1-1-2014

Management Of Plug-In Electric Vehicles And Renewable Energy Sources In Active Distribution Networks

Junhui Zhao
Wayne State University,

MANAGEMENT OF PLUG-IN ELECTRIC VEHICLES AND RENEWABLE ENERGY SOURCES IN ACTIVE DISTRIBUTION NETWORKS

by

JUNHUI ZHAO

DISSERTATON

Submitted to the Graduate School

of Wayne State University,

Detroit, Michigan

in partial fulfillment of the requirements

for the degree of

DOCTOR OF PHILOSOPHY

2014

MAJOR: ELECTRICAL ENGINEERING

Approved by:

_____

Advisor Date

_____

_____

_____

_____

DEDICATION

To my family

ACKNOWLEDGMENTS

Above all, I would like to express my great appreciation to my advisor Dr. Caisheng Wang. I especially thank him for providing me with lots of guidance not only of academic research but of career and personal development. It is his encouragement that inspires me to pursue a faculty position after graduation. I appreciate his precious support and help; and it is my honor to be his first Ph.D. student.

I would thank my co-advisor Dr. Feng Lin. His personal integrity and expectations of excellence always encourage me to advance higher in the study and research.

I would also like to express my sincere gratitude to other members of the dissertation committee, Dr. Le Yi Wang, Dr. Mark Ming-Cheng Cheng, and Dr. Wen Chen who gave me many professional ideas and stimulated my thinking in different ways so that I could improve my research study.

My sincere thanks also go to collaborators, Yang Wang, Lijian Xu, Zhong Chen, Zhongyang Zhao, Chang Fu, Saeed Alyami, Daniel Bral, Lezhang Liu, and Xuebin Tan, for their valuable discussions and suggestions in my research and study.

Special thanks go to my father Lijie Zhao and my mother Yanqin Shi, I would have never come so far without their unconditional support and love. Thanks to my father-in-law, Youmin Chen, and mother-in-law, Songluo Lin for their love and encouragement. Finally, I wish to thank my wife, Lan, for sharing the joys and sorrows of life with me. It is her countless encouragement and love inspire me go further and further.

TABLE OF CONTENTS

.

LIST OF TABLES

LIST OF FIGURES

CHAPTER 1 INTRODUCTION AND LITERATURE REVIEW

1.1 Motivation

Smart Grids have been widely hailed as the future infrastructure of electrical power generation for secure, efficient and sustainable energy development. Electric power distribution networks (DNs) have been a fundamental element and a large part of the power grid infrastructure. They will become even more critical and should be given the priority in developing future smart grids. This is because distribution networks are where most end users, distributed generation (DG) sources and plug-in electric vehicles (PEVs) are connected. Near 160 million customers in the U.S.A. are served via distribution networks [1]. The increasing penetration level of DG and PEVs, the implementation of smart distribution technologies such as advanced metering/monitoring infrastructure (AMI); and the adoption of smart appliances, have changed DNs from passive to active. The next-generation of DNs should be efficient and optimized system-wide, highly reliable and robust, and capable of effectively managing highly-penetrated PEVs, DG sources and other controllable loads. To meet new challenges, next-generation DNs need active distribution management (ADM).

Various distribution management technologies, such as distribution automation, AMI, fault location, automated reconfiguration and VAR control, have been studied and some of them have been successfully implemented in today's distribution networks [1]. Different aspects of optimization of DN planning have also been investigated, including optimal deployment of capacitor and other VAR compensation devices, section-reclosers, and DG sources [2-5]. Moreover, advances in new DG technologies, new power electronic converters (PEC) such as solid state transformers capable of regulating real and reactive power flows [6], the expanding

use of intelligent appliances and other controllable loads [7], and the application of home and office automation networks [8], all make ADM for next-generation DNs possible.

Therefore, it is vital and urgent to study the active management of DN with DGs and PEVs by taking advantage of novel management strategies and emerging technologies.

1.2 Literature Review

1.2.1 Active management framework of distribution networks

In an ADM scheme, the proper coordination of DGs, voltage regulators, shunt capacitors, and other devices in a DN is critical to achieve high system security and operation efficiency [9]. Generally, the management framework of the ADM can be categorized into three types: centralized, decentralized, and hybrid hierarchical management (HHM) frameworks.

1.2.1.1 Centralized management framework

In the centralized management framework, the voltage, power flow, and equipment status measurements at selected locations in the DN are sent to the distribution network central controller (DNCC), as shown in Figure 1.1. Similar to the supervisory control and data acquisition (SCADA) of transmission system, the DNCC is able to manage the DN through dispatching active and reactive power from DGs and assigning operation commands to other network elements.

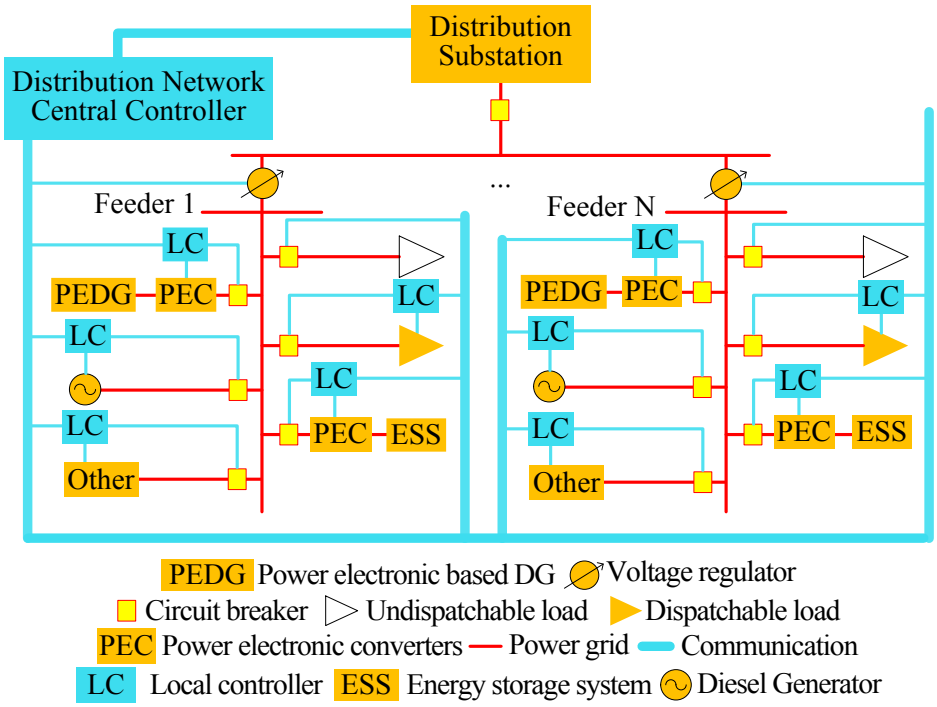

Figure 1.1 Illustration of a centralized control framework.

In addition, the DNCC coordinates available devices in the DN to enhance the operation efficiency and keep the voltage and frequency within security range. In [9], a central Distribution Management System Controller was proposed to deliver real-time measurements and network data into a state estimation algorithm to control active devices in the DN. Reference [10] presented an optimal algorithm to coordinate DGs with other devices, such as load ratio control transformer, step voltage regulator, shunt capacitor, shunt reactor, and static VAR compensator to adjust voltage of each node with necessary communication supports. In [11], to efficiently exchange information, a remote terminal unit (RTU) is placed at each DG and each switched capacitor in the system; and then by reading and analyzing the information provided by the RTUs, a central voltage controller adjusts the settings of the voltage regulators on different feeders to coordinately regulate the voltage within the acceptable range. A statistical state estimation method was utilized in [12] to estimate the voltage at each node, and correspondingly set the target voltage of relays and the DGs' output to maintain the voltage profile.

However, as stated in [16], the centralized control is against the "distributed" nature of DN, in which the electrical devices are usually dispersed. Though the centralized control strategy is the most straightforward way to achieve the management and optimization of the overall network, it certainly has several drawbacks: (1) A failure of the central controller may cause the crash of the whole system; (2) the amount of data and communication traffic may quickly exceed the level that can be handled; (3) high investment in communication and data processing; (4) onerous testing is required for even just a few modifications on the control algorithm; and (4) the shutdown of the whole system for maintenance.

1.2.1.2 Decentralized management framework

To follow the distributed nature of DN, an opposite way to centralized ADM is to develop a decentralized control system. As shown in Figure 1.2, the devices in decentralized methods can be autonomous. The control decisions of local controllers could be made according to only the local information or coordination with neighboring devices [13, 14]. For example, by using the local voltage and frequency information, the real and reactive power of DGs and energy storages could be adjusted through f/P and V/Q droop controllers [15-17].

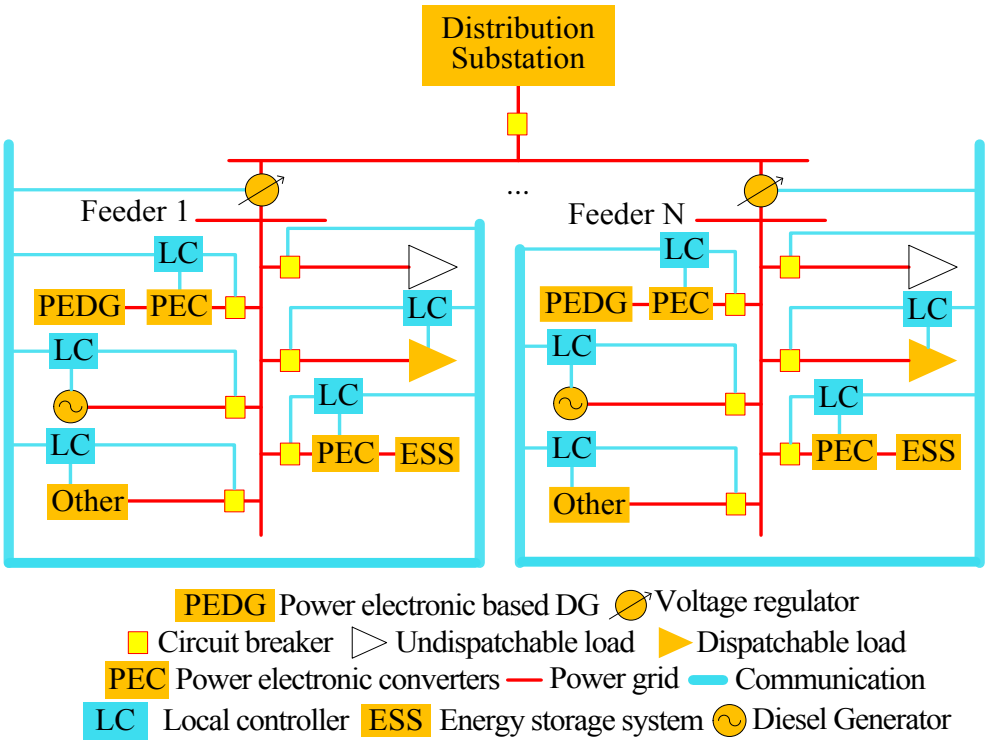

Figure 1.2 Illustration of a decentralized control framework.

By coordinating DGs and conventional voltage regulation devices, the voltage could be regulated within the security range in a local/distributed way. In [18], cooperated with line drop compensator, on-load tap changers (OLTC) were controlled to avoid local voltage problems in a medium voltage feeder with DGs installed. It concluded that the parameters and structure of a feeder and DG's connection point jointly affect the effectiveness of the proposed methods. In [19], a large and meshed network is firstly divided into many sub-networks based on the ε-decomposition of the sensitivity matrix; and then the devices in the same sub-network coordinate together to adjust the local voltage within the limitation.

In addition, a popular approach for distributed control scheme is agent based management (ABM), which has been widely studied for the power flow, protection, restoration and voltage regulation in transmission networks [20], and has drawn the attentions of its applications in DN management [21]. The definition of an agent in ABM, adapted from [22], is an entity of software

and/or hardware embedded in the DN and is able to change the network, be affected by a set of tendencies, and interact with other agents. A system containing two or more coordinated agents is named as multi-agent system (MAS). The management of various devices in the ABM received extensive studies. In [23], the ability of the agents to monitor the local voltage sensitivities was enhanced to facilitate the injection of plug-and-play DGs into the DN. Reference [24] focused on the operation of microgrid in DN through the ABM. In the three-layer ABM, every DG or controllable load determines the best behaviors by themselves. As for the intermittency of DGs, a persistent method was used by assuming that the average energy production for the next short period will be consistent with the current one. However, as it was stated in [25], in an ABM system, agents consider their own benefits more than the global optimization. Therefore, the solution provided by MAS may be sub-optimal.

An interesting paper [26] compared the centralized and decentralized control frameworks from the aspects of total allowed injection capacity and losses. It arrives at a conclusion that the two methods show similar influence on maximizing the DGs' penetration capacity without causing voltage rise issues. However, the two strategies both cause a significant increase of power losses, which is about five times higher than the constant power factor control method.

1.2.1.3 Hybrid hierarchical management framework

Hybrid hierarchical management (HHM) is a more practical framework to manage large distribution networks. It combines centralized and decentralized control and has a multi-layer structure, as shown in Figure 1.3.

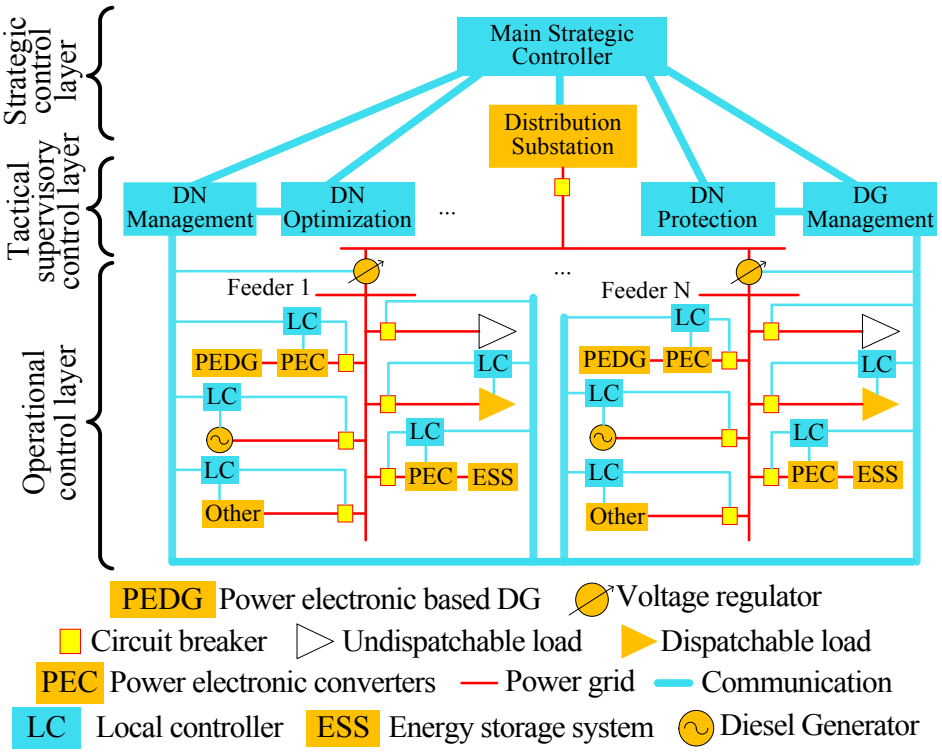

Figure 1.3 Illustration of a hybrid hierarchical control framework.

The HHM usually consists of several supervisory control layers [27-29]. In the top strategy layer, the controller carries out the functions of display, monitoring, operation and management by collecting the information of lower layers and market information. Based on the strategic orders, controllers in the lower tactical supervisory control layer perform different predefined functions to generate optimal settings for the local controllers in the lowest operational control layer. Analogous to a global manufacture standard, ISA-95, a general hierarchical control structure of microgrid was proposed in [30]. In the proposed scheme, the four layers from the top down are tertiary control layer, the secondary control layer, the primary control layer, and the inner control layer. The method could be extended to a cluster that has multiple microgrids and finally control the overall distribution network.

1.2.2 Voltage and energy management methods of active distribution networks

Within a given management framework, it is still challenging to develop practical strategies for power and energy management. On the energy-supply side, how to economically integrate DG sources and how to control these sources to regulate system voltage need more research. On the customer side, one challenging issue is how to solve the voltage and power issues caused by the proliferation of new loads such as PEVs.

1.2.2.1 Optimization of DGs in distribution networks

To economically integrate DGs into DNs, the location and sizing of DGs should be optimized. In [31], the optimal allocation and sizing of DG and ESS were calculated by a genetic algorithm, and the results showed that using DGs and ESS was able to economically improve the energy-not-supplied index of the DN. Reference [32] presented analytical approaches for optimal placement of DGs based on the network parameters, such as bus admittance matrix, generation information and load distribution of the system. In [33], a modified particle swarm optimization (PSO) algorithm with both of the technical and economic constraints was proposed to determine the optimal location of DGs and ESS in DN.

In addition, there are numerous objectives in optimization problems of DG-dispatching in DN. A common objective is to mitigate the power congestion and to defer the system upgrade [34, 35]. Energy losses minimization is another common objective in DN to optimally dispatch DGs [32, 36]. Some researchers consider the enhancement of reliability of power supply as another objective [37, 38]. Multi-objective optimization has also been extensively explored. In [39], a multi-objective mixed integer programming algorithm was proposed to optimize three objectives together by economically dispatching DGs in DN.

1.2.2.2 Active voltage management through DGs

Traditionally distribution network operators (DNOs) manage DGs in a unit power factor control mode; however, it ignores the fact that some DGs may be capable of providing reactive power support as well. With increasing needs for the reactive power support, it is very likely that, in the future, DGs will be required to provide such support. The studies to utilize DGs to actively compensate reactive power and regulate voltage in DN could be categorized into dynamic control [40-44] and steady-state dispatching [23, 45, 46].

The study on dynamic Volt/VAR control of DGs focuses on the design of the power inverter controllers of electronic-interfaced DGs. In [40] and [41], V/Q droop controllers were used to dynamically adjusting the reactive power generation of DGs to regulate the local voltage. Reference [42] introduced the control of the back-to-back voltage source converter of a wind turbine generator. The authors designed the three-stage controllers, rotor-side converter controller, DC-link controller, and grid-side converter controller. In addition, the real and reactive power operating limits were integrated into the design of the controllers. Based on these controllers, the reactive power is actively controlled for voltage regulation without violating the power limits. The authors of [43] proposed an algorithm to control the voltage by automatically adjusting the parameters of the controllers according to the system dynamics. With respect to the limit of reactive power generation of DGs, the work [44] realized that $|Q_{max}| \leq 0.45P_{rated}$ (where Q_{max} and P_{rated} are the reactive power generation capacity and the rated real power output of DGs respectively) was reasonable because it required no significant extra cost of inverters.

The steady-state analysis mainly commits to formulate the voltage support by DGs as a reactive power dispatching problem. In [23], with fast communications among DGs and voltage regulators, an agent based method was introduced to facilitate a model-free control procedure to

dispatch reactive power generation of DGs in an optimal manner. In [46], the reactive power of DG was regarded as a controllable variable and was coordinately dispatched with the OLTC and shunt capacitors. The results showed that the location and the capability of reactive power generation of DGs and other factors determined the performance of the voltage regulation.

Overvoltage is a common and important issue for DN with high penetration of DGs. For the worst scenario that the installed devices are unable to keep voltage below the upper limit, a straight forward method was proposed by reducing DGs' power production [47, 48]. Based on the dynamic Thevenin equivalent, a real-time prediction algorithm was proposed in [49] to calculate the active power limit as a reference of the power. However, for a feeder with multiple DGs, how to fairly curtail power of DGs that belong to different owners deserves more studies because unfair curtailment may cause conflict of interest between DG owners and DNOs. The simplest method is to equally curtail the power output of DGs once the voltage issue happens [47].

In addition, the study in [50] showed that the allowable penetration level of DGs could be increased if DGs were used as voltage regulators. In the above paper, three different power factor modes of distributed generators were compared which are unitary, capacitive and inductive power factor modes. It concluded that the voltage control mode for the DG helped maximize the allowable penetration of distributed synchronous generation in DN.

1.2.2.3 Active management of plug-in electric vehicles

To reduce CO2 emissions and oil dependency, transportation electrification is an important and viable way. By 2030, the cumulative sales of plug-in electric vehicles (PEVs) could be as high as 16 million [51]. The increasing number of PEVs will become a large load to the power grid when they are being charged. In [52], the impact of the PEVs on the Belgium DNs with the consideration of the traffic and driving patterns was studied. After the simulation studies for

different scenarios on a 34-node test feeder, it concluded that the large injection of PEVs can cause a significant amount of power losses and voltage deviations. At the same time, the analysis of the paper also showed that the voltage issue and energy deficiency could be mitigated if the charging of PEVs was actively managed. Therefore, the impacts of PEVs on DN must be measured and controlled to maintain the DN's stability. An active management of PEVs was proposed in [53] and [54]. PEVs and other loads in a DN were modeled by a method of finite state machine with variables, and then a safety controller was proposed to locally manage the dis-/charging of PEVs and other controllable loads on a node. With the coordination of controllers at all nodes, the peak power needed is shifted, and the safety of the feeder transformer is guaranteed.

Besides exerting great stress on DNs, the PEVs' injection also provides an opportunity to assist the ADM [55] via vehicle to grid (V2G). With the ability of V2G, PEVs are capable of exchanging energy and control information with DNOs to improve the voltage stability and energy security of the grid. In addition, PEVs could be used to balance the intermittent outputs from renewable sources via V2G techniques [56].

1.2.2.4 Demand side management

Demand side management (DSM) allows customers to take an active role in the ADM [57, 58]. By taking advantage of the bidirectional information and communication techniques, the customers are encouraged to shift their power consumption toward off-peak periods to reduce the maximum and/or total power needed, therefore reinforcing the energy security and reliability and maximizing the efficiency. When electricity demands are high, reducing peak usage and temporarily employing DGs are a solution that draws more and more attention [59].

Load demand modeling is important for the development of the DSM. A state-queueing model to study the price response of thermostatically controlled appliances (TCA) was proposed

in [60]. The model successfully simulates the dynamic response of the TCA type of load along with the price changes. In [61], the residential loads, with customized priority and convenience settings, were categorized into controllable and critical groups for the DSM strategy. With the proposed model, a load shaping tool was designed to not only manage the total demand under the limitation of transformers, but guarantee customers' comfort to a great extent.

The DSM has the potential to improve the investment efficiency in DN. It could be helpful in increasing the penetration level of DGs in the DN by managing the demand-supply balance [62]. The increased DGs help reduce the peak load of both cables and transformers and relieve congestion in substations. As a result, the upgrade of network could be deferred. As for how to overcome the intermittency of some DGs (i.e. photovoltaic resources, wind power generation) by DSM, a model predictive controller was proposed to predict the power consumption in a DN with high wind penetration in [63]. Integrated with the weather forecast and dynamic pricing information, the proposed algorithm could successfully realize a predictive demand dispatch in a real test platform.

1.2.3 Protection and fault location of distribution networks

In the DN with a large penetration of DGs, the traditional protection and fault-location methods may not work properly since most of them are based on unidirectional power/current flow along radial feeders. Therefore, active methodologies have to be developed to guarantee the security of DN.

1.2.3.1 Active distribution network protection

There are tremendous challenges that protection engineers have to deal with regarding the integration of DGs: Fuse and switchgear coordination, feeding faults after utility protection opens, interrupting ratings of devices, sympathetic tripping, protection relay desensitizing, recloser

coordination, and islanding [64]. For instance, when a DG tries to maintain the voltage stability under a fault condition, the reduction of the current seen by relays may induce the relay desensitizing [65]. In addition, both the direction and magnitude of the fault current seen by protection relays can be changed because of the injection of DGs [66]. To deal with the uncertainty of the fault current, an adaptive protection strategy was proposed in [67]. By only collecting the local information of the operating status and the faulted section, the trip characteristics of the relays are timely updated. And the use of microprocessor-based directional overcurrent relays, whose tripping characteristics could be chosen accordingly, brings the adaptive protection into effect [67].

Moreover, islanding is a noteworthy emerging challenge as the penetration of DGs increases. It is a situation that a DN or a portion of the DN has been isolated from the main power grid, but continually supplied by the DGs within it [68]. Such a situation may threaten the safety of line workers, cause distorted voltage and frequency, and lead to unwanted out-of-phase reclosing of the DGs [69, 70]. To detect the islanding, a remote (centralized) strategy will have to rely on communication [71] and advanced monitoring system, such as SCADA [72]. Decentralized strategies try to locally detect islanding by either passively measuring varying parameters such as voltage, frequency and harmonic distortion [73], by actively introducing perturbation to induce a significant change [74], or by hybrid methods to integrate both passive and active strategies [75].

1.2.3.2 Active fault location in distribution networks

There has been increased research effort on fault location for distribution network with DGs [1] [76-79]. In [76], a general method was given to locate faults for distribution networks with DGs. The method uses synchronized voltage and current measurements at the interconnection points of DG units and is able to adapt to variations in the topology of the system. The authors of [77] proposed a fault location method based on a binary hybrid algorithm of particle swarm

optimization and differential evolution, which targeted for solving "premature convergence" issues. It is a two-population evolution scheme with information exchange mechanism and is able to adaptively accommodate the changes caused by multiple fault sections in DN with multiple DGs. In [78], a multiagent management strategy was proposed to enhance the security of DN. By compromising the rule-based expert systems, the proposed intelligent agent could quickly locate and isolate the fault with assistance of the power line communication. A distribution fault anticipation technique, based on large database records of electrical waveforms of failing apparatus, was discussed in [79]. The technique was proposed for failures detection by monitoring sensitive signals. It can be extended to include a larger database with equipment parameters and system constraints [1].

1.2.4 Emerging technologies

In this section, the emerging technologies that enable the novel management methods and strategies aforementioned are reviewed.

1.2.4.1 Advanced power electronics

PECs are interfaces of the energy conversion for DGs and are the basic platform for DNOs to actively manage the DGs. With proper control strategies, PECs facilitate and regulate the power flow in DN, regulate the voltage where DGs are connected, compensate reactive power if needed, provide certain protection to the distributed generators, and help DGs rapidly and smoothly share load when the system islands [80].

In addition, assisted or even redesigned using power electronic techniques, some conventional devices are endowed with novel functions and applications. One example is new solid-state transformers (SST). By using semiconductor-based devices, they are much more flexible in handling high power levels with very fast switching [6, 81]. An SST is able to (1) change

the voltage and frequency of the power it produces; (2) has both AC and DC inlet/outlet; (3) directly take in power from wind and PV and (4) connect to the grid through proper power conversion. Another example is the solid-state fault current limiter (SSCL) [82]. Because the increased penetration of DG sources in DN in turn can cause the fault current exceed the ratings of existing power devices, the SSCL was proposed to limit the fault current and reduce oscillations by using series connected capacitors to act as large turn-off snubbers [83]. In the future, the built-in processors and communications will enable SST and SSCL to be key parts in the actively managed DN [1, 84].

Furthermore, the applications of flexible alternating current technologies in DN (DNFACT) enhance the controllability of the ADM. The devices of this kind include Distribution Static Compensator, Dynamic Voltage Restorer, and Solid State Transfer Switch. Reported in [85], DNFACTs were installed close to the load side for improving the system stability and the power supply quality.

Lower cost is always the highest priority in designing and developing PECs. It is critical to have cost effective PECs to integrate and manage various kinds of distributed generation sources and storage units in DNs. To achieve the goal, the effort has to be made at both the levels of hardware (topologies and components) and software (control and management). On the one hand, as reviewed in the previous sections, more features/functions such as reactive power support may be required from future PECs, which may increase their cost. Hence, the power converter manufactures need to come out with new ways to reduce the cost. Modular design that has been explored and used in the past [86-88] is a possible way. On the other hand, new control methods should be proposed to achieve the same control objectives without adding too much burden on the power electronic hardware side. For instance, a real power management strategy for PVs is

welcome if it can achieve the same voltage management goal since it will not increase the converter power ratings while the reactive power support features may.

1.2.4.2 Communication and information technology

Communication and information technology (CIT) provide data and information connectivity among active devices in the DN, including DGs, protection devices and loads. It enables distant control for DNs on a continuously increasing scale, and is viewed as one of the deciding factors for the successful realization of the ADM. In a CIT-based project of Distributed Intelligence in Critical Infrastructures for Sustainable Power (CRISP) [89], it has shown the CIT's important functions in protection, control and management, and network reconfiguration. Two important techniques to realize CIT in ADM are an advanced metering infrastructure (AMI) and phasor measurement units (PMU).

a) *Advanced metering infrastructure:* an AMI bridges smart meters, customers, energy resources, and various energy management systems. The various uses of metering data provided by AMIs were deeply explored in [90]. To provide advanced functionalities, the requirements for the AMI are to provide sufficient data to cover the network, to utilize powerful engine to store and analyze the data, and to employ accurate links among customer, transformers and substations. Based on these key elements, the AMI is able to monitor the performance of transformers, cables and circuits. In addition, by discovering outage disturbances, the AMI is capable of predicting pending failures in the DN.

b) *Application of Phasor Measurement Units*: With respect to the applications of PMUs in DNs, two constraints have to be carefully considered: The total vector error of frequency between different buses is very small [91]; and specific synchrophasor estimation algorithms are needed to tolerate high level harmonic distortions in the DN [92]. A specially

designed PMU and a novel algorithm to deal with the aforementioned two constraints are proposed in [92]. More importantly, due to the extremely large number of components in DNs, a distribution PMU technology should also be economically feasible. In addition, PMUs support the state estimation of DN. In [93], a method of designing the measurement infrastructure to maintain a desired accuracy of state estimation with trade-offs among the number of PMUs and the number of other measurement devices was proposed. The optimal placement of PMUs was determined by an optimization algorithm based on the generic algorithm [93]. Furthermore, PMUs help achieve a better protection of DN. In [94], PMUs were used to measure the phase error between the utility grid and DGs to detect loss of mains.

c) *IEC Standards*: Two important standards regarding the CIT in power systems are International Electrotechnical Commission (IEC) 61400-25 and IEC-61850 [95]. Their extensions to support the injection of wind energy in ADM were introduced in [95]. Depending on the actual CIT-based network management systems, DGs are smoothly integrated via an optimization algorithm for cost minimization and constraints management [95].

1.2.4.3 Smart appliances

The study and application of smart appliances (SA) have been extensively explored from smart thermostats to a series of home appliances which include but not limited to smart refrigerators/freezers, clothes washers/dryers, room air conditioners, and dishwashers [8] [96, 97]. By shifting the operation from on-peak hours to off-peak hours, SA is an effective tool for demand side management. In addition, by curtailing the operation temporarily in response to requests, the SA behaves as spinning reserves which is costly in the grid. Furthermore, the demand and the

supply from undispatched renewable energy resources (RES) could be well leveled by the SA thereby increasing the penetration of RES. In [96], the benefits of implementing SA were evaluated in terms of peak load shifting and spinning reserves. The calculation based on the price information from real wholesale markets indicates that the annual benefits by using SA are far more than the cost.

1.2.4.4 Energy storage system

The applications of ESS in ADM potentially benefit the DN [98], by:

- deferring system upgrade by peak load shaving;
- avoiding widespread outages together with demand response;
- mitigating the intermittency of some renewable energy sources while performing load and frequency regulation ;
- increasing penetration level of DGs in the DN;
- increasing the effective distribution capacity by using the storage devices that have extremely rapidly dis/charge rate; and
- enhancing system reliability.

Among various types of ESS, the battery energy storage system (BESS) takes a large part in smoothing the intermittency of RES in DN. However, the BESS sometimes is unable to act fast enough to follow high-frequency fluctuations. On the other hand, handling a large burst of current, such as in the scenarios of motor startup and rapid increase in solar generation, degrades battery plates and even shortens the life expectancy of BESS. An alternative way is to combine ultracapacitor and BESS in a hybrid energy storage system [99]. This hybrid solution was originally used to quickly capture the braking energy in hybrid electrical vehicles [100], and was

further introduced to smooth the intermittency of PV generation [101]. By implementing a high-pass filter, the high-frequency fluctuation and low-frequency continuous parts are separated. The battery can supply/absorb continuous energy, and the ultracapacitor is used to smooth the sudden change of load demand or energy generation.

In addition, along with the increasing of PEVs and resident-owned RES in DN, how to enhance the reliability in response to contingencies at the consumer-end is a new challenge. A solution is to install distributed small energy storage units in the residential community, which is referred to community energy storage (CES) [102]. Because the CES units are close to residents, they are able to serve as backup power, mitigate flickers, and integrate local PEVs and RES. Moreover, the clustered CES units perform as bulk energy storage at the substation to level supply and demand, improve the power quality, and even provide ancillary services.

1.2.5 Discussions on future development

The advancement of electricity distribution has been evolving very dynamically in various aspects including the areas reviewed in the previous sections. In this section, the discussion is focused on the future development in the following selected areas: Energy storage, customer participation, and the concept of virtual microgrid for active management of distribution network.

1.2.5.1 Community energy storage using retired electrical vehicle batteries

A surge of retired electrical vehicle (EV) batteries will soon be seen as more and more EVs hit the road. The treatment of old EV batteries is another important aspect for the whole EV development cycle. It needs to be investigated right now to provide a chance for repurposing them to support distribution grid. Old EV batteries that are not suitable for vehicle applications can still have substantial amount (up to 75%) of capacity left [103]. One million of retired 15 kWh/40kW EV batteries with an average of 50% remaining power and energy capability can provide 7,500

MWh energy capacity and 20,000 MW power capacity, a huge waste if not utilized in their secondary applications, such as energy storage for grid support [103-105]. Sandia National Laboratories released a report on the technical and economic feasibility of such approaches several years ago [103]. Recently, several EV manufacturers have announced their plans on using old EV batteries for stationary energy storage. For instance, General Motors, teamed with ABB, is developing 50 kWh of energy storage systems by using retired Chevy Volt batteries for CES applications [104]. However, management of used EV batteries is far more difficult than their primary EV usage. First, they must be re-characterized for the remaining capacity, internal impedance, and voltage/SOC curves. Secondly, different battery modules, in terms of their size, chemistry, voltage/current rating, capacity, etc., must be integrated. More research is also needed on new PECs and novel characterization and management of energy storage systems consisting of heterogeneous, retired EV batteries.

1.2.5.2 Customer participation

Customer participation is critical to many ADM technologies such as demand side management, smart appliance adoption and all other customer based approaches. Various incentives from federal and state governments to utilities have been made available to customers to encourage them to participate in a more active way for electricity distribution and management [106]. Though customer behaviors are affected by many factors, technologies can make them more aware and become more responsible for sustainable energy development and usage. Smart phone applications, for example, can provide an effective feedback path for customers, particularly young generations, to make information-aware decisions.

A smart phone application, called Home Emissions Read-Out (HERO), has been created by researchers at Wayne State University to provide consumers with real-time information about

local air emissions resulting from their energy choices [107, 108]. HERO can help users make environmentally-informed decisions about the best time to use their electricity to reduce emissions due to electricity generation and usage. The similar idea can be extended to other demand side management programs. According to a FERC report [109], the residential class represents the "most untapped potential for demand response".

Meanwhile, it is also important to guarantee customers fair participation and shared responsibility. For example, it is desired to give different renewable sources (owned by different owners) the equal opportunity to deliver their powers and to fairly distribute the responsibility when the renewable output powers need to be regulated. Similarly, PEV owners want their PEVs to be charged and to participate in possible V2G applications in a fairly defined way. This unique characteristic of fairness of power management in distribution networks has been realized by researchers recently. New methods such as cooperative and consensus control schemes have been proposed for fair power generation and sharing in distribution networks [110-112].

1.2.5.3 Concept of virtual microgrid

Though microgrids have been intensively explored and widely reviewed as a promising platform to integrate the intermittent renewable sources and electric drive vehicles to the grid [113-118], the extension of the concept to distribution network management largely remains as an unexplored area. Currently, most microgrids are operated as an attachment or extension to the existing grid and do not cover the major part of distribution networks. The potential of leveraging and expanding microgrid concept and technologies in ADM should be carefully investigated and deserves more research effort in future.

A concept of virtual microgrid (VMG) for ADM has been proposed in [119]. As shown in Figure 1.4, in this concept, a distribution network will be virtually or physically partitioned into

VMGs based on the physical feeder topologies, protection zones, or other partition and reconfiguration methods. A VMG, a portion of the distribution network, is controlled and managed just like any real microgrids. The whole distribution system will then have a hierarchical structure of at least two different levels/layers: the distribution grid level, the VMG level, and possibly sub-VMG levels. At the VMG level, each VMG controller will manage the components and network within its own scope and communicate information with and receive orders from the upper level controller, i.e. the grid controller. The grid controller will treat each VMG as a single control entity to achieve a system-wide power and energy management system for the whole distribution network.

However, there are many challenging issues that need to be addressed before the VMG concept can be used for managing real distribution networks. For example, how to form a virtual microgrid (or how to partition original distribution networks into VMGs) is one of the critical tasks. Moreover, VMG modeling and new management and control scheme based on the VMG concept should be interesting research topics in future.

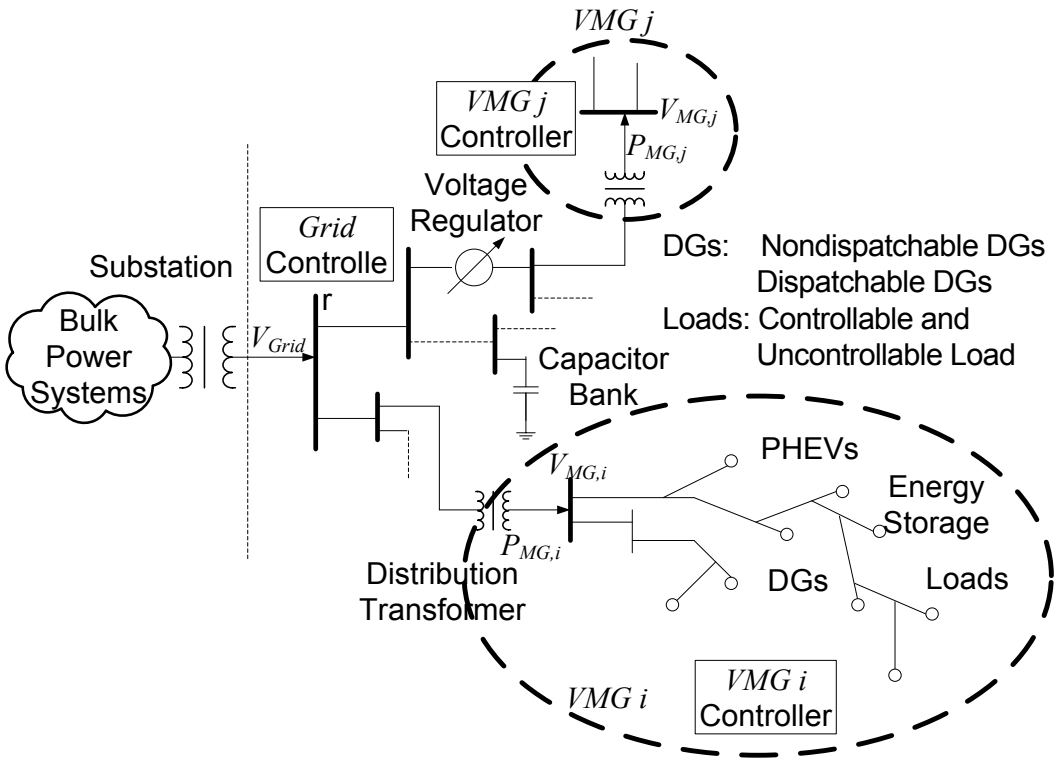

Figure 1.4 Illustration of a hybrid hierarchical control framework [119].

1.2.6 Summary

A review of the recent development in technologies and methods for the active distribution management is provided. Different management frameworks, active voltage and energy management methods, and active protection and fault location techniques for ADM were reviewed. In addition, some specific new strategies of the active management, such as optimization of DGs in DN, demand side management, and agent-based management were also reviewed. Emerging distribution technologies, such as advanced power electronics, communication and information technology, smart appliances, and energy storage systems have been illustrated. Finally, the future trends of energy storage, customer participation, and the concept of virtual microgrid for active management of distribution network were discussed.

1.3 Scope of the Study

Among the aforementioned topics in the active management of DNs, the main focus of the dissertation is the management of PEVs and renewable energy sources in DNs to avoid power shortage and voltage issues. A novel method of Finite State Machine with Variables and corresponding safety control are used to model and control PEVs. In addition, the optimal management of PEVs to prevent the violation of voltage stability will be investigated on system operation level. Furthermore, an algorithm to regulate the voltage in a microgrid by coordinating the reactive power generation from multiple distributed generations will be studied.

1.4 Organization of Dissertation

The remainder of the dissertation is organized as follows:

Chapter 2 and 3 discuss the active management of plug-in electric vehicles (PEVs) in a DN. In Chapter 2, PEVs are modelled as controllable loads by Finite State Machine with Variables (FSMwV) and managed by a safety controller. We proposed a novel discrete-event modeling method to model PEVs and other loads in DN. Chapter 3 presents a novel optimization algorithm to integrate as many PEVs as possible in DNs without causing voltage issues, including the violation of acceptable voltage ranges and voltage stability issues. To further explore the active management of PEVs in the DNs, we developed a universal demonstration platform, consisting of software package and hardware remote terminal units (RTUs), which is introduced in Chapter 4. The demonstration platform is designed with the capabilities of measurement, monitoring, control, automation, and communications.

The second part of the dissertation, Chapter 5, studies the reactive power management in microgrids, a special platform to integrate distributed generations (DGs) and energy storage in distribution networks.

CHAPTER 2 SAFETY CONTROL OF PEVS IN DISTRIBUTION NETWORKS USING FINITE STATE MACHINES WITH VARIABLES

2.1 Introduction to Discrete Event System

Discrete Event System (DES) is a system has discrete states, and of which the state evolution depends totally on the occurrence of asynchronous discrete events. In the definition, the event is an instantaneous action to drive the system moving forward or backward. Examples of DES include manufacturing systems, networks, computer databases, digital circuits, traffic networks, etc.

In this section, some basic notions and definitions are introduced, including finite state machine and supervisory control theory [120-122].

2.1.1 Language

For an event set Σ, a *language* is defined as a set of all finite symbol sequences, which is also called strings, formed from events in Σ [121]. Letting Σ^* denotes the set of all finite strings of elements in Σ including the empty string ϵ, obviously a language, L, over Σ is a subset of Σ^*.

If t is a prefix of s, where $s, t \in \Sigma^*$, the language of the *prefix closure* of L, denoted by $\bar{L}$ is defined by:

$$\bar{L} := \{s \in \Sigma^* : (\exists t \in \Sigma^*)[st \in L]\} \tag{2.1}$$

L is prefix-closed if $L = \bar{L}$.

Generally, it is more convenient to represent and analyze the properties and the specification of DES in the formal language setting [123]. Using sequences of events, the language describes the behavior of the system in a theoretic-based representation.

2.1.2 *Finite state machine*

A *finite state machine* (FSM) is usually selected to represent a language within the framework of predefined rules. In our study, the FSM is described by a 5-tuple [121]

$$\text{FSM} = (\Sigma, Q, \delta, q_0, Q_m) \tag{2.2}$$

where Σ is the (finite) event set, Q the (finite) state set, δ: $\Sigma \times Q \rightarrow Q$ the transition function and $\delta(q_1, \sigma) = q_2$ means there is an event σ that drives the system transition from state q_1 to state q_2; q_0 is the initial state, and Q_m the marked (or final) states. The FSM is said to be *deterministic* if there is only one transition with an event label out of a state; otherwise, it is defined as *nondeterministic*.

By following the rules that $\delta(q, \epsilon) = q$ and $\delta(q, s\sigma) = \delta(\delta(q, s), \sigma)$, we can recursively extend the transition function δ from $Q \times \Sigma$ to $Q \times \Sigma^*$, where $q \in Q, s \in \Sigma^*$, and $\sigma \in \Sigma$. Then we can define:

(1) *Generated language* of FSM by:

$$L(FSM) \coloneqq \{s \in \Sigma^* : \delta(q_0, s) \in Q\} \tag{2.3}$$

which is the set of all strings generated by FSM; and

(2) *Marked language* of FSM by:

$$L_m(FSM) \coloneqq \{s \in \Sigma^* : \delta(q_0, s) \in Q_m\} \tag{2.4}$$

which is the set of all strings that drive the FSM from state q_0 to a marked state q_m in Q_m.

Given two FSMs $\text{FSM}_1 = (\Sigma_1, Q_1, \delta_1, q_{01}, Q_{m1})$ and $\text{FSM}_1 = (\Sigma_2, Q_2, \delta_2, q_{02}, Q_{m2})$, an operation, *synchronous composition* of FSM_1 and FSM_2 to form a composite finite state machine (CFSM) is defined as:

$$\begin{aligned} \text{CFSM} &= \text{FSM}_1 \parallel \text{FSM}_2 \\ &= (\Sigma_1, Q_1, \delta_1, q_{01}, Q_{m1}) \parallel (\Sigma_2, Q_2, \delta_2, q_{02}, Q_{m2}) \\ &= (\Sigma_1 \cup \Sigma_2, Q_1 \cup Q_2, \delta_1 \cup \delta_2, q_{01} \cup q_{02}, Q_{m1} \cup Q_{m2}) \\ &= (\Sigma, Q, \delta, q_0, Q_m) \end{aligned} \tag{2.5}$$

The *synchronous composition* is usually employed to combine FSMs in the system to form a single FSM without loss of characteristics of system.

2.1.3 Supervisory control of DES

The target of DES control is to design controllers and control strategy to ensure the system satisfy certain desired qualitative constraints, which sometimes means the system is controlled without visiting undesirable states.

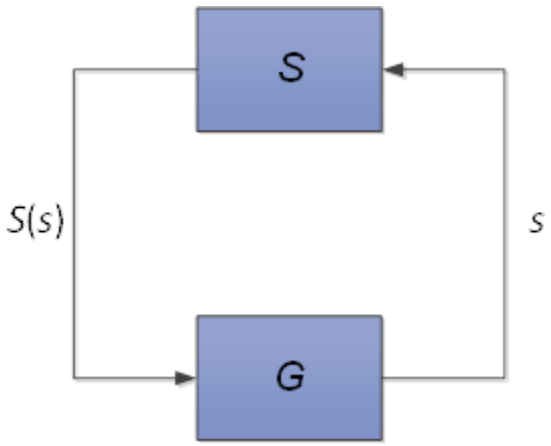

Figure 2.1 Feedback loop of supervisory control.

In the control framework proposed by Ramadge and Wonham [120], the control of DES is based on the principle of feedback. Based on observed information, the controller is used to generate input to the system so that the control specifications can be met. The feedback loop of supervisory control is shown in Figure **2.1**. Generator, *G* represents FSM defined in (2.2) and is also known as an object to be controlled. *S* is called as a supervisory controller. The supervisory control theory was introduced to synthesize the controller *S* and the specifications for the given

generator *G*. To incorporate the control information into the system, the set Σ is partitioned into subsets: (1) the *controllable events* Σ_c, *i.e.* those events that can be disabled by an external controller; and (2) the *uncontrollable events* Σ_{uc} which cannot be prevented from occurring.

The *control pattern set* is defined by:

$$\Lambda := \{\lambda | \Sigma_{uc} \subseteq \lambda \subseteq \Sigma\} \subseteq 2^{\Sigma} \tag{2.6}$$

The control pattern is interpreted that the controller *S* is an external agent which is able to observe the behaviors of the system *G* and control *G* through enabling and disabling the controllable events.

Formally, a *supervisor S* for system *G* is a function:

$$S: L(G) \to \Lambda \tag{2.7}$$

where *L*(*G*) is the language generated by *G*, and *S*(*s*) is the set of eligible events that can be executed after a string $s \in L(G)$. Then the language of the controlled system, *L*(*S*/*G*), to denote the closed behavior of G under the supervision of S is defined recursively as follows

- $\epsilon \in L(S/G)$
- $s \in L(S/G), s\sigma \in L(G), and\ \sigma \in S(s), then\ s\sigma \in L(S/G)$
- *No other strings belong to* $L(S/G)$

The marked language by S/G is defined by

$$L_m(S/G) = L(S/G) \cap L_m(G) \tag{2.8}$$

where $L(S/G)$ represents the system behaves in a desired way under the supervision and control of *S*. To show whether *G* is controllable, the controllability is formulated in [124]:

Consider a discrete event system, $FSM = (\Sigma, Q, \delta, q_0, Q_m)$. *Let* $L(G) = \overline{L(G)}$ *be a prefix-closed language. Let K and L(G) be languages over an event set Σ. The language K is said to be controllable w.r.t, L(G) and the set of uncontrollable events* Σ_{uc} *if*

$$\overline{K}\Sigma_{uc} \cap L(G) \subseteq \overline{K} .$$

The supervisory control theory [120-122, 125] based on finite state machines has been well developed as it addresses the fundamental issues in control of DES.

2.2 Problem Formulation

Modeling and control of DES have been studied by control engineers and scientists for more than 25 years. During this period, many modeling approaches have been proposed, including most notably automata or finite state machines [120, 121], Petri nets [126, 127] and their variations such as vector DES [128, 129] and event graphs [130], queuing systems [121] and generalized semi-Markov processes [130]. Among these models, FSM is the most straightforward for control. We now have a good understanding of problems such as controllability, observability, coobservability, normality, decentralization, nondeterminism, etc. We believe that an important reason we have gone this far in a relatively short time period is that we adapted a simple model of FSM. Because of this, we can focus our attention on and see the essence of the control problem.

However, FSM model has long suffered from the problem of state explosion that renders it unsuitable for some practical applications. For example, to model a buffer of *n* capacity using a FSM would require at least *n* states. On the other hand, by using an integer variable to describe the content of the buffer, the number of states required can be drastically reduced. Furthermore, in the case that the capacity of the buffer changes, we can simply modify the range of the variable without remodeling the system.

Meanwhile, the traditional supervisory control techniques focus on (passively) maintaining system safety and liveness by the means of disabling some controllable events. It has neglected the possibility of actively enforcing certain events that is widely practiced in the control of real

world DES applications. Event enforcement can be quite useful in both "driving" the system toward the given objective (e.g., marked states) and actively maintaining system safety.

To mitigate the problem of state explosion, we propose to employ both FSM and sets of variables in modeling discrete event systems. We call our representation Finite State Machines with Variables (FSMwV) (formerly, it was called Finite State Machines with Parameters [131]). We show that our FSMwV can represent a broader class of discrete event systems with far smaller numbers of discrete states. The definition of our FSMwV is similar to the Extended Finite State Machines (EFSM) described in [132]. However, the EFSM mechanism was developed for the design verification of circuits but not for the modeling of general discrete event systems. Hence, variables in EFSM are mainly for describing the contents of the circuit inputs/outputs rather than for describing system resources and possible time/resource constraints that FSMwV is designed for. Furthermore, neither concepts of system composition nor control synthesis were developed under the EFSM scheme.

Recently, a method using EFSM to implement the supervisory map as an embedded control was developed [133]. The method was extended to decentralized control in [134]. EFSM was also used to verify supervisory control properties in [135]. In [136], the authors proposed to transform a set of extended automata into a set of ordinary automata with equivalent behavior, but no control synthesis methods were discussed. [137] developed the supervisory control for concurrent systems with EFSM modeled subsystems. In [138], a symbolic transition system model was used, which defines the concept of controllability by applying it to the guards of symbolic transitions, instead of to the events. Neither [138] nor [137] investigated the synthesis of optimal (least restrictive) controllers. They also did not consider enforceable events.

In this chapter, our focus is on control synthesis using FSMwV. We first extend the scope of the traditional DES control to include both event disablement and event enforcement. We then propose an offline safety control synthesis procedure that takes the advantage of both event disablement and enforcement in order to prevent the controlled system from venturing into the prohibited state space. To address the practical concern of real world implementations, we further present a set of safety control synthesis procedures, based on the limited and/or variable lookahead policies [139, 140] that generate the control policies online under the FSMwV modeling framework.

The theoretical results on modeling and control of DES using FSMwV are applied to the safety control of PEVs in the electric power distribution network. DES theories have been explored for applications in power systems [141-144]. Supervisory control using DES was applied and reported in [141] for line restoration. Hybrid automaton and Petri Nets was used to model power systems for handling inverse problems such as parameter uncertainty and parameter estimation [143]. DES was used in [144] to describe cascading events such as blackouts in power systems. A number of potential power system control problems were discussed in [142]. However, most of the results obtained so far in the area are still preliminary. The relevance and applications of DES to power systems remain not so clear [142]. We model a distribution network by an FSMwV in this chapter. We consider both conventional uncontrollable loads and controllable loads (such as plug-in hybrid electric vehicles) by using appropriate variables to avoid possible state explosion. A supervisor is then designed to ensure the network is fully utilized and never overloaded.

The rest of the chapter is organized as follows: We present the FSMwV model and its system composition mechanism in Section 2.3. Some preliminary work on FSMwV was presented in [131]. In Section 2.4, we describe our notion and means of control and present an offline safety

control synthesis algorithm. In Section 2.5, we present an online synthesis algorithm (and its variations) for safety control policies. In Section 2.6, we apply the results to the safety control of PEVs in the power distribution network. We conclude this chapter in Section 2.7.

2.3 Finite State Machines with Variables

To introduce variables into an FSM, let $p \in P$ be a vector of variables, where P is some vector space. P can be either finite or infinite. More often, P is over the set of natural numbers. We also introduce guards $g \in G$ that are predicates on the variables p. The transition function δ can be defined as a function from $\Sigma \times Q \times G \times P$ to $Q \times P$ as illustrated in Figure 2.2. The transition shown is to be interpreted as follows: If at state q, the guard g is true and the event σ occurs, then the next state is q' and the values of variables will be updated to $f(p)$. We denote such a transition by $(q, g \wedge \sigma / p := f(p), q') \in \delta$.

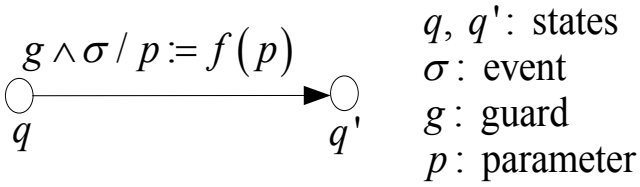

Figure 2.2 A transition in FSMwV.

If g is absent in the transition, and then the transition takes place when σ occurs. Such a transition is called event transition. If σ is absent, then the transition takes place when g becomes true. Such a transition is called dynamic transition. If $p:=f(p)$ is absent, then no variable is updated during the transition. In summary, a finite state machine with variables can be viewed as a 7-tuple

$$\text{FSMwV} = (\Sigma, Q, \delta, P, G, (q_0, p_0), Q_m) \tag{2.9}$$

where p_o is the initial value of variables at the initial state q_o.

Without much difficulty, we can regard finite state machines with variables as a special type of Hybrid Machines (HMs) introduced in [145]. In particular, an FSMwV has no continuous dynamics (i.e. $\dot{p} = 0$ at any state). The only way to change values of variables is by updating (or re-initialization).

Similar to FSMs and HMs, we can define parallel composition of several FSMwVs running in parallel to form a composite finite state machine with variables (CFSMwV)

$$\text{CFSMwV} = \text{FSMwV}_1 \,\|\, \text{FSMwV}_2 \,\|\cdots\|\, \text{FSMwV}_n \tag{2.10}$$

To define a CFSMwV, we assume that any variable can only be updated by at most one FSMwV. Variables that are not updated by any of the FSMwVs are updated by the unmodeled environment. In general, a variable updated by one FSMwV can be used in another FSMwV. That is, a guard in one FSMwV may depend on a variable updated by another FSMwV.

To simplify the following definition of parallel composition, we assume that, without loss of generality, all transitions in an FSMwV have been decomposed into event transitions and dynamic transitions, as this can always be done. Hence,

$$\begin{aligned}
\text{CFSMwV} &= \text{FSMwV}_1 \|\ldots\| \text{FSMwV}_n \\
&= \left(\Sigma_1, Q_1, \delta_1, P_1, G_1, (q_{o1}, p_{o1}), Q_{m1}\right) \|\cdots\| \left(\Sigma_n, Q_n, \delta_n, P_n, G_n, (q_{on}, p_{on}), Q_{mn}\right) \\
&= \left(\Sigma_1 \cup \ldots \cup \Sigma_n, Q_1 \times \ldots \times Q_n, \delta_1 \times \ldots \times \delta_n, P_1 \cup \ldots \cup P_n, G_1 \cup \ldots \cup G_n,\right. \\
&\quad \left.(q_{o1}, \ldots, q_{on}, p_{o1}, \ldots, p_{on}), Q_{m1} \times \ldots \times Q_{mn}\right) \\
&= (\Sigma, Q, \delta, P, G, (q_o, p_o), Q_m),
\end{aligned} \tag{2.11}$$

where the transition function $\delta = \delta_1 \times \cdots \times \delta_n$ is defined as illustrated in Figure 2.3 and Figure 2.4 for n=2. In the figures, l_i can be either an event ($l_i = \sigma_i$) or a guard ($l_i = g_i$). If $l_1 \neq l_2$, then the situation is illustrated in Figure 2.3. That is, if the transition l_1 occurs at state (q_1, q_2), then the next state is (q_1', q_2). Variable p_1 is updated to $f_1(p_1)$ while p_2 is not updated. On the other hand, if $l_1 = l_2 = l$, then the situation is illustrated in Figure 2.4. That is, if the transition l occurs at state

(q_1, q_2), then the next state is (q_1', q_2'). Variables p_1 and p_2 are updated to $f_1(p_1)$ and $f_2(p_2)$ respectively.

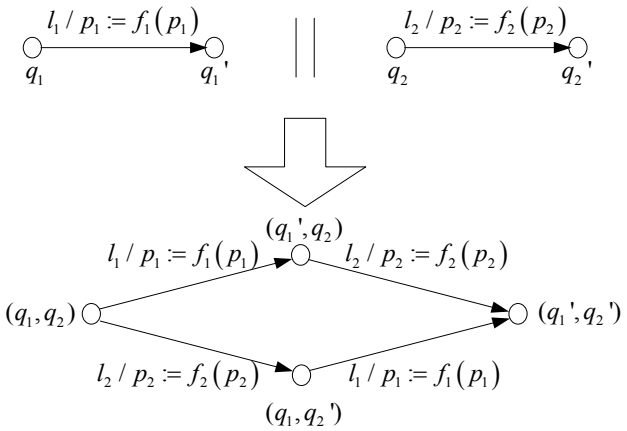

Figure 2.3 Parallel composition: $l_1 \neq l_2$.

We note that this definition is an extension to that of FSM [121]. Using this parallel composition, we can build large systems from simple components. This procedure can be automated.

To describe the behaviour of an FSMwV, (Σ, Q, δ, P, G, (q_0 , p_0), Q_m), we define a run of an FSMwV as a sequence

$$r = (q_0, p_0) \xrightarrow{l_1} (q_1, p_1) \xrightarrow{l_2} (q_2, p_2) \xrightarrow{l_3} (q_3, p_3) \cdots \tag{2.12}$$

where l_i is (the label of) the ith transition and (p_i, q_i) is the state and variable values after the ith transition. We denote the set of all possible runs of FSMwV as

$$R(\text{FSMwV}) = \{r: r \text{ is a run of FSMwV}\} \tag{2.13}$$

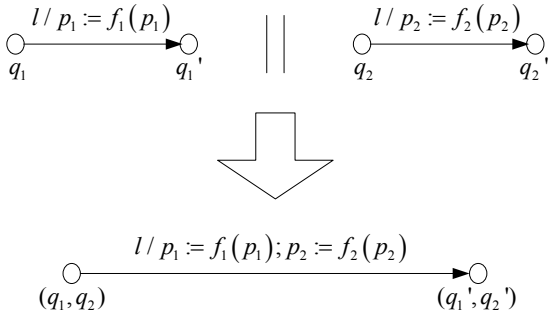

Figure 2.4 Parallel composition: $l_1 = l_2 = l$.

A trace of a run is the sequence of event transitions in the run

$$s = \sigma_1\sigma_2\sigma_3 \cdots \tag{2.14}$$

That is, *s* is obtained from *r* by deleting the state information and dynamic transitions.

If an FSMwV is deterministic (which we assume throughout this chapter), then a run is uniquely determined by its trace. That is, we can reconstruct a run by looking at its trace and the FSMwV. The set of all traces of an FSMwV is a language denoted by

$$L(\text{FSMwV}) = \{s: s \text{ is a trace of FSMwV}\} \tag{2.15}$$

This language is called the language generated by FSMwV. The language marked by FSMwV is defined as

$$L_m(\text{FSMwV}) = \{s \in L(\text{FSMwV}): \text{the run of } s \text{ ends in a marked state } q \in Q_m\} \tag{2.16}$$

Since CFSMwV and FSMwV have the same structure, runs, traces, and languages for CFSMwV are defined similarly.

We often use a legal specification $E \subseteq R(\text{CFSMwV})$ to specify the legal behaviour of the system modeled by a CFSMwV: a run *r* is legal if and only if it belongs to *E*. We call this type of specifications dynamic specifications. On the other hand, if the legal behaviour is specified in terms of legal and illegal states, that is, a run *r* is legal if and only if it does not visit any illegal state, then the specification is called a static specification. It is well known in supervisory control [146] that a dynamic specification can always be translated into a static specification (perhaps at the cost of having more states). Therefore, we will use static specifications in safety controller synthesis.

2.4 Safety Controller

In this section, we study how to design a safety controller, that is, a controller that guarantees the system will never enter some illegal states. We assume that the system to be controlled is modeled by a CFSMwV:

$$\text{CFSMwV} = (\Sigma, Q, \delta, P, G, (q_0, p_0), Q_m) \tag{2.17}$$

and the safety requirement is given by a set of illegal states $Q_b \subseteq Q$. Note that the specifications in terms of illegal states are very general and cover a large class of practical situations. For example, we can translate the specification "the variable p shall always be less than a constant c" into an illegal state specification as shown in Figure 2.5.

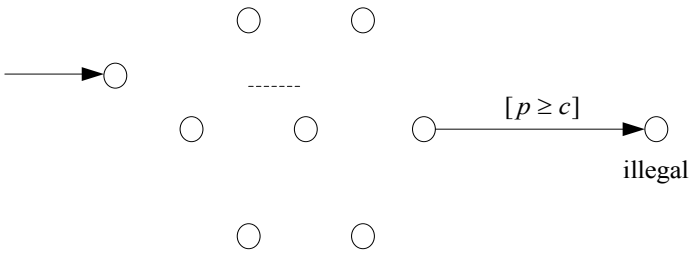

Figure 2.5 An illegal state specification for $p \geq c$.

The control objective is to make sure that the system never visits any illegal state in Q_b. We assume that there are two control mechanisms that can be used to achieve the control objective.

(1) Disablement: Events in $\Sigma_c \subseteq \Sigma$ can be disabled by a controller. Events $\sigma \in \Sigma_c$ are called controllable events.

(2) Enforcement: Events in $\Sigma_f \subseteq \Sigma$ can be enforced by a controller. Events $\sigma \in \Sigma_f$ are called enforceable events.

We assume that an uncontrollable event cannot be enforced, that is, $(\Sigma - \Sigma_c) \cap \Sigma_f = \phi$, where ϕ denotes the empty set. We also assume that the system is deterministic. That is, any transition in CFSMwV can only lead to one state.

The behavior of the uncontrolled system is described by the set of runs generated by CFSMwV, R(CFSMwV). The legal behaviour of the system is described by a subset of runs in R(CFSMwV) that does not visit illegal states:

$$E = \{r \in R(\text{CFSMwV}): r \text{ does not visit any illegal states in } Q_b\} \tag{2.18}$$

In order to simplify the analysis and synthesis of controllers, we will treat all transitions, including event transitions and dynamic transitions, in a unified manner. To this end, we introduce an artificial uncontrollable event σ_u and extend the event set Σ to include σ_u. To simplify the notation, we will still use Σ to denote the expended event set in the rest of the chapter. With σ_u, a dynamic transition $(q, g/p := f(p), q')$ is equivalent to $(q, g \wedge \sigma_u/p := f(p), q')$ for the purpose of controller analysis and synthesis and an event transition $(q, \sigma/p := f(p), q')$ can be viewed as $(q, g \wedge \sigma/p := f(p), q')$ if we let $g = T$.

To investigate the control in a generalized framework, we use generalized control patterns [147] as follows:

$$\Gamma = \{\gamma \subseteq \Sigma: \Sigma - \Sigma_c \subseteq \gamma \vee \gamma \subseteq \Sigma_f\} \tag{2.19}$$

This set of control pattern allows two types of control: (1) Disabling some controllable events (that is, those in $\Sigma - \gamma$, if the first disjunction is satisfied); and (2) Enforcing some enforceable events (that is, those in γ, if the second disjunction is satisfied). This is a generalization from pure disablement of standard supervisory control.

Proposition 1: The set of control patterns Γ is closed under union, that is, for all control patterns γ_1, γ_2

$$\gamma_1 \in \Gamma \wedge \gamma_2 \in \Gamma \Longrightarrow \gamma_1 \cup \gamma_2 \in \Gamma \tag{2.20}$$

Proof: Assume that $\gamma_1, \gamma_2 \in \Gamma$, that is $\Sigma - \Sigma_c \subseteq \gamma_1 \vee \gamma_1 \subseteq \Sigma_f$ and $\Sigma - \Sigma_c \subseteq \gamma_2 \vee \gamma_2 \subseteq \Sigma_f$. Consider four possible cases.

(1) $\Sigma - \Sigma_c \subseteq \gamma_1 \wedge \Sigma - \Sigma_c \subseteq \gamma_2 \Longrightarrow \Sigma - \Sigma_c \subseteq \gamma_1 \cup \gamma_2 \Longrightarrow \gamma_1 \cup \gamma_2 \in \Gamma$.

(2) $\Sigma - \Sigma_c \subseteq \gamma_1 \wedge \gamma_2 \subseteq \Sigma_f \Longrightarrow \Sigma - \Sigma_c \subseteq \gamma_1 \cup \gamma_2 \Longrightarrow \gamma_1 \cup \gamma_2 \in \Gamma$.

(3) $\gamma_1 \subseteq \Sigma_f \wedge \Sigma - \Sigma_c \subseteq \gamma_2 \Longrightarrow \Sigma - \Sigma_c \subseteq \gamma_1 \cup \gamma_2 \Longrightarrow \gamma_1 \cup \gamma_2 \in \Gamma$.

(4) $\gamma_1 \subseteq \Sigma_f \wedge \gamma_2 \subseteq \Sigma_f \Longrightarrow \gamma_1 \cup \gamma_2 \subseteq \Sigma_f \Longrightarrow \gamma_1 \cup \gamma_2 \in \Gamma$.

Therefore, Γ is closed under union.

The controller is defined as a mapping from the set of runs *R*(CFSMwV) to the set of control pattern Γ:

$$\psi: R(\text{CFSMwV}) \rightarrow \Gamma \tag{2.21}$$

The behavior of the controlled system, denoted by *R*(CFSMwV, ψ), is given as follows:

(1) $\varepsilon \in R(\text{CFSMwV}, \psi)$, where ε denotes the empty trace (empty run);

(2) Then inductively,

$$\left(\forall r = (q_0, p_0) \xrightarrow{l_1} (q_1, p_1) \cdots \xrightarrow{l_n} (q_n, p_n) \in R(CFSMwV, \psi)\right)(\forall l_{n+1} = g \wedge \sigma)$$

$$r \xrightarrow{l_{n+1}} (q_{n+1}, p_{n+1}) \in R(CFSMwV, \psi)$$

$$\Leftrightarrow r \xrightarrow{l_{n+1}} (q_{n+1}, p_{n+1}) \in R(CFSMwV) \wedge \sigma \in \psi(r)$$

In other words, a transition $(q_n, p_n) \xrightarrow{l_{n+1}} (q_{n+1}, p_{n+1})$ is possible in the closed-loop systems if and only if it is possible in the open-loop system (hence the guard is true) and the event is enabled or enforced. Our goal is to synthesize a controller such that *R*(CFSMwV, ψ) = *E* if

possible. To find a necessary and sufficient condition for the existence of a controller, controllability is generalized as follows.

Definition 1: A set of possible runs $K \subseteq R$(CFSMwV) is *controllable* with respect to R(CFSMwV) and Γ if

$$(\forall r \in \bar{K})(\exists \gamma \in \Gamma)\left(\Sigma_{R(CFSMwV)}(r) - \Sigma_K(r)\right) = \Sigma_{R(CFSMwV)}(r) - \gamma \qquad (2.22)$$

where $\bar{K}$ denotes the prefix-closure of K, $\Sigma_{R(CFSMwV)}(r) = \left\{\sigma \in \Sigma : r \xrightarrow{g \wedge \sigma} (q,p) \in R(CFSMwV)\right\}$, and $\Sigma_K(r) = \left\{\sigma \in \Sigma : r \xrightarrow{g \wedge \sigma} (q,p) \in \bar{K}\right\}$.

The following theorem says that controllability is a necessary and sufficient condition for the existence of a controller.

Theorem 1: Given a system CFSMwV and a specification $K \subseteq R$(CFSMwV), a controller ψ exists such that R(CFSMwV, ψ) = K if and only if K is closed and controllable.

Proof: (ONLY IF) Let ψ be a controller such that R(CFSMwV, ψ) = K. Clearly K is closed. We show that K is controllable as follows:

$$K = R(CFSMwV, \psi)$$

$$\Rightarrow (\forall r \in K)\Sigma_K(r) = \Sigma_{R(CFSMwV,\psi)}(r)$$

$$\Rightarrow (\forall r \in K)\Sigma_K(r) = \Sigma_{R(CFSMwV)}(r) \cap \psi(r)$$

$$\Rightarrow (\forall r \in K)\Sigma_{R(CFSMwV)}(r) - \Sigma_K(r) = \Sigma_{R(CFSMwV)}(r) - \Sigma_{R(CFSMwV)}(r) \cap \psi(r)$$

$$\Rightarrow (\forall r \in K)\Sigma_{R(CFSMwV)}(r) - \Sigma_K(r) = \Sigma_{R(CFSMwV)}(r) - \psi(r)$$

$$\Rightarrow (\forall r \in K)(\exists \gamma = \Psi(r) \in \Gamma)\Sigma_{R(CFSMwV)}(r) - \Sigma_K(r) = \Sigma_{R(CFSMwV)}(r) - \gamma$$

Therefore, K is controllable.

(IF) Since K is closed and controllable,

$$(\forall r \in K)(\exists \gamma \in \Gamma)\sum_{R(CFSMwV)}(r) - \sum_K(r) = \sum_{R(CFSMwV)}(r) - \gamma.$$

Let us define the controller ψ: R(CFSMwV)→Γ as follows: For $r \in K$, let $\psi(r)$ be the largest γ satisfies the above equation. By Proposition 1, the largest γ exists. For $r \in R$(CFSMwV)−K, let $\psi(r)=\Sigma-\Sigma_c$. We can prove $r \in R$(CFSMwV, ψ) $\Leftrightarrow r \in K$ by induction on the length $|r|$ of r as follows:

Base: Since K is closed, $\varepsilon \in K$. By the definition of R(CFSMwV, ψ), $\varepsilon \in R$(CFSMwV, ψ). Therefore,

$$\varepsilon \in R(\text{CFSMwV}, \psi) \Leftrightarrow \varepsilon \in K.$$

Induction Hypothesis (IH): Assume that for all r such that the length $|r| \leq d$, and d is a positive integer.

$$r \in R(\text{CFSMwV}, \psi) \Leftrightarrow r \in K.$$

Induction Step: We need to prove that for all $r \xrightarrow{g\wedge\sigma} (q,p)$ such that $\left|r \xrightarrow{g\wedge\sigma} (q,p)\right| = d+1$,

$$r \xrightarrow{g\wedge\sigma} (q,p) \in R(CFSMwV,\psi) \Leftrightarrow r \xrightarrow{g\wedge\sigma} (q,p) \in K.$$

Indeed,

$$r \xrightarrow{g\wedge\sigma} (q,p) \in R(CFSMwV,\Psi)$$

$$\Leftrightarrow r \xrightarrow{g\wedge\sigma} (q,p) \in R(CFSMwV) \wedge \sigma \in \Psi(r) \wedge r \in R(CFSMwV,\Psi)$$

$$\Leftrightarrow r \xrightarrow{g\wedge\sigma} (q,p) \in R(CFSMwV) \wedge \sigma \in \Psi(r) \wedge r \in K \qquad \text{By IH}$$

$$\Leftrightarrow \sigma \in \sum_{R(CFSMwV)}(r) \wedge \sigma \in \Psi(r) \wedge r \in K$$

$$\Leftrightarrow \sigma \in \sum_{R(CFSMwV)}(r) \wedge \sigma \notin \sum_{R(CFSMwV)}(r) - \Psi(r) \wedge r \in K$$

$$\Leftrightarrow \sigma \in \sum_{R(CFSMwV)}(r) \wedge \sigma \notin \sum_{R(CFSMwV)}(r) - \sum_K(r) \wedge r \in K$$

$$\Leftrightarrow \sigma \in \sum_{R(CFSMwV)}(r) \wedge \sigma \in \sum_K(r) \wedge r \in K$$

$$\Leftrightarrow r \xrightarrow{g\wedge\sigma} (q,p) \in R(CFSMwV) \wedge r \xrightarrow{g\wedge\sigma} (q,p) \in K \wedge r \in K$$

$\Leftrightarrow r \xrightarrow{g\wedge\sigma} (q,p)\in K$

This proves the theorem.

Q.E.D

If the specification E is not controllable, we will find the largest subset of E that is controllable. In fact, we can show that the supremal controllable subset of E always exists. To this end, let us define the set of all controllable subset of E as

$C(E)=\{K \subseteq E$: K is closed and controllable with respect to R(CFSMwV) and $\Gamma\}$ (2.23)

Then we have the following theorem.

Theorem 2: If K_1, $K_2 \in C(E)$, then $K_1 \cup K_2 \in C(E)$. Therefore, the supremal controllable subset of E, denoted by sup$C(E)$, exists.

Proof: Let K_1, $K_2 \in C(E)$ and $K = K_1 \cup K_2$. Obviously K is closed. Since both K_1 and K_2 are controllable, we have

$$(\forall r \in K_1)(\exists \gamma_1 \in \Gamma)\sum_{R(CFSMwV)}(r) - \sum_{K_1}(r) = \sum_{R(CFSMwV)}(r) - \gamma_1,$$

$$(\forall r \in K_2)(\exists \gamma_2 \in \Gamma)\sum_{R(CFSMwV)}(r) - \sum_{K_2}(r) = \sum_{R(CFSMwV)}(r) - \gamma_2.$$

To prove K is controllable, we need to show

$$(\forall r \in K)(\exists \gamma \in \Gamma)\sum_{R(CFSMwV)}(r) - \sum_{K}(r) = \sum_{R(CFSMwV)}(r) - \gamma.$$

Since $K = K_1 \cup K_2$, there are three possible cases.

(1) $r \in K_1$ and $r \in K_2$: In this case, let $\gamma = \gamma_1 \cup \gamma_2$. By Proposition 1, $\gamma_1 \in \Gamma \wedge \gamma_2 \in \Gamma \Longrightarrow$ $\gamma_1 \cup \gamma_2 \in \Gamma$. Also $\sum_K(r) = \sum_{K_1 \cup K_2}(r) = \sum_{K_1}(r) \cup \sum_{K_2}(r)$. Therefore,

$$\Sigma_{R(CFSMwV)}(r) - \Sigma_K(r)$$

$$= \Sigma_{R(CFSMwV)}(r) - \Sigma_{K_1 \cup K_2}(r)$$

$$= \Sigma_{R(CFSMwV)}(r) - \left(\Sigma_{K_1}(r) \cup \Sigma_{K_2}(r)\right)$$

$$= \left(\Sigma_{R(CFSMwV)}(r) - \Sigma_{K_1}(r)\right) \cap \left(\Sigma_{R(CFSMwV)}(r) - \Sigma_{K_2}(r)\right)$$

$$= \left(\Sigma_{R(CFSMwV)}(r) - \gamma_1\right) \cap \left(\Sigma_{R(CFSMwV)}(r) - \gamma_2\right)$$

$$= \Sigma_{R(CFSMwV)}(r) - (\gamma_1 \cup \gamma_2)$$

$$= \Sigma_{R(CFSMwV)}(r) - \gamma$$

(2) $r \in K_1$ and $r \notin K_2$: In this case, let $\gamma = \gamma_1 \in \Gamma$. Then,

$$\Sigma_{R(CFSMwV)}(r) - \Sigma_K(r)$$

$$= \Sigma_{R(CFSMwV)}(r) - \Sigma_{K_1 \cup K_2}(r)$$

$$= \Sigma_{R(CFSMwV)}(r) - \left(\Sigma_{K_1}(r) \cup \Sigma_{K_2}(r)\right)$$

$$= \Sigma_{R(CFSMwV)}(r) - \Sigma_{K_1}(r)$$

$$= \Sigma_{R(CFSMwV)}(r) - \gamma_1$$

$$= \Sigma_{R(CFSMwV)}(r) - \gamma$$

(3) $r \notin K_1$ and $r \in K_2$: In this case, let $\gamma = \gamma_2 \in \Gamma$. Then,

$$\Sigma_{R(CFSMwV)}(r) - \Sigma_K(r)$$

$$= \Sigma_{R(CFSMwV)}(r) - \Sigma_{K_1 \cup K_2}(r)$$

$$= \Sigma_{R(CFSMwV)}(r) - \left(\Sigma_{K_1}(r) \cup \Sigma_{K_2}(r)\right)$$

$$= \Sigma_{R(CFSMwV)}(r) - \Sigma_{K_2}(r)$$

$$= \Sigma_{R(CFSMwV)}(r) - \gamma_2$$

$$= \Sigma_{R(CFSMwV)}(r) - \gamma$$

So, in any case,

$$(\forall r \in K)(\exists \gamma \in \Gamma)\sum_{R(CFSMwV)}(r) - \sum_K(r) = \sum_{R(CFSMwV)}(r) - \gamma.$$

Q.E.D

By this result, we can find the least restrictive safety controller that ensures the closed-loop system will never visit illegal states. Our strategy to synthesize the least restrictive safety controller is as follows: Initially, the system can be in any legal state of the system. However, the system may move to an illegal state via some transitions. So it is important to study transitions on the boundary (from a legal state to an illegal state). If a transition is associated with a controllable event (i.e., transition $(q, g \wedge \sigma / p := f(p), q')$ with $\sigma \in \Sigma_c$) , then the transition can be disabled and we do not need to worry about it. On the other hand, if a transition is associated with an uncontrollable event, then we must prevent it from occurring by either making sure that its guard is not true or pre-empting the transition with an enforceable event if possible. This implies that we must strengthen (or tighten) the conditions under which the system can stay in legal states. We call these conditions safety conditions. We use I_q to denote the safety condition for state q. The key to synthesizing the least restrictive safety controller is to update I_q iteratively so that after the procedure converges, the transitions on the boundary are either disabled or pre-empted. To do this formally, let us denote the number of iterations by k. Initially, we let safety condition $I_q(0)=T$ for all legal states $q \notin Q_b$ and $I_q(0) = F$ for all illegal states $q \in Q_b$. For a legal state $q \notin Q_b$, its safety condition $I_q(k)$ is updated as:

$$I_q(k+1) = I_q(k) \wedge \left(\begin{array}{l} \neg \left(\bigvee_{(q, g \wedge \sigma / p := f(p), q') \in \delta \wedge \sigma \notin \Sigma_c} \left(g \wedge \neg I_{q'}(k)|_{p := f(p)} \right) \right) \\ \vee \left(\bigvee_{(q, g \wedge \sigma / p := f(p), q') \in \delta \wedge \sigma \in \Sigma_f} \left(g \wedge I_{q'}(k)|_{p := f(p)} \right) \right) \end{array} \right) \quad (2.24)$$

This formula implies that the new safety condition will be true only if the old safety condition $I_q(k)$ is true and either there are no uncontrollable transitions leading to illegal states, $\neg\left(\bigvee_{(q,g\wedge\sigma/p:=f(p),q')\in\delta\wedge\sigma\notin\Sigma_c}\left(g\wedge\neg I_{q'}(k)|_{p:=f(p)}\right)\right)$, or there are some enforceable transitions leading to legal states, $\left(\bigvee_{(q,g\wedge\sigma/p:=f(p),q')\in\delta\wedge\sigma\in\Sigma_f}\left(g\wedge I_{q'}(k)|_{p:=f(p)}\right)\right)$.

Since Q is finite by definition, whether the above iteration will converge (terminate) or not depends on the set P. If P is finite, then the iteration is guaranteed to converge. If P is infinite, then the iteration may or may not converge. In the example below, we show that in some cases even if P is infinite, the iteration still converges.

When the iteration converges, we have $I_q(k+1) = I_q(k)$. Denote $I^*_q = I_q(k+1) = I_q(k)$. We can obtain the controller ψ:R(CFSMwV)→Γ as follows: Let $r \in R$(CFSMwV) be a run ending at (q, p). Then

$$\psi(r)=\begin{cases}\{\sigma\in\Sigma:(q,g\wedge\sigma/\,p:=f(p),q')\in\delta\wedge\neg(g\wedge\neg I^*_{q'}|_{p:=f(p)})\}\cup(\Sigma-\Sigma_c) \\ \qquad\qquad \text{if } \neg\left(\bigvee_{(q,g\wedge\sigma/p:=f(p),q')\in\delta\wedge\sigma\notin\Sigma_c}(g\wedge\neg I^*_{q'}|_{p:=f(p)})\right) \\ \{\sigma\in\Sigma_f:(q,g\wedge\sigma/\,p:=f(p),q')\in\delta\wedge(g\wedge I^*_{q'}|_{p:=f(p)})\} \\ \qquad\qquad \text{otherwise.}\end{cases} \tag{2.25}$$

Clearly $\psi(r) \in \Gamma$ and under this control, the closed-loop system will satisfies safety condition I^*_q for all legal state $q\notin Q_b$. We show that ψ: R(CFSMwV)→Γ is indeed the controller we want.

Theorem 3: After the iteration converges, the controller ψ: R(CFSMwV)→Γ designed above generates the supremal controllable subset sup$C(E)$. In other words,

$$R(\text{CFSMwV}, \psi) = \sup C(E) \tag{2.26}$$

Proof: We need to prove (1) R(CFSMwV, ψ) is controllable; (2) R(CFSMwV, ψ) $\subseteq E$; and (3) for all other subset $K \subseteq R$(CFSMwV) such that K is controllable and $K \subseteq E$, $K \subseteq L$(CFSMwV, γ).

(1) R(CFSMwV, ψ) is controllable:

R(CFSMwV, ψ) is generated by a controller. By Theorem 1, it is controllable.

(2) R(CFSMwV, ψ) $\subseteq E$:

During the iteration, all safety conditions are strengthened, that is, $I_q^* \Longrightarrow I_q$ for all legal state $q \notin Q_b$. Therefore, R(CFSMwV, ψ) $\subseteq E$.

(3) For all other subset $K \subseteq R$(CFSMwV) such that K is controllable and $K \subseteq E$, $K \subseteq L$(CFSMwV,γ):

During the iteration, a safety condition is strengthened only if not doing so will result in violation of specification E. Hence, no other controller can generate a larger subset than L(CFSMwV,γ) without violating E. Since K is controllable, by Theorem 1, it can be generated by a controller. Therefore, K is controllable and $K \subseteq E$ imply $K \subseteq L$(CFSMwV,γ).

Q.E.D

Note that we assume that in the controlled system, the transitions enforced by the controller will occur before the occurrence of any uncontrollable transition. This assumption is reasonable because we do not consider time in the FSMwV model. If time is of importance, then we shall use hybrid machine model of [146] rather than FSMwV model. Let us now illustrate the above results by an example.

Example 1: Consider the system described by the CFSMwV in Figure 2.6. The CFSMwV has three events α, β, η and one variable $p \in P$, where P is the set of natural numbers. The illegal

state is $Q_b = \{6\}$ (shaded in the figures). The controllable events are $\Sigma_c = \{\beta, \eta\}$. The enforceable event is $\Sigma_f = \{\eta\}$. Our goal is to synthesize a safety controller to ensure that the system will never enter the illegal state.

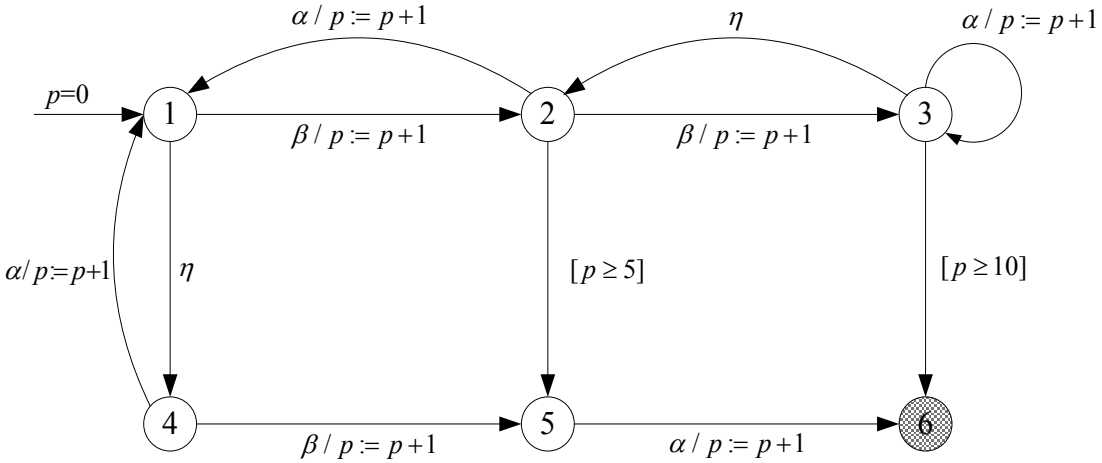

Figure 2.6 CFSMwV for Example 1.

The results of the iteration process to calculate I_q at different states is given in TABLE 2.1 and shown in Figure 2.7.

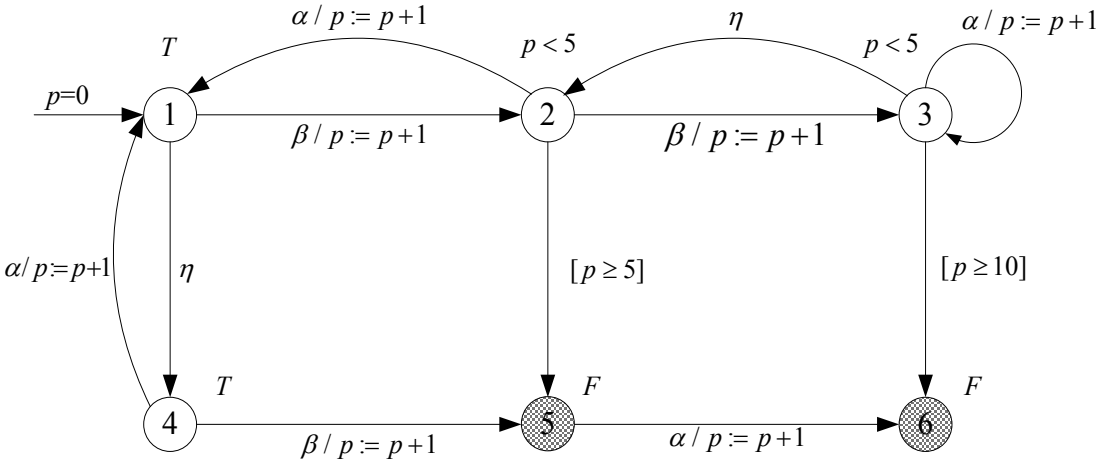

Figure 2.7 Resulting CFSMwV after the iteration converges.

The control is given as: at state 1 and 2, the controller will disable β if $p \geq 4$; at state 3, the controller will enforce η if $p \geq 4$; and at state 4, the controller always disables β.

Note that the controlled system can loop between states 1 and 4 infinitely many times. Hence, the value of p can increase unboundedly. This example shows that even if P is infinite (the set of natural numbers), the iteration still converges.

TABLE 2.1 CALCULATION OF I_Q AT SIX STATES

State k	1	2	3	4	5	6
0	T	T	T	T	T	F
1	T	T	T	T	$T \wedge \{\neg(T \wedge \neg F)\} = F$	F
2	T	$T \wedge \{\neg[(T \wedge \neg T) \vee (p \geq 5 \wedge \neg F)]\} = p<5$	$T \wedge \{\neg[(T \wedge \neg T) \vee (p \geq 10 \wedge \neg F)] \vee (T \wedge T]\} = T$	T	F	F
3	T	$p<5 \wedge \{\neg[(T \wedge \neg T) \vee (p \geq 5 \wedge \neg F)]\} = p<5$ **I_2*= I_2(2) = I_2(3), stop!**	$T \wedge \{\neg[(T \wedge \neg T) \vee (p \geq 10 \wedge \neg F)] \vee (T \wedge p<5)\} = p<10$	T	F	F
…	…	…	…	…	…	…
8	T	$p < 5$	$p<5$	T	F	F
9	T	$p < 5$	$p<5$ **I_3*= I_3(9)= I_3 (8), stop!**	T	F	F

2.5 Online Safety Controller

As it has been demonstrated in standard supervisory control theory, online synthesis of safety controllers has advantages in various applications. If the system to be controlled is large and complex, then offline control synthesis may not be feasible, because it tries to compute the control actions for all possible states and values of variables. Therefore, for large and complex systems, online synthesis is a good alternative because online synthesis only tries to compute the control action for the current state and the current values of variables. Furthermore, online synthesis can be used even if the system to be controlled is time-varying, while offline synthesis cannot be used

for time-varying systems. In this section, we will discuss online synthesis of safety controllers using FSMwV model.

To design a safety controller online, we can use either limited lookahead policies or variable lookahead policies [139, 140]. In both cases, a forward looking tree representing all possible future behaviour from the current state is constructed. Since the variable values at the current state are known (under our assumption of full observation), all guards can be evaluated. If a guard is true, the transition will be included in the tree; otherwise, the transition (and its continuation) will be discarded in the tree.

After the tree is constructed, the online control synthesis is similar to that of offline. It is actually simpler because of the following two reasons: (1) there are no loops in the tree structure; and (2) guards of all transitions have been evaluated as either true or false. Transitions with false guards are discarded. As before, dynamic transitions with true guards can be treated as same as uncontrollable event transitions by introducing a fictitious new uncontrollable event σ_u.

Since the offline synthesis algorithm has been discussed in the previous section, the key to controller synthesis is to construct the forward looking tree. This is the focus of this section.

During the tree construction, after evaluating guards, transitions of various types are replaced as follows:

(1) $q \xrightarrow{T\wedge\sigma} q'$ replace by $q \xrightarrow{\sigma} q'$

(2) $q \xrightarrow{F\wedge\sigma} q'$ discarded

(3) $q \xrightarrow{T} q'$ replace by $q \xrightarrow{\sigma_u} q'$

(4) $q \xrightarrow{F} q'$ discarded

For limited lookahead policies, the tree construction ends after *N* steps. The legality of the states at the boundary is determined by the attitude used. If the conservative attitude is used, then

all the states at the boundary are considered illegal. This guarantees that the resulting control policy is safe. However, conservative attitude may result in a smaller (that is, more restrictive) control policy or even an empty control policy, which means that the controller will have an error. On the other hand, if the optimistic attitude is used, then all the states at the boundary, except those belonging to Q_b, are considered legal. This attitude will result in a more flexible control policy. However, it may also lead to an unrecoverable error, as it may be too late for an optimistic controller to prevent some illegal behavior when it sees illegal states.

For variable lookahead policies, the tree construction will continue until some termination conditions are satisfied. We use the following three termination conditions:

(1) A branch terminates at state q if q is an illegal state;

(2) A branch terminates at state q if there is no forcible transition leaving q to a legal state but there is an uncontrollable transition leaving q to an illegal state. In this case, state q is illegal;

(3) A branch terminates at state q if all the transitions leaving q are controllable. In this case, state q is legal regardless of the legality of the following states.

If the tree construction for variable lookahead policies terminates, that is, if every branch ends with one of the three termination conditions satisfied, then the variable lookahead policy obtained is guaranteed to be safe and least restrictive. In other words, it will achieve the same performance as the controller synthesized offline.

Unlike limited lookahead policies, the tree construction for variable lookahead policies may not terminate. In such cases, we can combine limited lookahead policies with variable lookahead policies. In other words, we construct the tree as in variable lookahead policies until it

reaches the *N*-step boundary. We then use either conservative or optimistic attitude for the boundary state as in limited lookahead policies.

Example 2: Let us now demonstrate the online synthesis of the safety controller for the same system as in Example 1. We consider the initial state with *p=0*. The tree with *N=3* is constructed as shown in Figure 2.8. The shaded state is illegal.

If the conservative attitude is used, then all states at the bottom layer are considered illegal. By applying the synthesis algorithm, the illegal states are "propagated" upward as shown in Figure 2.9. The control action at the root (i.e. at the initial state) is to enable β, η and enforce nothing.

If the optimistic attitude is used, then all states at the bottom layer, except the left most one, are considered legal. The synthesis algorithm finds bad states as shown in Figure 2.10. The resulting control action at the initial state is the same as for the conservative attitude.

If variable lookahead policy is used, then some branches will terminate early as shown in Figure 2.11. This control synthesis results in the same control action at the initial state.

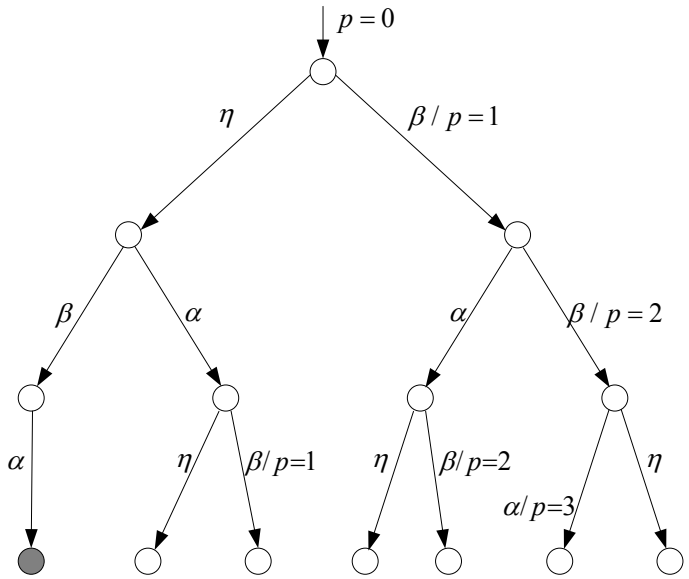

Figure 2.8 Online expansion of the CFSMwV in Figure 2.6, where $N = 3$.

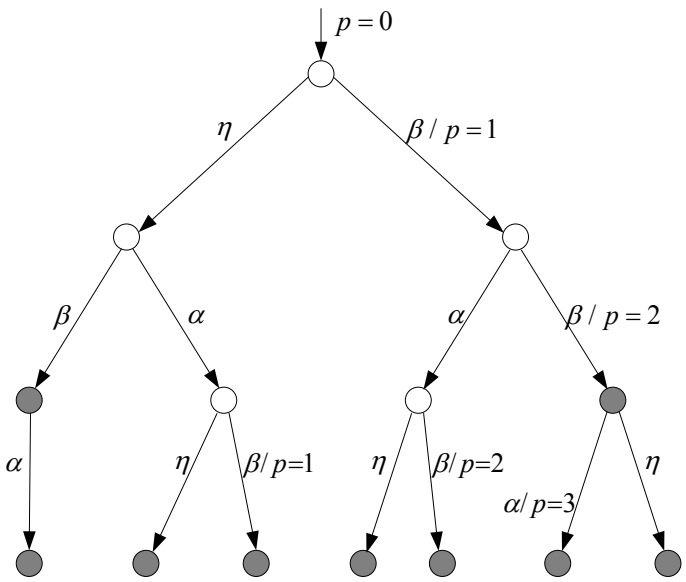

Figure 2.9 Online control synthesis in Example 2: with conservative attitude.

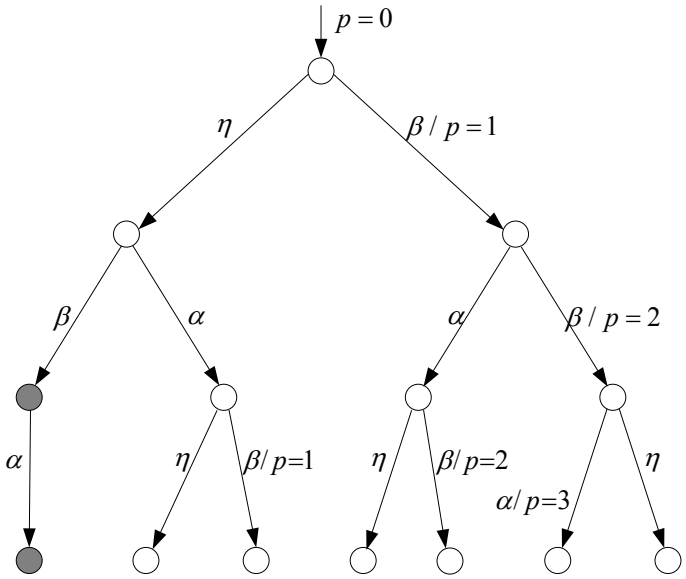

Figure 2.10 Online control synthesis in Example 2: with optimistic attitude.

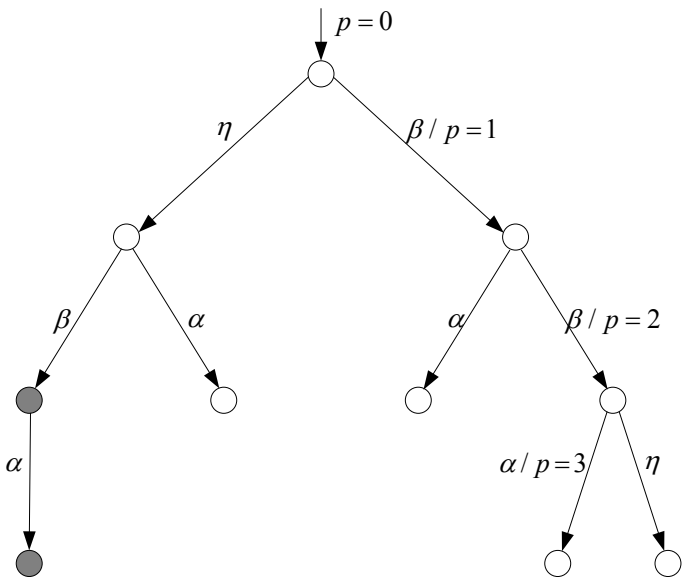

Figure 2.11 Online control synthesis in Example 2: with variable lookahead.

2.6 Applications to the Active Management of PEVs

In this section, we apply the results obtained in the previous section to power grids that needs to accommodate more and more use of PEVs. This is because transportation electrification is viewed as one of the most viable ways to reduce CO_2 emissions and the gasoline dependency. It is projected that the cumulative sales of electrical vehicles (EVs) and PEVs will reach 16 million by 2030 [51]. The increasing number of PEVs will post new challenges to the existing power grid, as they will become a large load to the grid [148, 149]. In the rest of the chapter, we will use FSMwV to model a small distribution network and use supervisory control to control the charging of PEVs.

2.6.1 Distribution networks

A distribution network connects the output terminals of a distribution substation to the input terminals of customer loads. Let us consider a typical distribution network shown in Figure 2.12. We assume that there are N nodes (or buses) in the distribution network. We consider radial distribution networks in this chapter. Interconnected distributed networks can also be considered,

but not discussed in this chapter. For each node i, all the conventional local loads are lumped together and denoted as $p_{i,i}$. For instance, all the local load at *Node 2* is denoted as $p_{2,2}$. All the power lines including transformers connected to *Node i* should not be overloaded. For example, for the local loads connected to *Node 2*, $p_{1,2}$, $p_{2,3}$ and $p_{2,2}$all should be within their corresponding limits $p_{1,2,m}$, $p_{2,3,m}$ and $p_{2,2,m}$. We call $p_{1,2}$ the incoming power to *Node 2*, at the same time, $p_{2,3}$ and $p_{2,4}$ are called the outgoing powers. At each node, there is a power meter to measure the power of each line connected to the node.

The power loss of the distribution network is neglected. We assume that if the power of a power line is 10% over its limit, the circuit breaker (CB) will trip to protect the line and other devices. This constraint can be readily changed to any actual protection setting in a distribution network. For the purpose of simplification, only PEVs are considered as controllable loads. The control target is to avoid the over loading type of tripping while satisfying all the load demands as much as possible. Therefore the only safety criterion considered now is the power limit of each node in the distribution network. Since the incoming powers and the outgoing powers are the summation of the local loads, the illegal condition can also be considered as the overload of every local load power line.

A PEV load is assume to be $n_i \times m$, where n_i is the number of PEVs being charged at the node i and m is the power consumed by each PEV at the unit of kilowatts (kW). Three scenarios were proposed in [150] to charge the PEVs and one of them, $m=6kW$, is used in this chapter. All local loads are calculated as conventional loads plus the PEV load, that is, $p_{i,i} + 6n_i$. For instance, the local loads at *Node 2* is $p_{2,2} + 6n_2$. The control must ensure that all local loads connected to all nodes do not exceed their limits. For example, for the local loads connected to *Node 2*, $p_{2,2} + 6n_2$ must be within its corresponding limit $p_{2,2,m}$.

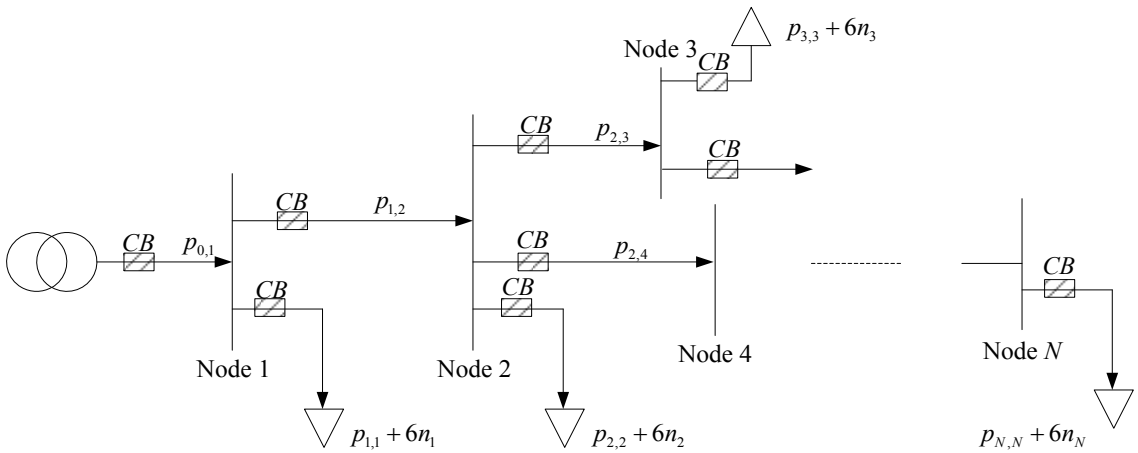

Figure 2.12 A distribution network with N nodes.

2.6.2 Offline safety control of DN

In this section, four scenarios will be analyzed for the distribution network with and without PEVs. Only conventional uncontrollable loads are considered in scenarios 1 and 2. On the other hand, the management of new PEV loads is considered and compared in scenarios 3 and 4. The method described in Section II is used to calculate safety conditions I_q iteratively. $p_{i,i,m}$ is set as 100 *kW*. In scenarios 1 and 2, no PEVs loads are considered in the distribution network, so that we could see the influence of the conventional load to the distribution network. The model is shown in Figure 2.13.

The states set $Q_{i,i}$ contains three states representing load level: the marked state N is for $0 \le p_{i,i} < p_{i,i,m}$; O is for $p_{i,i,m} \le p_{i,i} < 1.1 p_{i,i,m}$; D denotes for the dangerous state and at D the circuit breaker will be tripped to protect the power line thereby moving the system to the illegal state J.

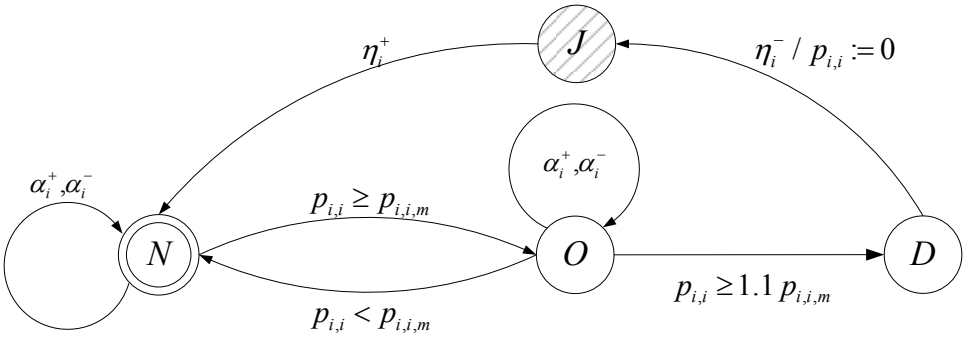

Figure 2.13 Local load FSMwV model at node i for Scenarios 1 and 2.

Three dynamic transitions are defined correspondingly as: $N \rightarrow O$ when $p_{i,i} \geq p_{i,i,m}$; $O \rightarrow N$ when $p_{i,i} < p_{i,i,m}$; $O \rightarrow D$ when $p_{i,i} \geq 1.1 p_{i,i,m}$.

Four events in $\Sigma_{i,i}$ are defined as follows: α_i^+ is for "increase the conventional load"; α_i^- is for "decrease the conventional load"; the uncontrollable event η_i^- is for "trip the circuit switch" and η_i^+ is for "restore the power line". One variables, the conventional loads $p_{i,i}$ will be updated with the occurrence of corresponding events as: α_i^+ with $p_{i,i} := p_{i,i} + 1kW$; α_i^- with $p_{i,i} := p_{i,i} - 1kW$; η_i^- with $n_i := 0$ and $p_{i,i} := 0$.

A. Scenario 1

In this scenario, only the uncontrollable conventional loads are considered. In other words, it is assumed the increase of the conventional loads is uncontrollable and unenforceable, so that we could track the change of the loads by the FSMwV model. The results of the iteration process to calculate I_q at different states is given in TABLE 2.2.

From TABLE 2.2, it is shown that all the states status will be updated as illegal since the unlimited increase of the conventional loads. This table gives us the intuitively image of the change of the states status and the update process of the safety area I_q, even though the unlimited increase of the conventional loads is not practical.

TABLE 2.2 CALCULATION OF I_q AT FOUR STATES FOR SCENARIO 1

State / k	N	O	D	J
0	T	T	T	F
1	T	T	T∧ {¬(T∧¬F)}= F	F
2	T	T∧{¬[(T∧¬T)∨(T∧¬T)∨ (p<100∧¬T)∨ (p≥110∧¬F)]} = p<110	F	F
3	T∧ {¬[(T∧¬T)∨ (T∧¬T)∨ (p≥100∧¬(p<110))]} = p<110	p<110∧ {¬[(T∧¬(p+1<110))∨ (T∧¬(p-1<110))∨ (p<100∧¬T)∨ (p≥110∧¬F)]} = p<109	F	F
4	p < 109	p<108	F	F
…	…	…	…	…
112	p < 1 ***F***	p<0 ***F***	***F***	***F***

B. Scenario 2

In this scenario, it is assumed that the actual load $p_{i,i}$ will not exceed the 0.9 $p_{i,i,m}$=90 kW. This assumption is not unrealistic because we usually have some estimate of the maximum possible load. It means that the guard $p_{i,i} \leq 90$ kW is added to the event α_i^+. Then the results of the iteration process to calculate I_q at different states is given in TABLE 2.3.

TABLE 2.3 CALCULATION OF I_q AT FOUR STATES FOR SCENARIO 2

State / k	N	O	D	J
0	T	T	T	F
1	T	T	T∧	F

			{¬(T∧¬F)} = F	
2	T	T∧{¬[(*p*≤90∧¬T)∨ (T∧¬T)∨ (*p*<100∧¬T)∨ (*p*≥110∧¬F)]} = *p*<110	F	F
3	T∧ {¬[(*p*≤90∧¬T)∨(T∧¬T)∨ (*p*≥100∧¬(*p*<110))]} = *p*<110	*p*<110∧{¬[(*p*≤90∧ ¬(*p*+1<110))∨ (T∧¬(*p*-1<110))∨ (*p*<100∧¬T)∨ (*p*≥110∧¬F)]} = *p*<110 **I_O*= I_O(3)= I_O (2), stop!**	F	F
4	*p* <110 **I_N*= I_N(4)= I_N (3), stop!**		***F***	***F***

It is clear from TABLE 2.3 that the safety area of state *O* and state *N* both converge to 110. It means that the state *O* and state *N* will stay safe because of the existence of the guard of event α_i^+. Intuitively, the conventional uncontrollable load will not increase once $p \le 110kW$.

The PEVs loads are considered in the distribution network in scenarios 3 and 4. The model of the local load $FSMwV_{i,i}$ is shown in Figure 2.14.

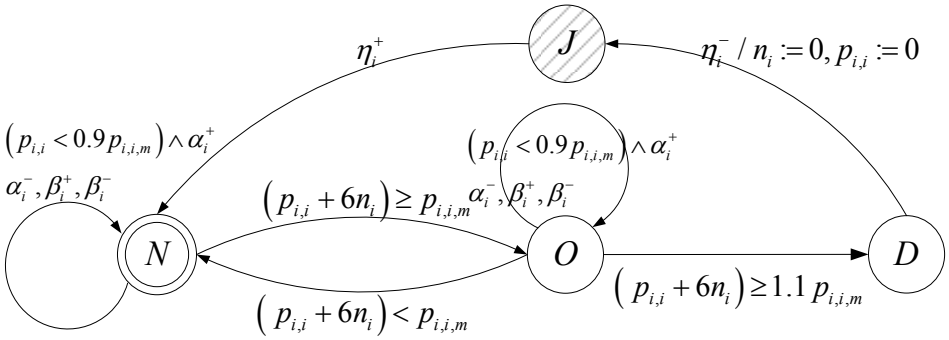

Figure 2.14 Local load FSMwV model at node *i* for Scenarios 3 and 4.

The states set $Q_{i,i}$ contains three states representing load level: the marked state *N* is for $0 \le (p_{i,i}+6n_i) < p_{i,i,m}$; *O* is for $p_{i,i,m} \le (p_{i,i}+6n_i) < 1.1p_{i,i,m}$; *D* denotes for the dangerous state and at

D the circuit breaker will be tripped to protect the power line thereby moving the system to the illegal state J.

Three dynamic transitions are defined correspondingly as: $N \rightarrow O$ when $(p_{i,i}+6n_i) \geq p_{i,i,m}$; $O \rightarrow N$ when $(p_{i,i}+6n_i) < p_{i,i,m}$; $O \rightarrow D$ when $(p_{i,i}+6n_i) \geq 1.1p_{i,i,m}$.

Six events in $\Sigma_{i,i}$ are defined as follows: α_i^+ is for "increase the conventional load"; α_i^- is for "decrease the conventional load"; β_i^+ is for "add one PEV"; β_i^- is for "remove one PEV"; η_i^- is for "trip the circuit switch" and η_i^+ is for "restore the power line". Two variables, the conventional loads $p_{i,i}$ and number of PEVs being charged n_i, will be updated with the occurrence of corresponding events as: α_i^+ with $p_{i,i} := p_{i,i}+1kW$; α_i^- with $p_{i,i} := p_{i,i}-1kW$; β_i^+ with $n_i := n_i+1$; β_i^- with $n_i := n_i-1$; η_i^- with $n_i := 0$ and $p_{i,i} := 0$. We assume that charging PEV can be controlled (disabled). Therefore, the controllable event set is $\Sigma_c = \{\beta_i^+\}$. We assume that the event in $\Sigma_f = \{\eta_i^+\}$ is enforceable.

As for the event β_i^-, we will consider two scenarios, one is uncontrollable and unenforceable (cannot unplug a PEV) and the other is enforceable (can unplug a PEV). We will discuss these two scenarios separately and compare their effects in the control.

Two assumptions for the FSMwV model of local loads are made as follows: (1) The occurrence of α_i^+ has a guard $p_{i,i} < p_{i,i,m}$ since the conventional local loads normally cannot exceed the limit; and (2) Initial limitation of the state O is set as: $(p_{i,i}+6n_i) < 1.1p_{i,i,m}$.

C. Scenario 3

When the event β_i^- is considered as uncontrollable and unenforceable, the safety regions representing safety conditions I_q of states N and O are shown in Figure 2.15 after 89 iterations. We do not show safety conditions I_T and I_D, because they are simple: I_T is always "False" and I_D is "False" after the first iteration since the transition from state D to state T is uncontrollable.

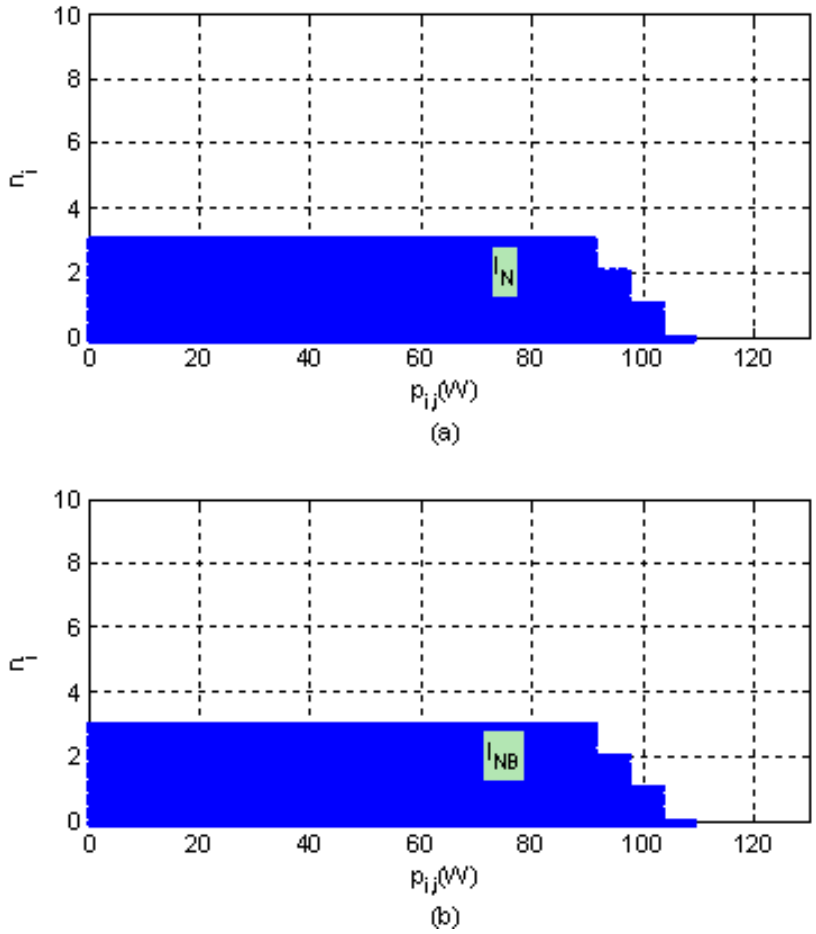

Figure 2.15 Safety regions when β_i^- is uncontrollable for (a) State *N*, (b) State *O*.

From Figure 2.15, we can see that the safety regions of states *N* and *O* are both very small. Intuitively, this is because if the controller cannot unplug PEVs, then it must be very conservative when it allows PEVs to charge. The maximal number PEVs can be charged is only 1. This is the case even if the conventional loads are very low. This means the capacity of the distribution network (and the generation capacity) is not fully utilized. This control is not suitable for the increasing use of PEVs.

D. Scenario 4

When the event β_i^- is considered as enforceable, the safety regions representing safety conditions I_q of states *N* and *O* are shown in Figure 2.16 after 32 iterations. The I_D is also "False" after the first iteration.

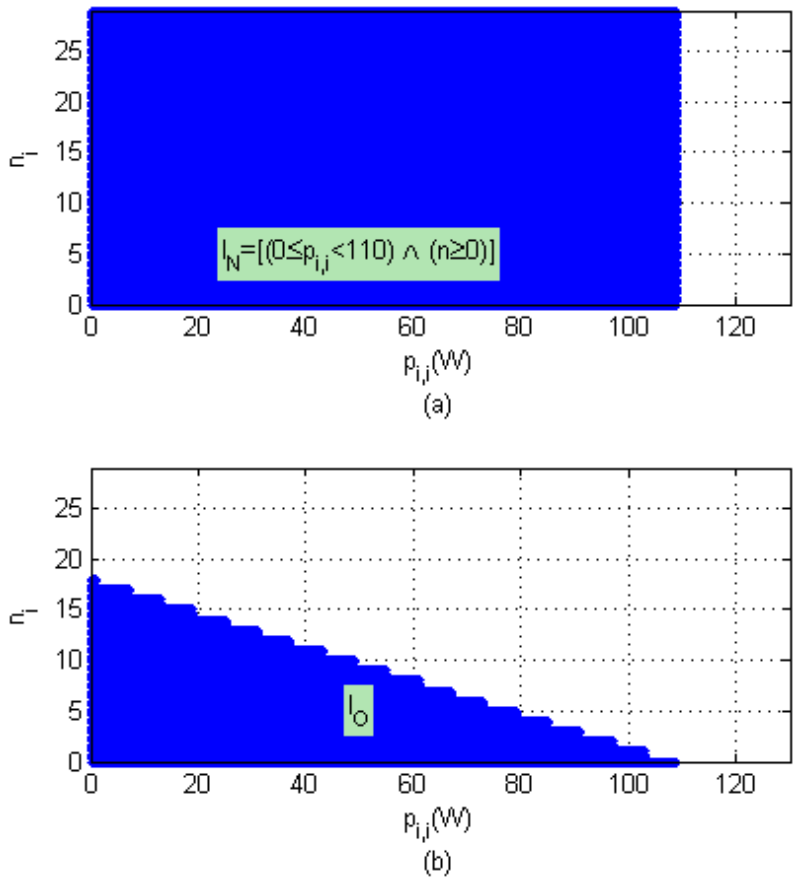

Figure 2.16 Safety regions when β_i^- is enforceable for (a) State *N*, (b) State *O*.

Figure 2.16 shows that the safety regions of states *N* and *O* are much bigger than Scenario 3. This is because if PEVs can be unplugged by the controller, then the control of charging of PEVs becomes more flexible. The control strategy is based on two premises: to guarantee the safety of the system (to avoid entering the illegal states) and to give preference to uncontrollable conventional loads. This control not only ensures the safety of the distribution network, but also takes full advantage of its capacity. It allows as many PEV to be charged as possible.

2.6.3 Offline safety control of DN with energy storage

Sometimes energy storage sources are used as backup to handle emergent situations, and the offline safety control of DNs with energy storage is also studied. The model of the local load FSMwV$_{i,i}$ is shown in Figure 2.17. Some states and events are of the same meaning in 2.6.2 and

are repeated here for convenience. The states set $Q_{i,i}$ contains six states representing load level: the marked state *N* is for $0 \leq (p_{i,i} + 6n_i) < p_{i,i,m}$; *O* is for $p_{i,i,m} \leq (p_{i,i} + 6n_i) < 1.1p_{i,i,m}$; *NB* is used to denote the state that the backup energy storage is used and $p_{i,i,m} \leq (p_{i,i} + 6n_i) < (p_{i,i,m} + p_b)$, where p_b denotes the capacity of the backup power source; *OB* is for $(p_{i,i,m} + p_b) \leq (p_{i,i} + 6n_i) < 1.1(p_{i,i,m} + p_b)$; *D* denotes for the dangerous state and at *D* the circuit breaker will be tripped to protect the power line thereby moving the system to the illegal state *T*. Six dynamic transitions are defined correspondingly as: $N \longrightarrow O$ when $(p_{i,i} + 6n_i) \geq p_{i,i,m}$; $O \longrightarrow N$ when $(p_{i,i} + 6n_i) < p_{i,i,m}$; $NB \longrightarrow OB$ when $(p_{i,i} + 6n_i) \geq (p_{i,i,m} + p_b)$; $OB \longrightarrow NB$ when $(p_{i,i} + 6n_i) < (p_{i,i,m} + p_b)$; $O \longrightarrow D$ when $(p_{i,i} + 6n_i) \geq 1.1p_{i,i,m}$; and $OB \longrightarrow D$ when $(p_{i,i} + 6n_i) > 1.1(p_{i,i,m} + p_b)$.

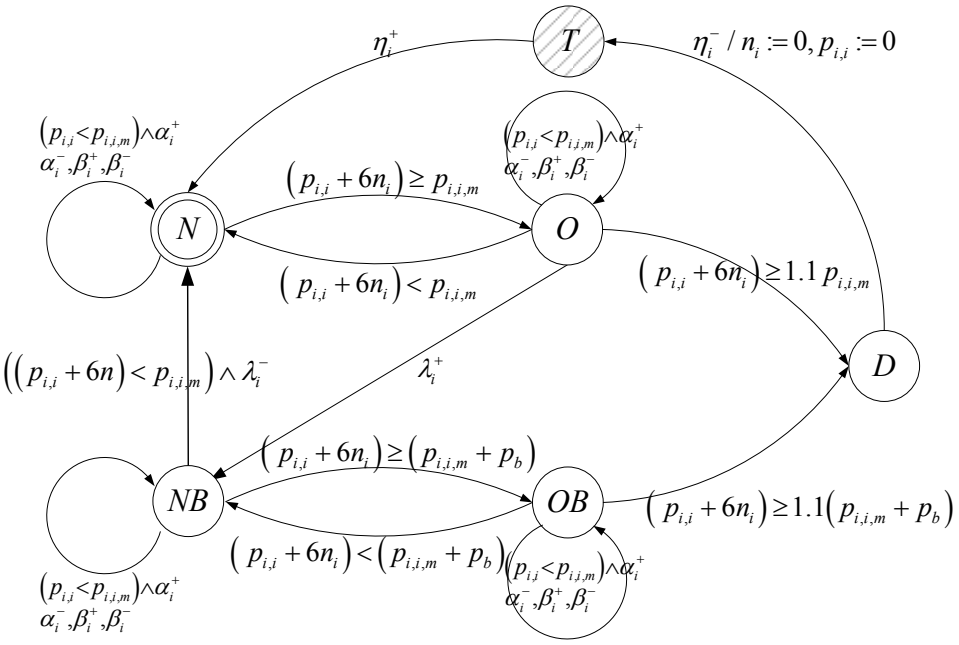

Figure 2.17 FSMwV model for local load at node *i*.

Eight events in $\Sigma_{i,i}$ are defined as follows: α_i^+ is for "increase the conventional load"; α_i^- is for "decrease the conventional load"; β_i^+ is for "add one PEV"; β_i^- is for "remove one PEV";

λ_i^+ is for "add the backup power source"; λ_i^- is for "remove the backup power source"; η_i^- is for "trip the circuit switch" and η_i^+ is for "restore the power line". Two variables, the conventional loads $p_{i,i}$ and number of PEVs being charged n_i, will be updated with the occurrence of corresponding events as: α_i^+ with $p_{i,i} := p_{i,i} + 1kw$; α_i^- with $p_{i,i} := p_{i,i} - 1kw$; β_i^+ with $n_i := n_i + 1$; β_i^- with $n_i := n_i - 1$; η_i^- with $n_i := 0$ and $p_{i,i} := 0$. We assume that charging PEV can be controlled (disabled). Therefore, the controllable event set is $\Sigma_c = \{\beta_i^+\}$. We assume that the events in $\Sigma_f = \{\lambda_i^+, \lambda_i^-, \eta_i^+\}$ are enforceable. As for the event β_i^-, we will consider two scenarios, one is uncontrollable and unenforceable (cannot unplug a PEV) and the other is enforceable (can unplug a PEV). We will discuss these two scenarios separately and compare their effects in the control.

Three assumptions for the FSMwV model of local loads are made as follows: (1) The occurrence of α_i^+ has a guard $p_{i,i} < p_{i,i,m}$; (2) The occurrence of λ_i^- has a guard $(p_{i,i} + 6n_i) < p_{i,i,m}$, because we cannot remove the backup energy storage if the system will be overloaded; and (3) Initial limitation of the state *OB* is set as: $(p_{i,i} + 6n_i) < 1.1(p_{i,i,m} + p_b)$.

We assign the variables as: $p_{i,i,m} = 100\ kW$, $p_b = 30\ kW$. Since the iterations are rather involved and time consuming, we write a computer program to do the calculations.

When the event β_i^- is considered as uncontrollable and unenforceable, the safety regions representing safety conditions I_q of states *N, NB, O* and *OB* are shown in Figure 2.18 after 101 iterations. I_T is always "False" and I_D is "False" after the first iteration since the transition from state D to state T is uncontrollable.

From Figure 2.18, we can see that the safety regions of states *N, NB, O* and *OB* are all very small. Intuitively, this is because if the controller cannot unplug PEVs, then it must be very conservative when it allows PEVs to charge. The maximal number PEVs can be charged is only

7. This is the case even if the conventional loads are very low. This means the capacity of the distribution network (and the generation capacity) is not fully utilized. This control is not suitable for the increasing use of PEVs.

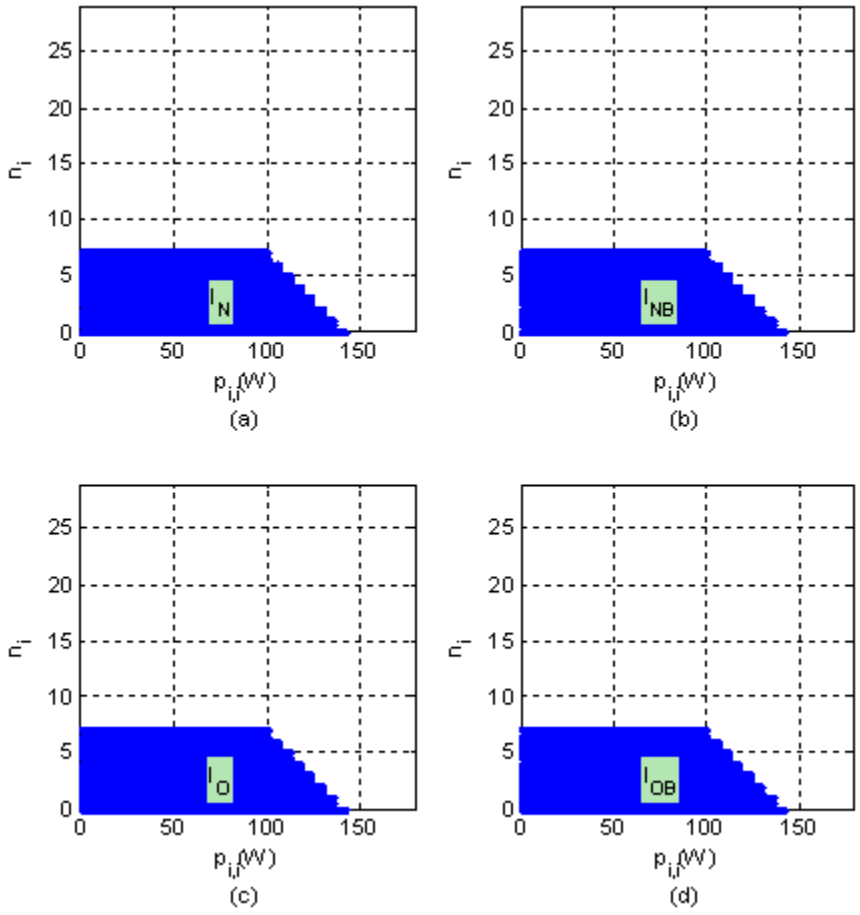

Figure 2.18 Safety regions when β_i^- is uncontrollable (a) State *N*, (b) State *NB*, (c) State *O* and (d) State *OB*.

When the event β_i^- is considered as enforceable, the safety regions representing safety conditions I_q of states *N, NB, O* and *OB* are shown in Figure 2.19 after 33 iterations. The I_D is also "False" after the first iteration.

It is clear from Figure 2.19 that the safety regions of states *N, NB, O* and *OB* are much bigger than the uncontrollable scenario. Same conclusion with the one in Scenario 4 in the Section

2.6.2 can be arrived that this control not only ensures the safety of the distribution network, but also takes full advantage of its capacity.

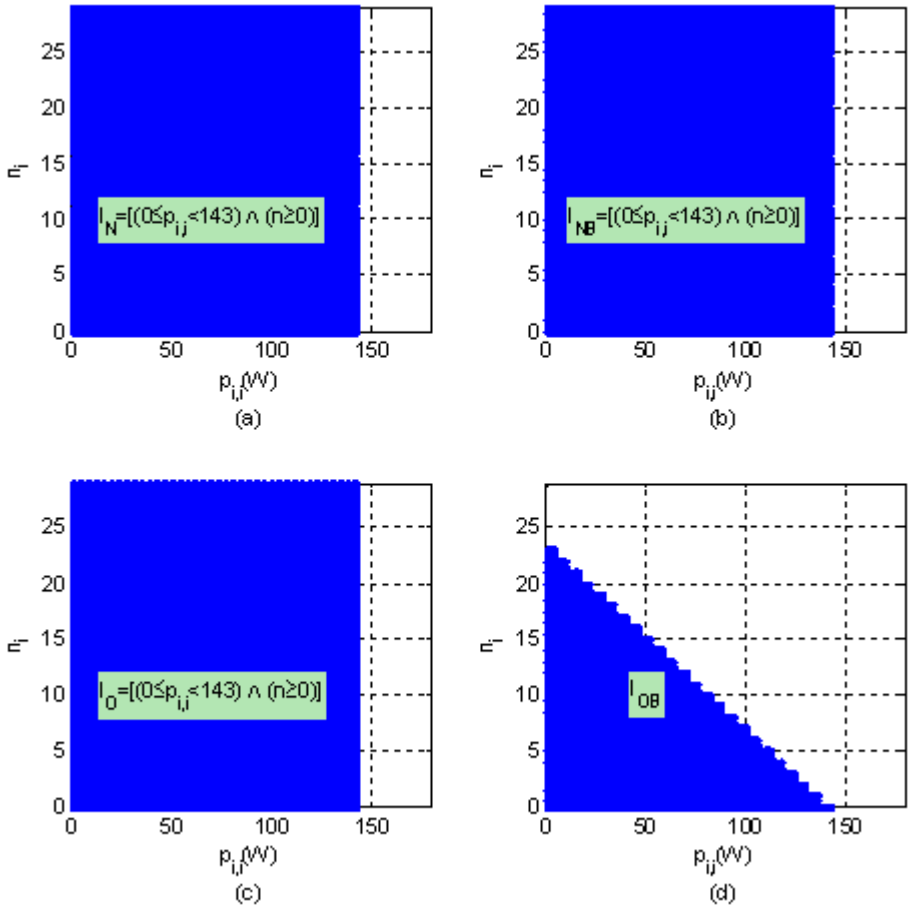

Figure 2.19 Safety area when β_i^- is enforceable event of (a) State *N*, (b) State *NB*, (c) State *O* and (d) State *OB*.

From the step by step analysis in Section 2.6.2 and Section 2.6.3, the change of the power grid is clearly shown and the management of the PEVs at a node could be achieved by the FSMwV and corresponding safety control. Since the model of multi-nodes distribution network could be constructed by the composing operation as CFSMwV, the corresponding safety controller can be designed by the same method.

2.7 Conclusion

In this chapter, we have presented our work on control synthesis under the modeling framework of Finite State Machine with Variables. We have described our extension of the scope of the traditional DES (*i.e.*, supervisory) control to include both event disablement and enforcement for the control of discrete event systems modeled as FSMwV. We have proposed an offline safety control synthesis procedure that takes the advantage of both event disablement and enforcement in order to prevent the controlled system from venturing into illegal states. We have further presented online safety control synthesis procedures based on the limited/variable lookahead policies to address the practical concern of real world implementation. We have also applied the theoretical results to control PEVs in power distribution networks with and without energy storage.

CHAPTER 3 MAXIMIZING THE PENETRATION OF PLUG-IN ELECTRIC VEHICLES IN DISTRIBUTION NETWORK

3.1 Introduction

Transportation electrification is viewed as one of the most viable ways to reduce CO2 emissions and oil dependency. The increasing number of PEVs will post new challenges to the existing power grid, as they as a whole will become a significant portion of the load to the power grid when they are being charged.

Active research work has been carried out in this emerging area [52-54, 151]. The impact of PEVs on Belgium's distribution networks (DNs) was studied with the consideration of the traffic and driving patterns in [52]. The simulation results for different scenarios on a 34-node test feeder showed that a significant amount of power losses and voltage deviations can be induced by wide adoption of PEVs. It concluded that, even in a small country like Belgium, the impacts of PEVs on DNs must be evaluated and controlled to maintain the DN's stability. In [151], PEVs were managed by deterministic and coordinated methods, respectively. The comparison results in the previous paper showed that the uncoordinated charging of PEVs could cause significant losses while coordinated charging had nearly no impact on DNs. From the aspect of available power in a DN, an active management of PEVs was proposed in [53, 54] and in Chapter 2. PEVs and other loads in a DN were modeled by a method of finite state machine with variables (FSMwV), and then a safety controller was proposed to locally manage the dis-/charging of PEVs and other controllable loads on a node. With the coordination of controllers at all nodes, the peak power needed is shifted, and the safety of the feeder transformer is guaranteed.

In addition, voltage problems in DNs are very important since they are directly related to stability, reliability and power quality of the power grid. Poor voltage profile can cause increased

system losses, possible damage to circuit devices and home appliances, and unsatisfactory customers. A number of papers discussed voltage stability indices (VSI) of a power system based on global information, such as the P-V and Q-V curves of the system [152], Jacobian matrix singularity indices [153, 154], and L-index [155]. On the other hand, VSIs can also be calculated by local information of power lines [156, 157] and nodes [158, 159]. However, the indices [152]-[159] that developed for transmission network may not be suitable for distribution network. For example, the method in [155] requires the calculation of bus admittance matrix which sometimes cannot be obtained because of the singularity.

A two-bus equivalent network was developed to analyze the voltage stability of DN in [160]. In this method, the singularity of Jacobian matrix was used to derive the VSI. To predict the voltage collapse triggered by contingencies and events, a new technique was developed to rank all contingencies [161]. This method overcomes the drawback of Jacobian-based methods which may be invalidated by the occurrence of the singularity of the matrix. In [162], the active and reactive powers on buses in DN were calculated without knowing the voltages at sending and receiving ends; and the VSI was formulated based on the proposed equations. Reactive power dispatch [163] and optimal network reconfiguration [164] were both studied to increase the loadability and minimize the losses of DN with the consideration of the safe voltage assessment. A system equivalent model using the concept of transfer impedance was proposed in [165], in which a VSI named equivalent node voltage collapse index (ENVCI) was developed to estimate system voltage stability. This method relieves the required computing burden and is able to real-time follow the variation of loads and generators. The ENVCI will be used in this study as the constraint of voltage stability in the optimization algorithm.

In this chapter, a method is proposed to maximize the injection of PEVs in DNs without violating power limitations and causing voltage problems. Section 3.2 formulates the problem and gives a brief overview of the objective and constraints of the optimization algorithm and the ENVCI. Section 3.3 presents and discusses the simulation results of the proposed method on a 33-bus test feeder. At the end, Section 3.4 concludes this chapter.

3.2 Voltage Stability Index Incorporated Optimization Algorithm

3.2.1 Problem formulation

The large injection of EVs in the distribution network will absorb lots of power from the power grid, cause the voltage decline and power losses, and threaten the safety of power supply to residents. One issue has not drawn much attention is the voltage stability in the DN. The voltage instability is the phenomenon that an uncontrolled voltage decline occurs on one or more buses, and then inducing the voltage collapse of the whole power system [166].

To avoid the voltage instability, the injection of PEVs in the DN should be controlled. It is easy to individually consider the voltage stability at certain buses by calculating the VSI through methods proposed in [160, 165] and then limiting the injection of PEVs to maintain the voltage stability. However, in order to maximize the injection of PEVs, the loads at different buses should be jointly considered since different buses normally have different PEV accommodation capabilities. For example, a bus closer to the feeder transformer is normally able to support a larger number of PEVs. On the other hand, the remote buses can support less because of the voltage drop and the power losses during the long distance delivery of power. Therefore, the problem of maximizing the injection of the PEVs in DNs requires the determination of the best combination of conventional loads and new PEV loads at considered buses so that DN has the best loadability and safe voltage profile. Furthermore, the optimization problem is complex and should consider

the practical limits of the power grid as constraints. The constraints include, but not limited to, the power balance, power supply limits, voltage stability, and thermal line limits. All of the above questions will be discussed and solved in the proposed optimization injection (OI) method.

3.2.2 Objective and constraints

In this study, the objective is to maximize the total injection of PEVs in a DN by minimizing f_{min} as following

$$f_{min} = \frac{1}{N_1+N_2+\cdots+N_M} \tag{3.1}$$

where N_k is the number of PEVs at node k, k=0, 1, 2 ⋯, M.

The optimization problem is subject to the following constraints:

1) Power balance equations: The sum of the real and reactive power from utility grid must be balanced by the local demand, PEVs consumption and the power loss in the lines

$$\begin{gathered} \sum P_{load} + \sum P_{PEVs} + \sum P_{loss} = P_{trans} \\ \sum Q_{load} + \sum Q_{loss} = Q_{trans} \end{gathered} \tag{3.2}$$

where P_{load}, P_{PEVs}, P_{loss}, and P_{trans} are the real power consumed by conventional load, and PEVs, the power loss, and the real power supplied by the feeder transformer, respectively; Q_{load}, Q_{loss}, and Q_{trans} are the reactive power of load and loss, and the reactive power supplied by the feeder transformer. PEVs are assumed to consume only real power, i.e. at unity power factor.

2) Power supply limits: The feeder transformer has its supply limit

$$\begin{gathered} P_{trans} \le P_{trans}^{max} \\ Q_{trans} \le Q_{trans}^{max} \end{gathered} \tag{3.3}$$

where P_{trans}^{max} and Q_{trans}^{max} are the upper limits of active and reactive power can be supplied by the feeder transformer.

3) Voltage stability index limits: The voltage stability index at each node has to be larger than the predefined *ENVCI* limitation:

$$ENVCI_k \geq ENVCI_k^{min} \tag{3.4}$$

where $ENVCI_k$ is the calculated value at node k; $ENVCI_k^{min}$ is the minimum allowed value of voltage stability index at node k. The calculation of ENVCI at each node will be shown in the Appendix A.

4) Voltage security limits: In addition to the voltage stability index limits, the voltage at each node should be within the security range:

$$V_k^{lower} \leq V_k \leq V_k^{upper} \tag{3.5}$$

where $[V_k^{lower}, V_k^{upper}]$ is the voltage security range and is defined as $[0.85\ \text{p.u.}, 1.06\ \text{p.u.}]$ in this study.

5) Thermal line limits: The thermal line limits constrain the apparent power flow along each line:

$$S_{l,t} < S_l^{max}, \forall l, t \tag{3.6}$$

where $S_{l,t}$ denotes the apparent power flow at line l and time t, and S_l^{max} is the apparent power limit for line l.

3.3 Simulation Results and Discussion

The proposed method is validated on the 33-bus test feeder [49] system, which is shown in Figure 3.1. The data of the test feeder is listed in TABLE 3.1. Simulations have been carried out based on Matlab/Optimization Toolbox [167], and MATPOWER [168].

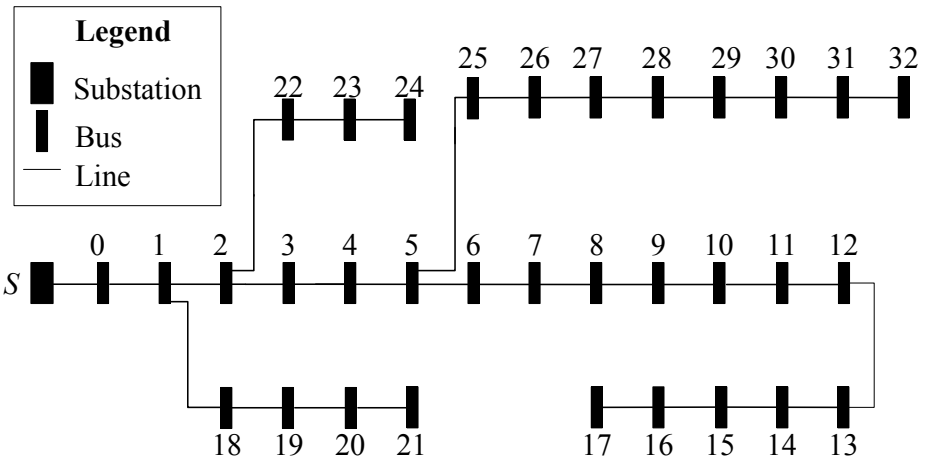

Figure 3.1 33-bus test feeder [49].

Four charging stations are connected to buses 17, 21, 24 and 32 in the 33-bus test system. The four buses are relatively far to the feeder transformer, and therefore are prone to voltage problems. Buses 17 and 32, which are far away from the feeder transformer, are prone to voltage issues caused by the variation of loads. Buses 21 and 24, which are much closer, are also invested for comparison and coordination with buses 17 and 32.

TABLE 3.1 DATA FOR 33-BUS TEST FEEDER

Line number	Sending Bus	Receiving Bus	Resistance (Ω)	Reactance (Ω)	Load at Receiving End Bus	
					Real Power (kW)	Reactive Power (kVAr)
1	0	1	0.0922	0.0477	100.0	60.0
2	1	2	0.4930	0.2511	90.0	40.0
3	2	3	0.3660	0.1864	120.0	80.0
4	3	4	0.3811	0.1941	60.0	30.0
5	4	5	0.8190	0.7070	60.0	20.0
6	5	6	0.1872	0.6188	200.0	100.0
7	6	7	1.7114	1.2531	200.0	100.0
8	7	8	1.0300	0.7400	60.0	20.0
9	8	9	1.0400	0.7400	60.0	20.0
10	9	10	0.1966	0.0650	45.0	30.0
11	10	11	0.3744	0.1238	60.0	35.0
12	11	12	1.4680	1.1550	60.0	35.0
13	12	13	0.5416	0.7129	120.0	80.0
14	13	14	0.5910	0.5260	60.0	10.0
15	14	15	0.7463	0.5450	60.0	20.0
16	15	16	1.2890	1.7210	60.0	20.0

17	16	17	0.7320	0.5740	90.0	40.0
18	1	18	0.1640	0.1565	90.0	40.0
19	18	19	1.5042	1.3554	90.0	40.0
20	19	20	0.4095	0.4787	90.0	40.0
21	20	21	0.7089	0.9373	90.0	40.0
22	2	22	0.4512	0.3083	90.0	50.0
23	22	23	0.8980	0.7091	420.0	200.0
24	23	24	0.8960	0.7011	420.0	200.0
25	5	25	0.2030	0.1034	60.0	25.0
26	25	26	0.2842	0.1447	60.0	25.0
27	26	27	1.0590	0.9337	60.0	20.0
28	27	28	0.8042	0.7006	120.0	70.0
29	28	29	0.5075	0.2585	200.0	600.0
30	29	30	0.9744	0.9630	150.0	70.0
31	30	31	0.3105	0.3619	210.0	100.0
32	31	32	0.3410	0.5302	60.0	40.0

Two scenarios are considered and simulated. In the first scenario, the total PEV loads at the four selected buses are optimized by the proposed OI method without violating the constraints especially the minimum voltage stability index, $ENVCI_k^{min}$. In the second scenario, the PEVs are uniformly incrementally injected at the selected buses, and the total added PEVs are viewed as the maximum injection once the *ENVCI* of any bus reaches $ENVCI_k^{min}$. In addition, five load levels are simulated, *i.e.*, base load, base load × 1.25, base load × 1.50, base load × 1.75, and base load × 2.0, in which the base load represents the active and reactive load at each bus shown in TABLE 3.1. The power to charge a PEV, P_{charge}=20kW is used in this chapter. The $ENVCI_k^{min}$ is set as 0.65.

TABLE 3.2 TOTAL ALLOWED NUMBER OF PEVS AT FIVE LOAD LEVELS

Load level / Total # of PEV	Base load	Base load ×1.25	Base load ×1.50	Base load ×1.75	Base load ×2.0
Optimized Injection	871	832	793	751	667
Uniform Injection	228	188	148	104	60

The total allowed PEVs for two scenarios at five load levels are compared in TABLE 3.2 and Figure 3.2. It is clearly shown that the total number of allowable PEVs drops down as the

increase of the load level for both scenarios. However, the allowable PEVs calculated by the OI method are far more than the number by the uncontrolled uniform injection (UI) method. The reason is that, in the UI method, the bus farthest away from the feeder transformer, which also has the lowest margin of the voltage stability, is easy to be affected by the large injection of PEVs and can only support the smallest number of PEVs. Therefore, the ability of charging PEVs is determined by the shortest board of the cask, which badly limits the loadability of the studied DN. However, the proposed OI method could coordinate charge PEVs according to the ability of different buses, thereby optimizing the total allowed injection of PEVs in the DN without going against the constraints. This statement is once again proved by the comparison of Figure 3.3 and Figure 3.4.

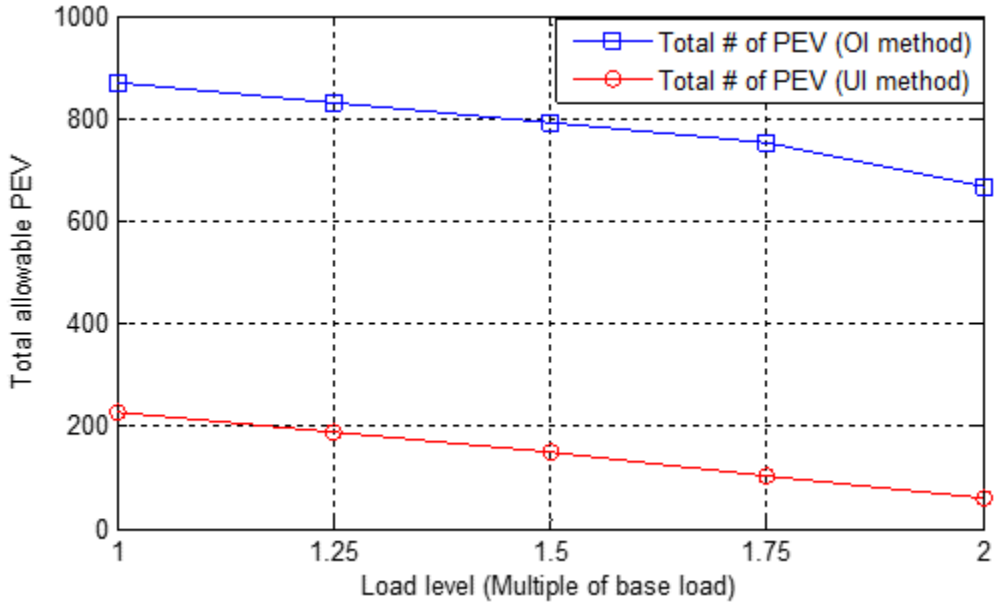

Figure 3.2 Total allowable PEVs for two scenarios at five load levels.

Figure 3.3 shows the voltage value (p.u.) and *ENVCI* at Bus 1-32 under five load levels by the UI method. It illustrates that the voltage and *ENVCI* reach the minimum value only at Bus 17, which is the most remote one from the feeder transformer and is the weakest bus. At the same time,

the *ENVCIs* at Buses 21, 24 and 32 are still far away from the dangerous edge of voltage instability, which means that the power resources in the studied DN are not fully utilized to charge the PEVs.

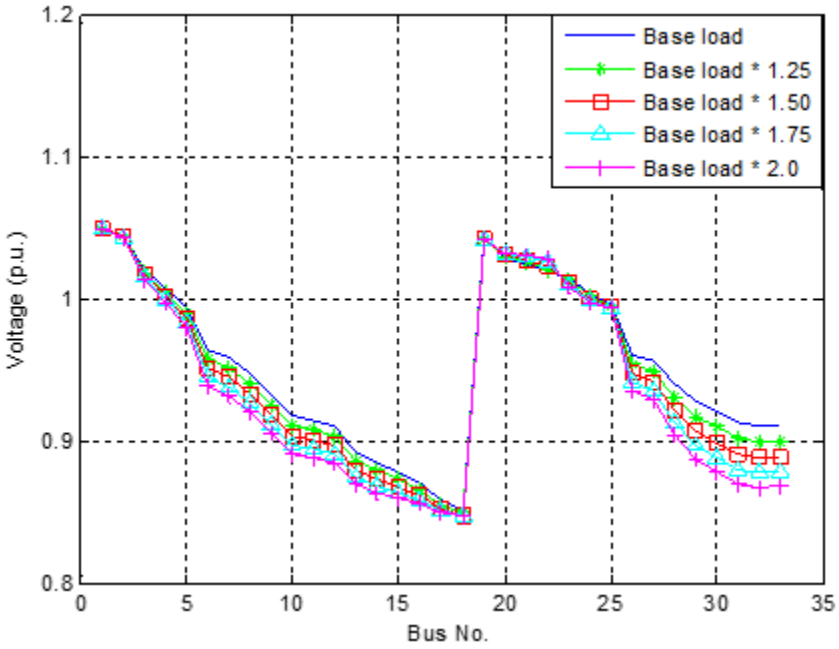

(a)

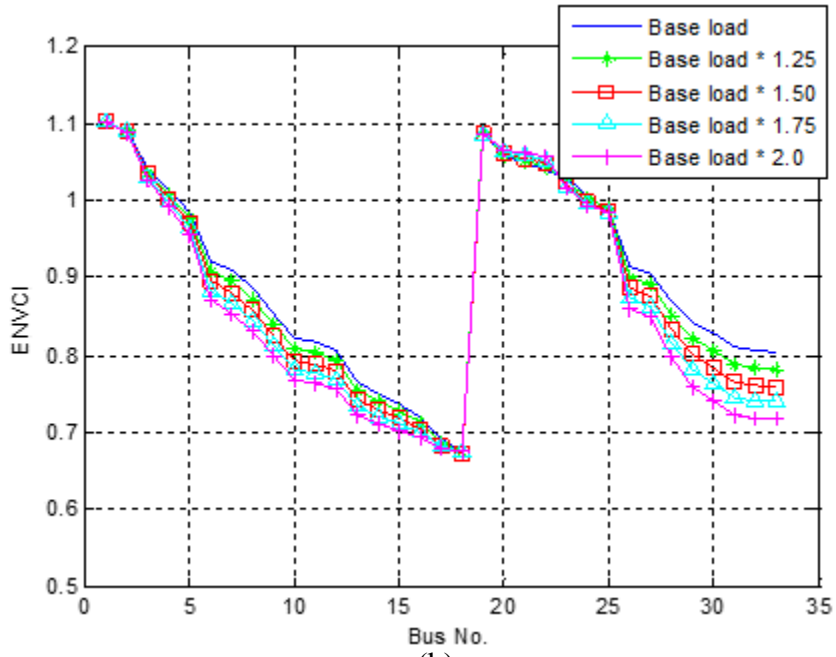

(b)

Figure 3.3 Simulation results by uniform injection method under five load levels, (a) voltage value (p.u.) at Bus 1-33, (b) ENVCI at Bus 1-33.

On the other hand, the voltage value (p.u.) and *ENVCI* at Bus 1-32 under five load levels by the proposed OI method, shown in Figure 3.4, shows the better utilization of DN to maximize the injection of PEVs. Because of the maximal injection of PEVs, the *ENVCIs* at selected buses all close to the $ENVCI_k^{min}$, which also corresponds to the voltage values in Figure 3.4(a).

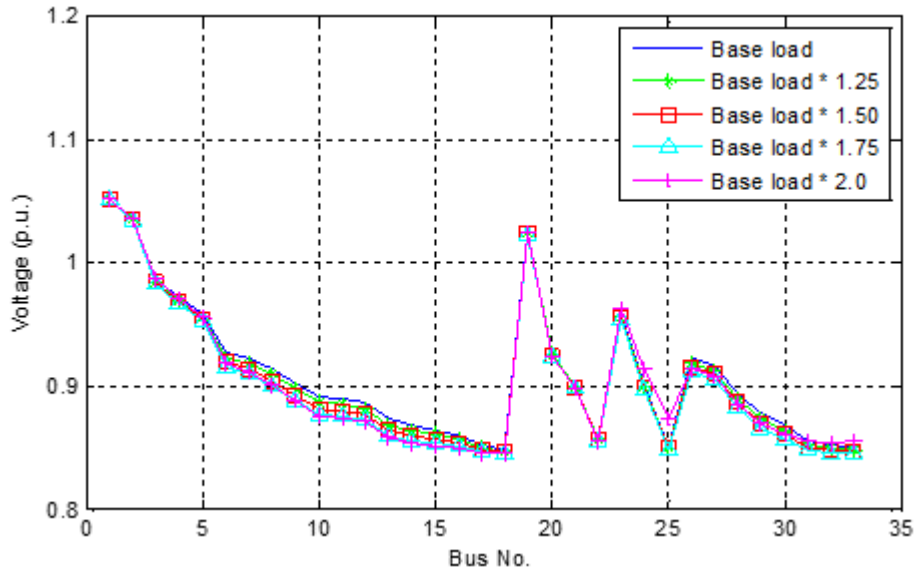

(a)

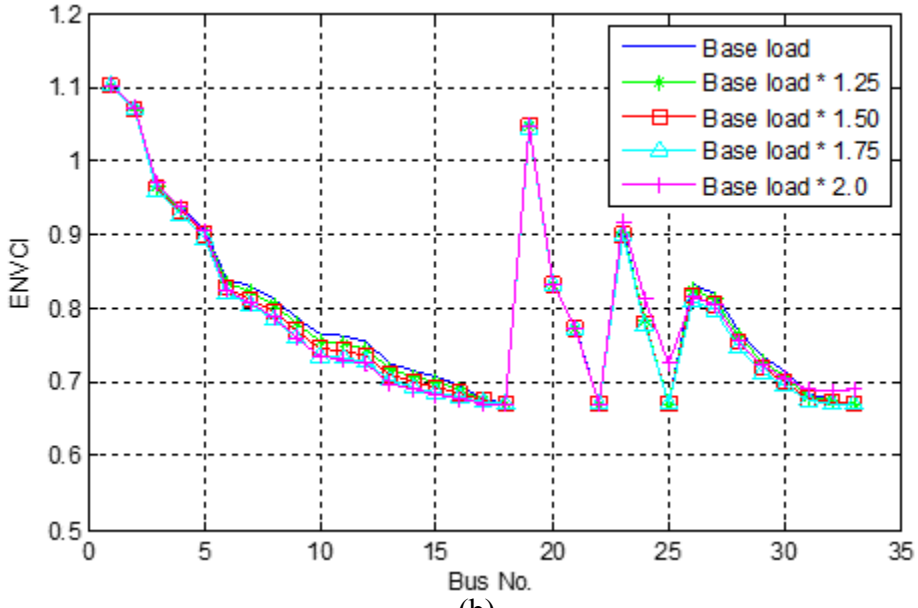

(b)

Figure 3.4 Simulation results by optimized injection method under five load levels, (a) voltage value (p.u.) at Bus 1-33, (b) ENVCI at Bus 1-33.

Figure 3.5 illustrates the number of PEVs at selected buses by optimized injection method under five load levels. It shows that the OI method lets stronger buses, Bus 21 and 24, support more PEVs than the weaker buses (Bus 17 and 32), to achieve the optimization target. With the good control of the charging of PEVs, the number charged in the DN could be optimized without causing safety issues.

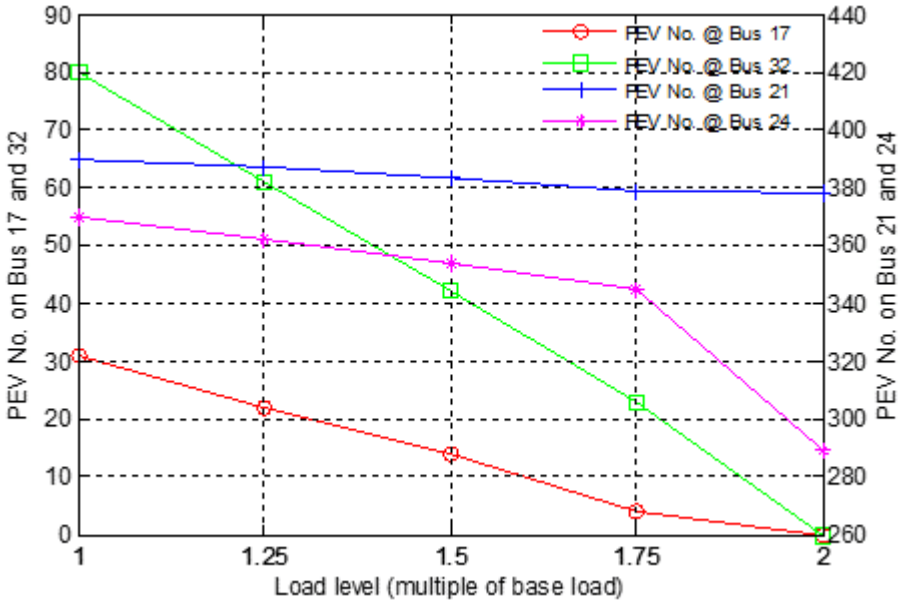

Figure 3.5 Number of PEVs at selected buses by the optimized injection method under five load levels.

According to the simulation studies of two scenarios on the 33-bus test feeder with five load levels, the following observations can be obtained:

- The total number of allowed PEVs drops down as the increase of the load level for both scenarios. It means the increase of PEVs is conflict with the gradually increasing conventional loads because the available power resources are finite. Therefore, it is essential to optimally utilize the available resources.
- The proposed OI method makes full use of the stronger buses to charge as many as PEVs in DN. Therefore the allowed PEVs calculated by the OI method are far more

than the numbers by the conventional UI method without causing the voltage instability.

- The OI method could automatically identify the capabilities of different buses to support added loads without causing voltage instability. It is a good reference for DNO to control the distribution of PEVs on different buses according to their capabilities and present capacity.

3.4 Conclusion

In this chapter, a voltage stability incorporated optimization method is proposed to maximize the injection of PEVs in DNs without violating power limits and causing voltage stability issues. The *ENVCI* is a powerful index used in this work to judge the voltage stability of DN. The simulation results on the 33-Bus test feeder show that the proposed optimization injection method can better utilize the power resources of DN to maximize the injection of PEVs. The allowed number of PEVs is much more than the allowed number by the conventional uniform increase method. This method can provide a clear reference to DNO to manage the charging of the PEVs in DNs.

CHAPTER 4 DEMONSTRATION OF ACTIVE MANAGEMENT OF PLUG-IN ELECTRIC VEHICLES

4.1 Introduction

We have discussed the safety control of PEVs by using FSMwV in Chapter 2 and the maximization of plug-in electric vehicles (PEVs) in DNs without violating voltage stability in Chapter 3 respectively. In the studies, the PEVs are charges by taking advantage of the resources in utilities as well as to keep the system secure. Both of the studies focus on the management strategy and algorithm development while considering the physical constraints in the DNs. To further explore the active management of PEVs in the DNs, we developed a universal demonstration platform, including the software package and the hardware remote terminal units (RTUs), as shown in Figure 4.1. The software package is based on the supervisory control theory, in which the master station (MS) collects data from local RTUs and makes decisions according to the real-time information and the predefined management algorithm. The objective of designing the management software is to charge as many PEVs as possible without violating the power and voltage limits. In addition, the software is flexible to integrate priority rules to regulate the charging sequence, such as first-come first-served. The RTUs are designed with the capabilities of measurement, monitoring, control, and communication. The communication between the MS and the RTUs is based on the IEC60870-5-104 communication protocol [169] which could work on Ethernet Passive Optical Network (EPON) communication system or 3G wireless communication system.

In this chapter, the demonstration of active management of PEVs is introduced. Section 4.2 discusses the design of the software and the management algorithm. Section 4.3 presents the

hardware platform to achieve the management via the RTUs. The application of the demonstration in active distribution network is discussed in Section 4.4. Section 4.5 concludes the chapter.

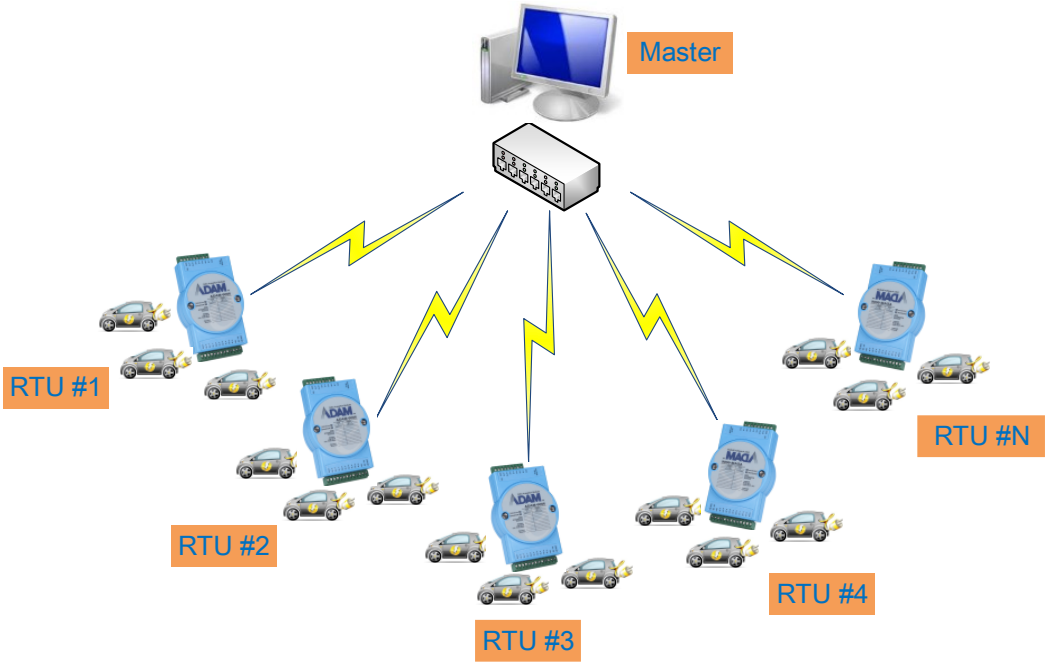

Figure 4.1 Diagram of the active management platform of PEVs

4.2 *Software and Management Algorithm*

To actively manage PEVs, the software has the functions of measurement, communication, monitoring, control, and decision making based on embedded algorithms. The user-friendly software interface is composed of three main parts: the setting interface, the interface of the MS and the interface of the RTUs. As shown in Figure 4.2, via the interface of parameter settings, it is able to set the IP address of the MS, make the function selection, and change settings of communication between the MS and the RTUs. It is the first step to setup the foundation of the MS and the RTUs.

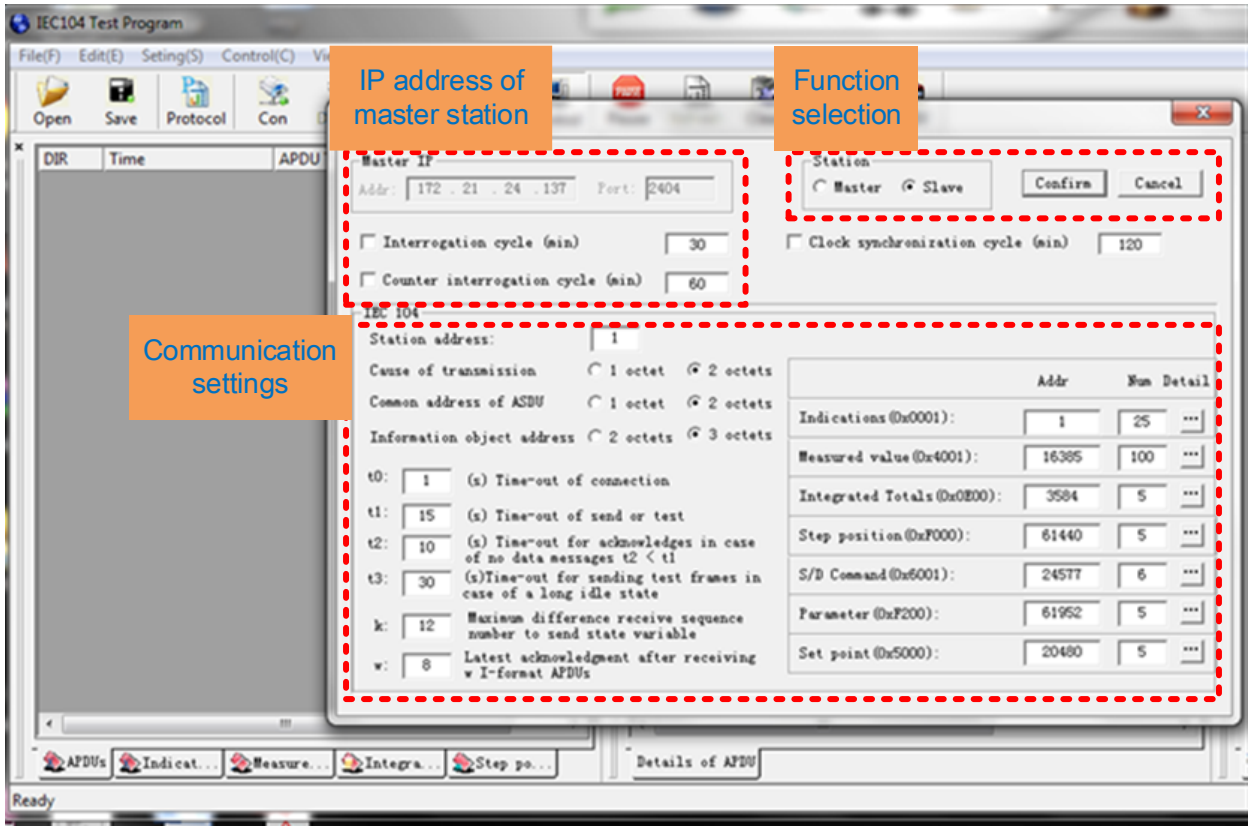

Figure 4.2 Software interface of the master station

The management algorithm of the MS is shown in Figure 4.3, and the software interface is presented in Figure 4.4. For every iteration, the MS first collects data from the RTUs, including voltage, power of uncontrollable loads, and the charging requests from PEVs. Based on the system information, the nominal power $(P_{N1}, P_{N2}, \cdots, P_{Nn})$ of $(RTU_1, RTU_2, \cdots, RTU_n)$ are determined and the total nominal power should not exceed the maximum available power, P_{max}, which could be the power limit of feeder transformers. The maximum number of allowed PEVs for RTU_n is also updated correspondingly by

$$PEV_{Mn} = floor\left(\frac{P_{Nn} - P_{un}}{P_c}\right) \tag{4.1}$$

where PEV_{Mn} is the allowed maximum number of PEVs for charging at RTU_n; P_{un} is the power of uncontrollable loads at RTU_n; P_c is the power consumed by charging a PEV. Then the

constraints $(P_{N1}, P_{N2}, \cdots, P_{Nn})$ and $(PEV_{M1}, PEV_{M2}, \cdots, PEV_{Mn})$ are sent to $(RTU_1, RTU_2, \cdots, RTU_n)$ for them to make local decisions.

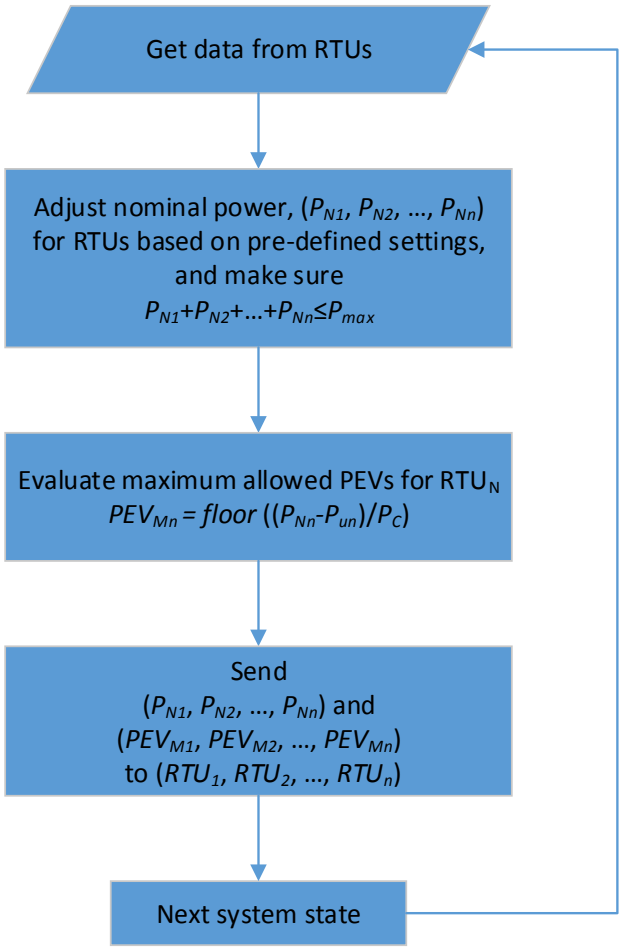

Figure 4.3 Management algorithm in the master station

The software interface of the MS is shown in Figure 4.4. The MS is able to communicate and control multiple RTUs, and we have two RTUs in the demonstartion. The simple and straightforward interface shows the imformation of the RTUs, including the assigned nominal power, current uncontrollable load level, allowed maximum PEVs and the actual requests from PEVs. The MS is able to get the information from the RTUs and send commands to the RTUs either automatically or manually.

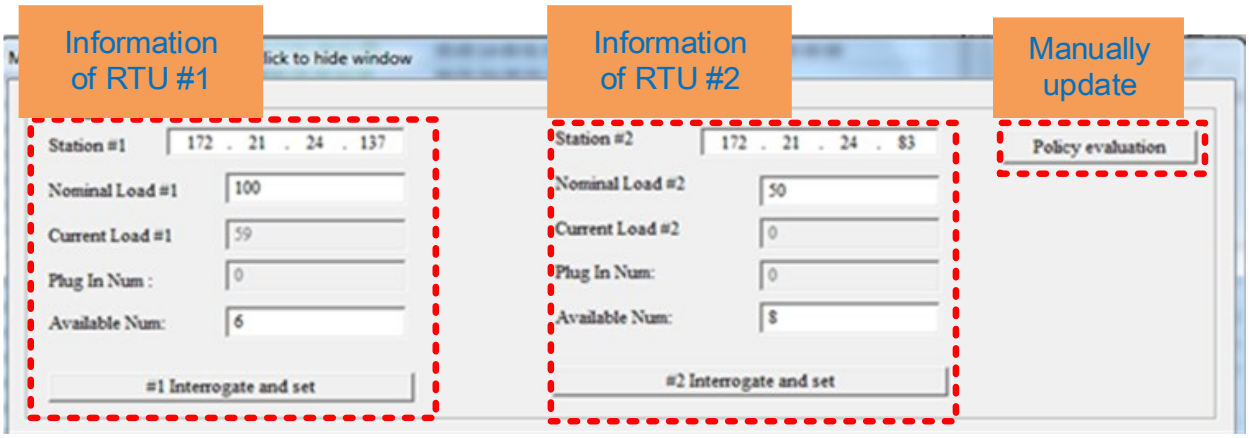

Figure 4.4 Software interface of the master station

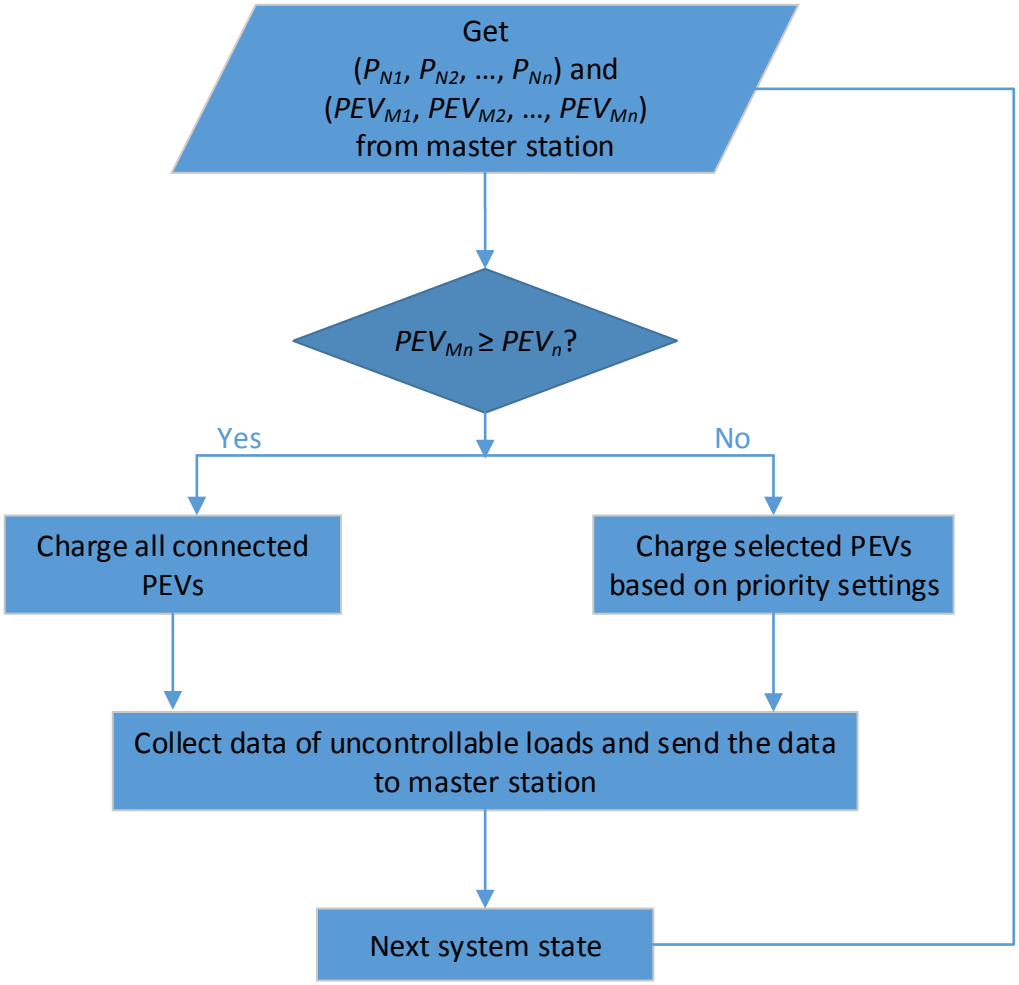

Figure 4.5 Management algorithm in the RTUs

The management algorithm of RTUs is shown in Figure 4.5. Once the RTUs get the information of the nominal power and the maximum allowed number of PEVs from the MS, the

charging strategy is chosen based on whether the PEV_{Mn} is equal to or larger than the actual charging requests, PEV_n. If it is yes, the RTU_n will satisfy all of the charging requests from PEVs. Otherwise, selected PEVs will be charged based on priority settings. In the priority algorithm, the charging requests are ordered based on predefined rules, such as the rule of first-come first-served or the higher priority is given to the customers who would like to pay more for their urgent charging demands. The priority algorithm is flexible to be a single rule or be jointly defined by multiple rules.

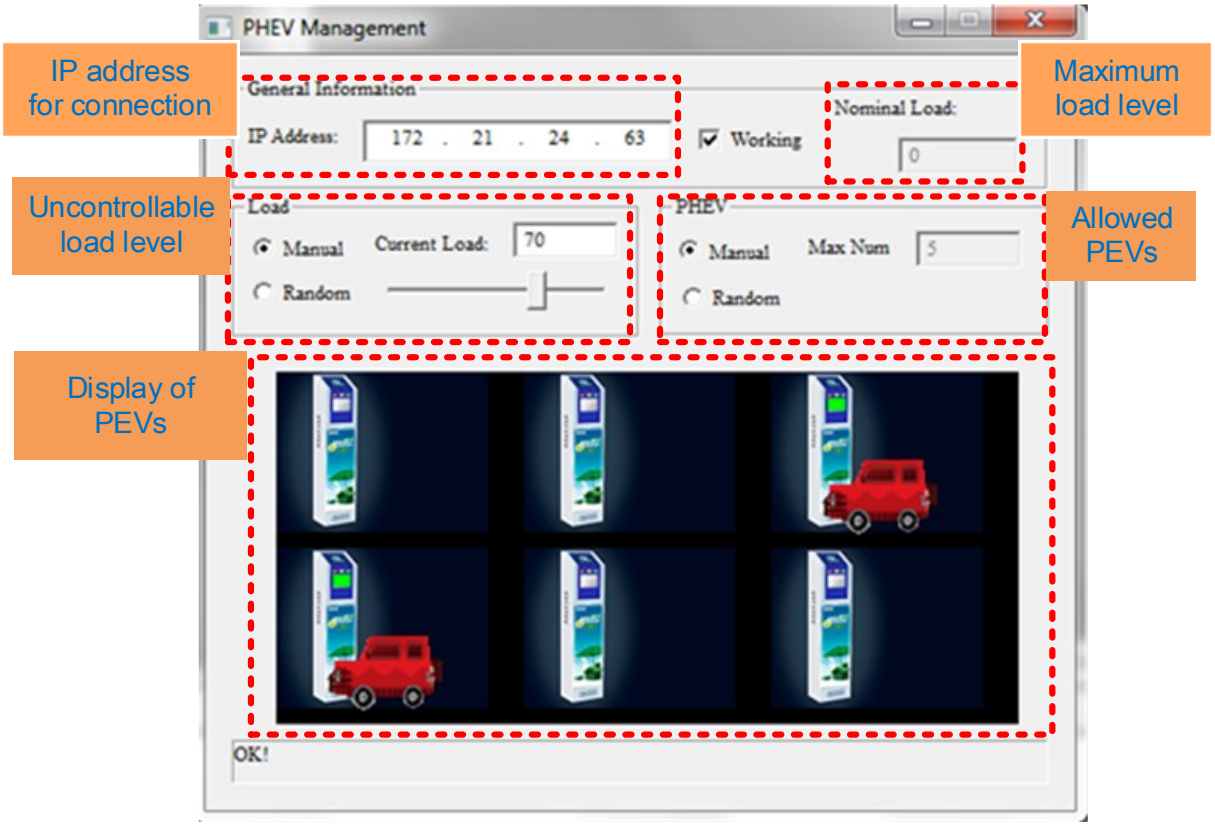

Figure 4.6 Software interface of RTUs

The software interface of RTUs is shown in Figure 4.6. The IP address is for the communication and control unit in the local charging station. The current load means the total power of the uncontrollabel loads. The PEV_{Mn} is shown in the PEV dialog box. In the demonstartion, there are six chargers in the charging station to be managed by every RTU. The

interface clearly shows how many requests in the station, where the requests are from, and what the charging status of each PEV is.

4.3 Hardware Platform

To execute the decisions, the hardware platform of RTUs is designed with the capabilities of measurement, monitoring, control, and communications, as shown in Figure 4.7.

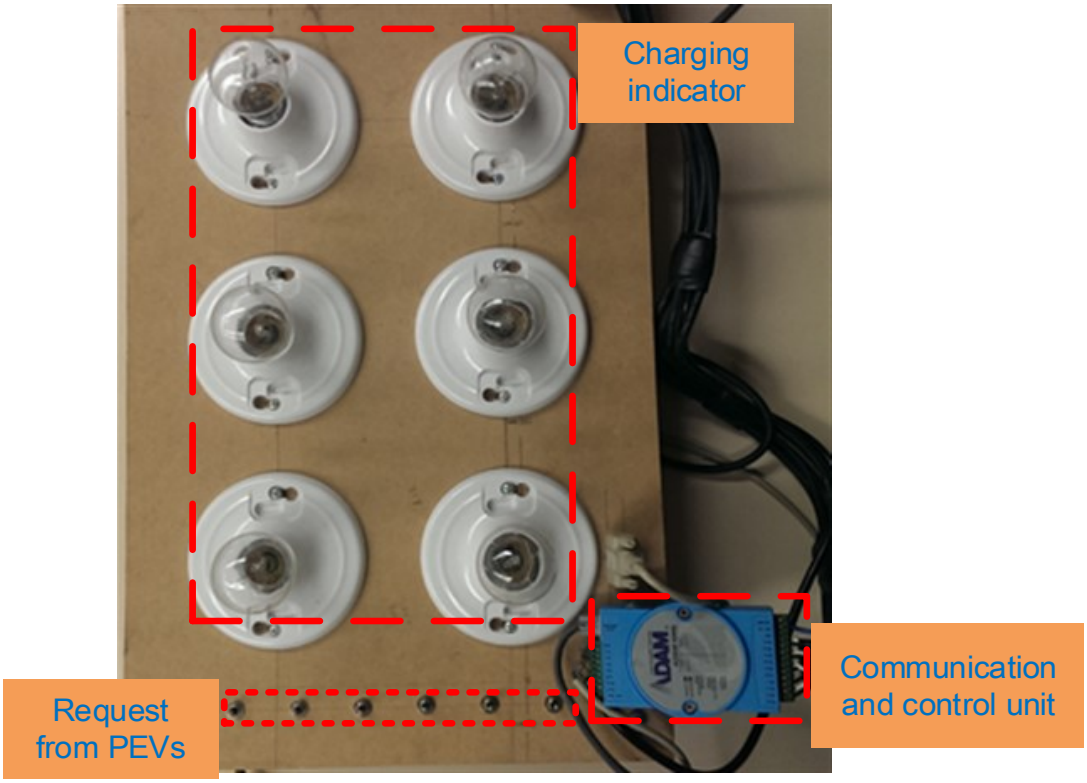

Figure 4.7 Hardware platform of local charging station

The charging station is composed of binary switches to simulate the requests from PEVs, light bulbs to indicate the charging status of PEVs, and a communication and control unit, ADAM-6066, to communicate with RTU and control the chargers to charge PEVs or not. When the PEVs send requests for charging to RTU_n, the RTU judges whether the total PEVs have exceeded PEV_{Mn}. If yes, the RTU will adjust the charging order based on the priority algorithm. The communication and control is performed by the ADAM-6066 module through Ethernet as shown

in Figure 4.8. The module can function as a product for measurement, control, monitoring and automation, and is flexible to be incorporated in the system without changing the entire architecture of the system. We have developed two sets of the charging stations, and the application of the demonstration in active PEVs management is presented in the next section.

Figure 4.8 ADAM-6066

4.4 Application in Active Distribution Network

The research reported in [170] considered the management of PEVs in traditional DN. As the smart grid technologies advance, it is necessary to study PEV's management in future active distribution networks (ADN). We are facing great challenges in how to utilize the ADN technologies (e.g., smart meters, advanced communication technologies) to provide service to more PEVs and how to reduce cost while developing a new paradigm of DN with more reliable and flexible control strategies.

The development of advanced metering infrastructure (AMI) including smart meters has laid the cyber-physical base for information acquisition and communication in future ADN.

Remote Terminal Unit (RTU), distribution Transformer Terminal Unit and Distribution Terminal Unit (DTU) are typical devices used in smart distribution networks, based on the IEC60870-5-104 communication protocol [16]. Figure 4.9 shows a simple example distribution grid with AMI infrastructure. As shown in the figure, zone H is a residential area and zone O is an office and business district. The circuit breakers CB_D, CB_O and CB_H are for the protection of the transformer, zone O and zone H, respectively. The protection settings of these circuit breakers are fixed since the design of the distribution grid. During the operation, they cannot be adjusted or adjusted frequently according to the change of the corresponding loads in a traditional way.

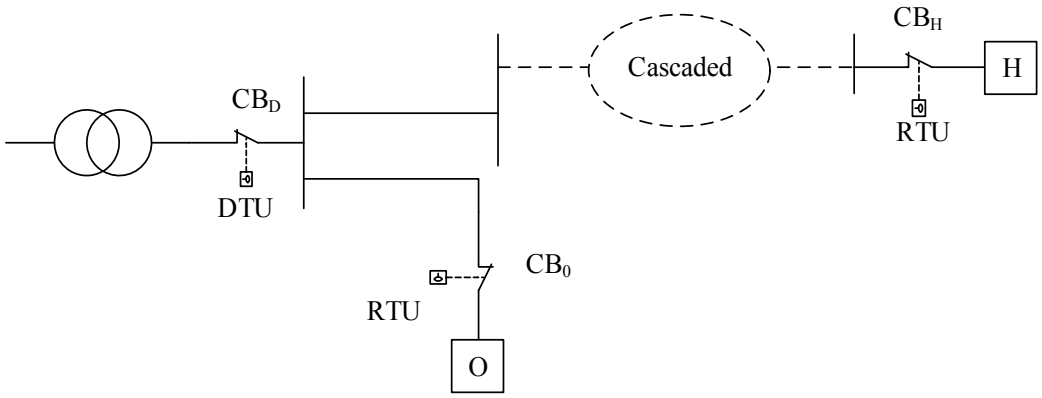

Figure 4.9 Management of PEVs in active DNs.

Since the PEVs are moving around, they can cause load shifts among different zones in the network. For example, most of them may be parked in zone O at daytime and move to zone H at night.

For the movement of PEVs, most of them are parked in the zone O in daytime and in the zone H at night, which cause two issues:

(1) At the design stage. For a new distribution grid design, the settings and ratings of CB_H and CB_O should be set to handle possible charging peak demands of PEVs. Based on the traditional peak demand design, the capacity of transformer and the setting of CB_D will be almost double what the actual need for PEVs. As a result, the system investment

will increase.

(2) At the operation stage. For an existing distribution grid, with high penetration of PEVs, a portion of the distribution grid may get overloaded for a period of time in a time due to PEV load shift. This will cause some PEVs not be charged or fully charged as needed. For the system shown in Figure 4.9, both zones may see a need for upgrade if the total PEV charging demand is over the limit of each them. However, the reality is that the chance for the two zones to have peak PEV charging demands at the same time is almost zero.

The smart grid communication technologies make it possible for us to rethink the aforementioned problems. One way is to develop a supervisory control strategy to adaptively re-set the protection settings at different zones to accommodate the load changes. For example, for the system of Figure 4.9, at day time, the load demand in the zone H may decrease while the load demand will increase in zone O. We can then lower the protection settings of CB_H increase that of CB_O. In the evening we can do in the opposite way to accommodate more PEVs at zone H. Therefore, the resources in the utilities are fully utilized to charge PEVs and support ever-increasing loads.

4.5 Conclusion

To further explore the active management of PEVs in the DNs, we developed a universal demonstration platform. The platform is composed of software for a MS and RTUs and hardware set of charging stations. The management algorithm for the MS and the RTUs are flexible to integrate priority algorithm of charging to meet the demands from PEV owners. Based on the ADAM-6066 modules, the RTUs are able to communicate with the MS and the charging stations

and carry out the demands to charge PEVs accordingly. The demonstration is suitable for the application in active distribution networks to manage PEVs.

CHAPTER 5 MICROGRID POWER MANAGEMENT DURING AND SUBSEQUENT TO ISLANDING PROCESS

5.1 Introduction

A microgrid (MG) can operate in the grid-tied mode under normal operating conditions and switches to the islanded mode when severe grid disturbances occur. The transition from the grid-tied mode to the standalone mode is referred to as the islanding process of MG.

For fault-induced islanding, the voltage of MG can drop to as low as 0.2 p.u.; and it usually takes more than 30 cycles for the voltage to recover to its nominal value [171]. This voltage recovery process may take much longer if the MG is heavily penetrated with dynamic loads, e.g., single phase induction motors (SPIMs). The main problem lies in the stall of these motors under low voltage condition (<0.87 p.u.), during which they absorb two to three times the rated current, making voltage issues in MG [172]. It has been claimed that penetration of SPIMs in a distribution system could reach as high as 75% due to government incentives and energy efficiency requirements [173]. It is risky to keep voltage low for a long period of time since the load will be shed by under-voltage load shedding protection schemes. Solutions need to be developed to ensure the MG voltage profile during and subsequent to the islanding process.

It is a possible solution of using the reactive power generated from distributed energy resources (DERs) for MG voltage regulation. Such ideas have been demonstrated in [173-175]. Presently, although many DERs are capable of producing and controlling reactive power, the industry practice and standards still require them to operate under unity power factor. Examples of such include inverters for photovoltaic (PV) systems and wind turbine power converters. In a recent amendment of IEEE Standard 1547, the distributed generators (DGs) are allowed to provide reactive support to regulate local voltage [176]. The problem then becomes how to control reactive

power generation and how to properly share it among electronic-interfaced distributed generators (EIDGs).

The idea of droop control is a classical solution that solves the reactive power sharing problem among DGs. By drooping voltage references of DG controllers against the real or reactive power outputs, the sharing of real and reactive power among DGs is enabled [177, 178]. However, the droop control is based on local voltage measurements only and is incapable of regulating the voltage at buses that have no DG installed or nearby.

A voltage sensitivity based method was proposed to regulate the voltage at a specific bus [179]. By adjusting the reactive power output of a wind generator, based on its active power generation, the voltage at a targeted bus is constrained to a certain limit. This method may work well when the MG is operating at steady-state with only one DG, but it does not consider the MG under transients or with multiple DGs.

In this chapter, the voltage sensitivity based method is extended to multiple DGs and to MG transient conditions (MG islanding). When islanding occurs, the proposed algorithm helps restore voltages at weak buses that are heavily penetrated with dynamic loads like SPIMs. The proposed reactive power compensation algorithm works in two stages according to the status of the system. During the islanding process, when system voltage falls/stays below a pre-defined threshold, EIDGs are dispatched to generate maximum possible reactive power to help shorten the voltage recovery process. When system voltage reaches the pre-defined threshold, a voltage sensitivity aided linear programming problem is formulated and solved recursively to determine the optimal sharing of reactive power among EIDGs. To validate the proposed method, a modified IEEE standard 13-bus system is simulated in Matlab/Simulink to work as a MG test-bed. Description of the testbed and the proposed algorithms are detailed in the following sections.

5.2 Microgrid Under Study

5.2.1 IEEE 13-bus test feeder

To investigate the voltage issues in a MG covering a reasonable size area, the 4.16 kV IEEE standard 13-bus test feeder [180] is studied. As shown in Figure 5.1, some modifications are made to this standard test feeder to make it a MG. A static switch is added between the utility grid and bus 650. Three distributed generators are modeled, including a 3.125MVA diesel generator at bus 650, a 600kW PV system at bus 680, and a 1.2MWh 600kW battery at bus 675. In the grid-tied mode, all DGs are under P&Q control, following the voltage and frequency (V & f) of the utility grid. In the islanded mode, MG enters the master/slave control mode with the diesel generator selected as the "master" and the rest selected as the "slaves" [181].

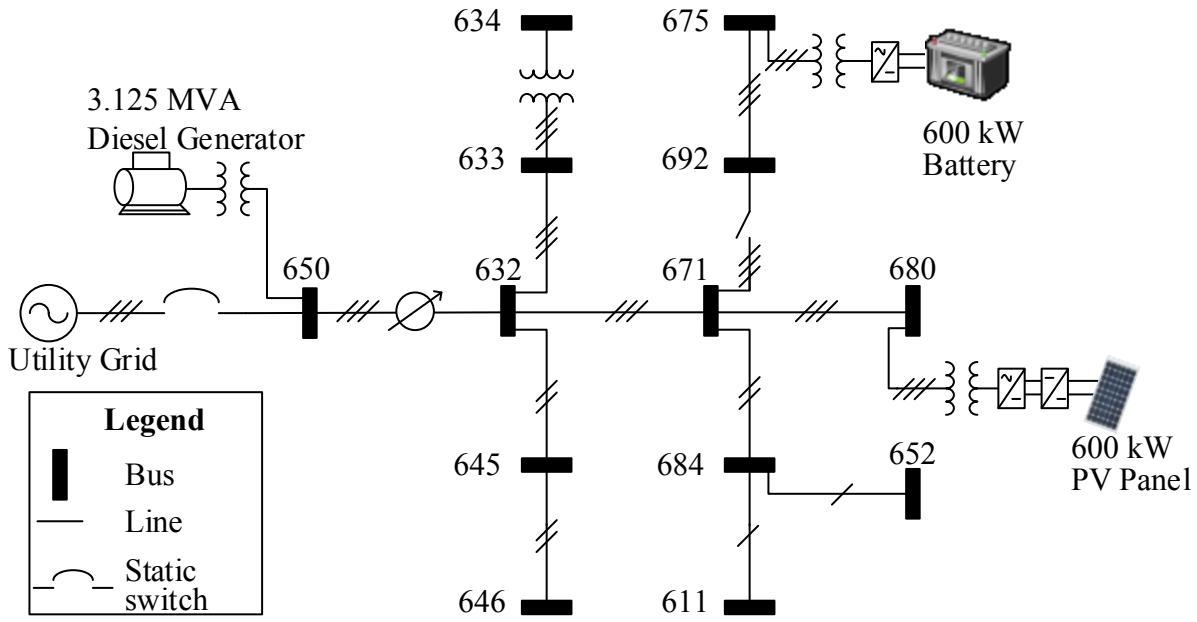

Figure 5.1 Diagram of the MG.

The battery and PV are connected at the remote buses through transformers. Since the voltage and frequency are defined by utility grid or diesel generator, they are controlled in current mode to follow the references of real and reactive powers. In this study, the reactive power of battery and PV are controlled to help the system to maintain the voltage within safe range.

5.2.2 Diesel generation system

The diesel generation system (DGS) in this MG consists of a turbine, two governors, an excitation system, and a synchronous generator (SM), which is shown in Figure 5.2. It is connected with the grid through a step-up transformer.

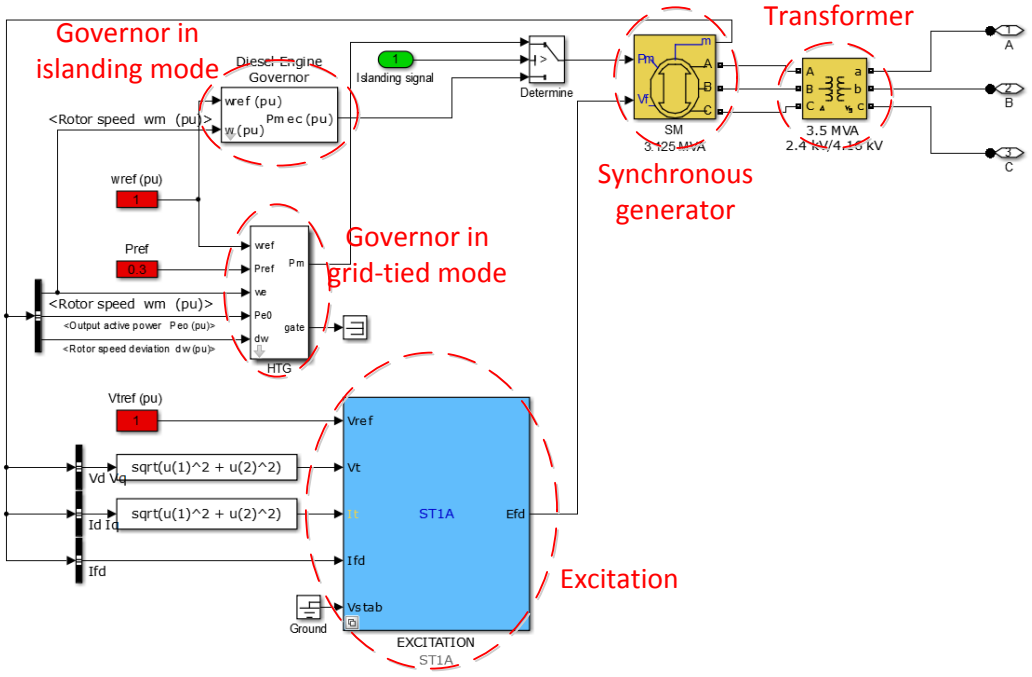

Figure 5.2 Diagram of the diesel generator and controllers.

In the grid-tied mode, the governor controls the SM to follow the reference of electric power without change the voltage and frequency of the grid which is shown in Figure 5.3 [182]. In the governor, a PI controller, $K_p + K_i/S$, is used to regulate electric power error. Then the output of the PID controller is sent to the servo motor. K_a and T_a are gain and time constant of the servo motor respectively. S means the derivative calculation. Together with the speed change rate, they are sent to model of turbine to get the reference of the mechanic power of the synchronous generator, P_{mec}^{ref}. The parameters are given in TABLE 5.1.

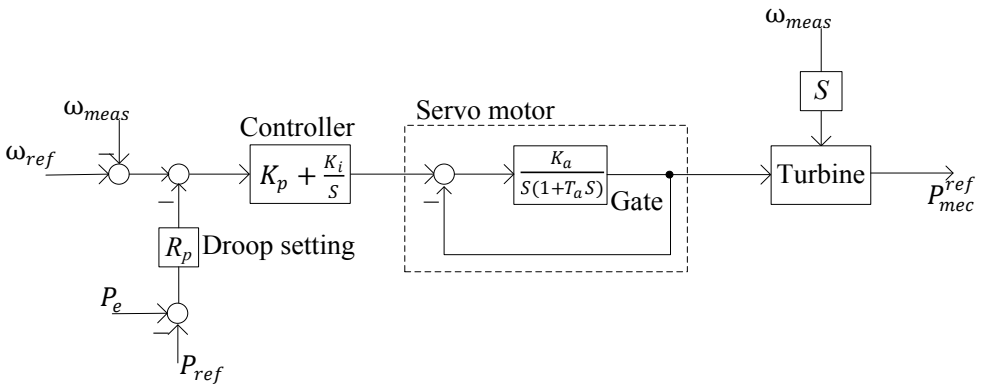

Figure 5.3 Diesel governor model in grid-tied mode.

TABLE 5.1 PARAMETERS OF DIESEL GOVERNOR IN GRID-TIED MODE

K_a	3.33
T_a	0.07
K_p	1.163
K_i	0.105
R_p	0.05

The diesel engine and governor to guarantee the speed to follow the reference in the standalone mode are presented in Figure 5.4. In the governor, a lead-lag controller is selected to adjust speed error [183]. K is the controller gain and T_1, T_2 and T_3 are the time constants of the lead-lag controller. T_4, T_5 and T_6 are the time constants of the actuator. T_D is the time delay of the engine, and its output products speed to get the P_{mec}^{ref}. The parameters are given in TABLE 5.2.

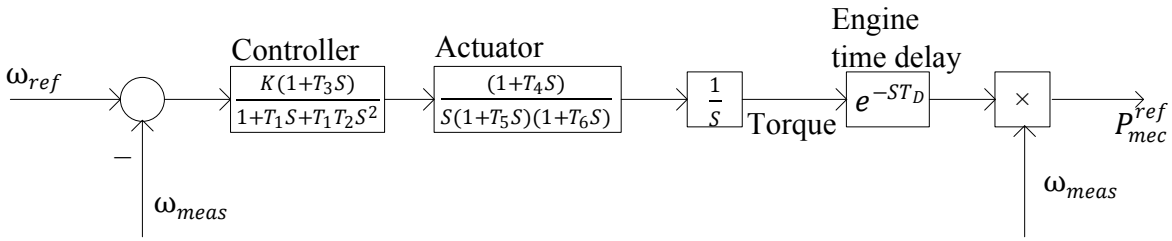

Figure 5.4 Diesel engine and governor model in standalone mode.

TABLE 5.2 PARAMETERS OF DIESEL ENGINE AND GOVERNOR IN STANDALONE MODE

K	80
T_1	0.01

T_2	0.02
T_3	0.01
T_4	0.25
T_5	0.009
T_6	0.0384
T_D	0.024

Among excitation systems in IEEE Standard [184], an AC1A excitation system is selected to control the field voltage of the synchronous generator. To guarantee the safety of power supply, the power rating of the synchronous generator is chosen about 1.8 times of the total loads. The parameters of the synchronous generator are given in TABLE 5.3.

TABLE 5.3 PARAMETERS OF SYNCHRONOUS GENERATOR

Generator Type	Salient pole type
Nominal Power	3.125 MVA
Nominal L-L Voltage	2400 V
Nominal Frequency	60 Hz
Number of Poles	4
Stator Resistance (R_s)	0.0036 p.u.
Leak Reactance (R_l)	0.052 p.u.
Direct Axis Reactance (X_d)	1.56 p.u.
Transient Direct Axis Reactance (X'_d)	0.296 p.u.
Subtransient Direct Axis Reactance (X''_d)	0.177 p.u.
Quadrature Axis Reactance (X_q)	1.06 p.u.
Subquadrature Axis Reactance (X''_q)	0.177 p.u.
Inertia Coefficient	0.57 s

Since the MG is operated in both grid-tied and standalone modes, two control schemes are designed and implemented. Under the grid-tied mode, the diesel generator works in P&Q

control mode; when MG is islanded, the diesel generator switches from P&Q to V&F control mode to actively regulate the V & f of the MG.

5.2.3 Model of PV panel

To reduce the cost and take advantage of the green energy resources, a 600 kW PV generation system is included in the studied microgrid. The PV panel is built up with series/parallel connected total 3600 PV solar cells, and the parameters of which are listed in TABLE 5.2. The PV cell is modeled by the one diode equivalent circuit in Figure 5.5 [185].

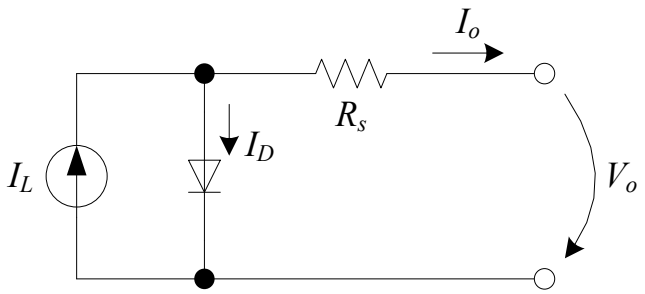

Figure 5.5 Equivalent model for a PV cell.

The output voltage V_o and the load current I_o has the relationship as:

$$I_o = I_L - I_D = I_L - I_0\left[e^{\left(\frac{V_o + IR_S}{\alpha}\right)} - 1\right] \tag{5.1}$$

where I_L is light current (A), I_0 is the saturation current, I_O is the output current, V_O is the output voltage, R_S is the series current and α is the thermal voltage timing completion factor. The PV is connected to a DC/DC converter with MPPT control, the output of which is further connected to a DC/AC inverter with *dq0* based PQ control.

TABLE 5.4 PV PANEL PARAMETERS

Module unit	153 cells, 173W @1kW/m^2, 25^{0}C
Module number	300×12=3600
Power rating	3600×173=622.8 kW

5.2.4 Model of battery

In case of emergent power demand, a 500 kW, 1000 kWh battery is included in the microgrid. Its equivalent model is presented in Figure 5.6 [186].

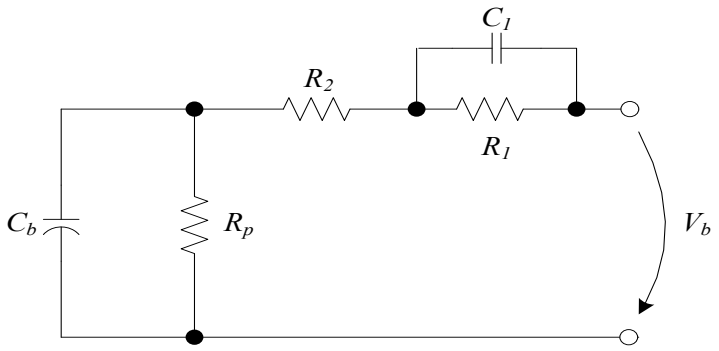

Figure 5.6 Equivalent model for lead acid batteries.

In the equivalent model, C_b is the battery capacitance, R_p is the self-discharge resistance, R_2 is the internal resistance, R_1 is the overvoltage resistance and C_1 is the overvoltage capacitance.

The SOC of the battery is calculated as:

$$SOC(t) = SOC(t_0) - \frac{\int_{t_0}^{t} id\tau}{Q} \tag{5.2}$$

where Q is the battery capacity (Ah), and i is the output current (A), t_0 is the initial time.

The battery is also connected to the microgrid via a DC/AC converter with the PQ controller. It has the same control scheme with the PV panel through controlling the real power and reactive respectively which will be introduced in the following section.

5.2.5 Control of power electronic inverters

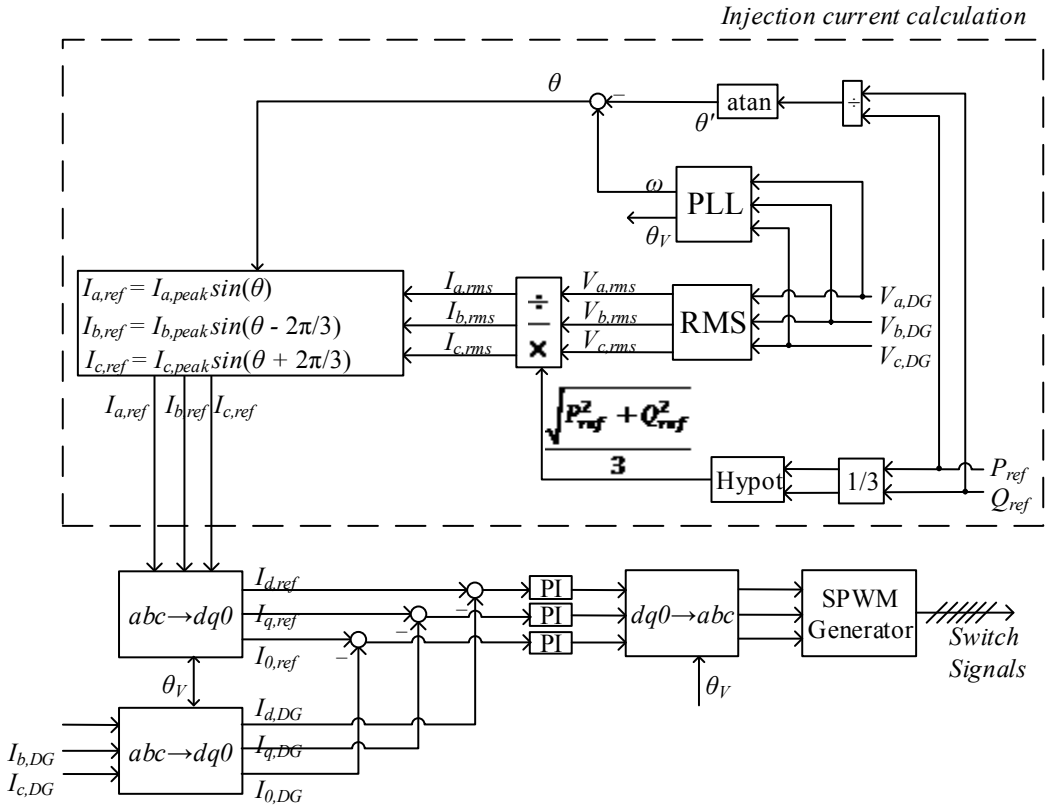

Figure 5.7 Control scheme of the EIDGs

The current injection control scheme is utilized in this study to control the real and reactive power of PV and battery [187]. However, the design of the conventional controller does not consider the possible voltage unbalance in the low voltage DN. The three-phase injected real and reactive powers should be controlled separately based on their voltage magnitudes. In addition, after the transformation of three-phase currents from *abc* to *dq*0 coordinate, it may not correctly reflect the dynamics of the system by overlooking the zero current, I_0. In unbalanced power grid, the zero current also influences the dynamic performance of the controller and should be controlled. The diagram of the PQ controller is shown in Figure 5.7.

As shown in Figure 5.7, the "Injection current calculation" block calculates the 3-phase current reference based on the measured 3-phase voltage phasors at the inverter output. Both the

3-phase reference and the measured currents are transformed from the *abc* frame into the *dq0* frame using *Clarke Transformation*. The calculation of the magnitudes and angles of the three-phase reference current is shown in (5.3)-(5.5). The difference between the reference and the measured currents are fed into PI current controllers. Then the control signals are transformed into the *abc* frame using *Inverse Clarke Transformation* with the angle reference, θ_V of the power grid. Through SPWM generator, the three phase control signals are transformed into PWM signals to yield required real and reactive power.

$$\begin{cases} I_{a,ref} = \sqrt{3} I_{a,rms} \sin(\theta) \\ I_{b,ref} = \sqrt{3} I_{b,rms} \sin(\theta - 2\pi/3) \\ I_{c,ref} = \sqrt{3} I_{c,rms} \sin(\theta + 2\pi/3) \end{cases} \tag{5.3}$$

$$\begin{cases} I_{a,rms} = \dfrac{\sqrt{P_{ref}^2 + Q_{ref}^2}}{3} \div V_{a,rms} \\ I_{b,rms} = \dfrac{\sqrt{P_{ref}^2 + Q_{ref}^2}}{3} \div V_{b,rms} \\ I_{c,rms} = \dfrac{\sqrt{P_{ref}^2 + Q_{ref}^2}}{3} \div V_{c,rms} \end{cases} \tag{5.4}$$

$$\theta = \omega - atan \frac{Q_{ref}}{P_{ref}} \tag{5.5}$$

5.2.6 Model of single phase induction motor

A capacitor-start motor is chosen for the study, which is modeled with two windings: main winding and auxiliary winding as shown in Figure 5.8. The equations to model the dynamic characteristics are listed as follows [172].

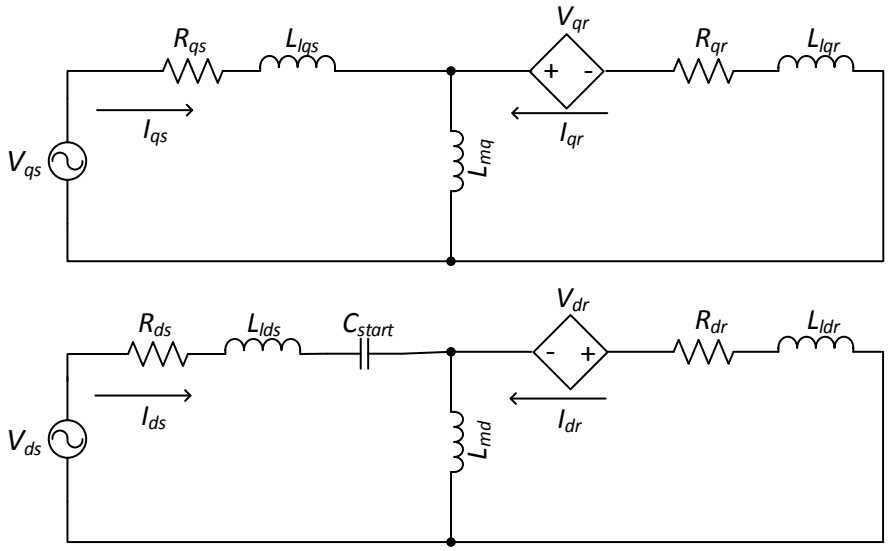

Figure 5.8 Equivalent circuit of the single phase induction machine dynamic model.

Voltage equations in *dq* reference frame are:

$$\begin{cases} V_{qs} = R_{qs}I_{qs} + \dfrac{d\lambda_{qs}}{dt} \\ V_{ds} = R_{ds}I_{ds} + \dfrac{d\lambda_{ds}}{dt} + V_c \\ 0 = R_{qr}I_{qr} + \dfrac{d\lambda_{qr}}{dt} - N_{qd}\omega_r\lambda_{dr} \\ 0 = R_{dr}I_{dr} + \dfrac{d\lambda_{dr}}{dt} + N_{dq}\omega_r\lambda_{qr} \end{cases} \tag{5.6}$$

where V_{ds} and V_{qs} are stator voltage on *d* and *q* axis respectively; V_{dr} and V_{qr} are rotor voltage on *d* and *q* axis respectively; R_{ds} and R_{qs} are the stator resistors on *d* and *q* axis respectively; R_{dr} and R_{qr} are the rotor resistors on *d* and *q* axis respectively; I_{ds} and I_{qs} are stator currents on *d* and *q* axis respectively; I_{dr} and I_{qr} are rotor currents on *d* and *q* axis respectively; λ_{ds} and λ_{qs} are stator *d* and *q* axis fluxes; λ_{dr} and λ_{qr} are rotor *d* and *q* axis fluxes; V_c is the voltage of the starting capacitor; N_{qd} is the ratio of number of main winding's effective turns over the number of auxiliary winding's effective turns, and N_{dq} is its reciprocal; ω_r is the electrical angular velocity.

Flux equations and inductance equations are:

$$\begin{cases} \lambda_{qs} = L_{qs} I_{qs} + L_{mq} I_{qr} \\ \lambda_{ds} = L_{ds} I_{ds} + L_{md} I_{dr} \\ \lambda_{qr} = L_{qr} I_{qr} + L_{mq} I_{qs} \\ \lambda_{dr} = L_{dr} I_{dr} + L_{md} I_{ds} \end{cases} \tag{5.7}$$

$$\begin{cases} L_{qs} = L_{lqs} + L_{mq} \\ L_{ds} = L_{lds} + L_{md} \\ L_{qr} = L_{lqr} + L_{mq} \\ L_{dr} = L_{ldr} + L_{md} \end{cases} \tag{5.8}$$

here L_{ds} and L_{qs} are the stator inductances on d and q axis respectively; L_{dr} and L_{qr} are the rotor inductances on d and q axis respectively; L_{md} and L_{mq} are main winding magnetizing inductance on main and auxiliary winding respectively; L_{lds} and L_{lqs} are stator leakage inductance on d and q axis respectively; L_{ldr} and L_{lqr} are rotor leakage inductance on d and q axis respectively.

Mechanical equations are:

$$T_e = \frac{P}{2}\left(N_{dq} \lambda_{qr} I_{dr} - N_{qd} \lambda_{dr} I_{qr}\right) \tag{5.9}$$

$$J\left(\frac{P}{2}\right)\frac{d\omega_r}{dt} = T_e - T_L \tag{5.10}$$

where P is the number of poles; J is the inertia coefficient; T_e is the electromagnetic torque; T_l is the load torque.

Since the existence of the starting capacitor, the auxiliary winding current on d axis during startup is represented by:

$$C\frac{dV_C}{dt} = -I_{ds} \tag{5.11}$$

According to the typical torque speed characteristic of a capacitor-start motor shown in Figure 5.9, the torque of the by the SPIM could be very high when the motor starts because of the assistance of starting capacitor. When the speed rises to 0.75 p.u., a preset threshold, the starting capacitor will be isolated from the circuit by opening a centrifugal switch. Only main winding is left to support the running of the motor, and the torque drops around 1 p.u. to 2.5 p.u..

The stall of these motors under low voltage condition (<0.87 p.u.), during which two to three times the rated current are absorbed, makes voltage issues in the MG. It has been claimed that penetration of SPIMs in a distribution system could reach as high as 75% due to government incentives and energy efficiency requirements [173]. The motors are only equipped with thermal protections, which means the voltage issues during stalling can last 30 seconds to 2 minutes until thermal protection kicks in to isolate the motors from the grid. It is risky to keep voltage low for such a long period of time, and solutions need to be developed to ensure the MG voltage profile during and subsequent to the islanding process.

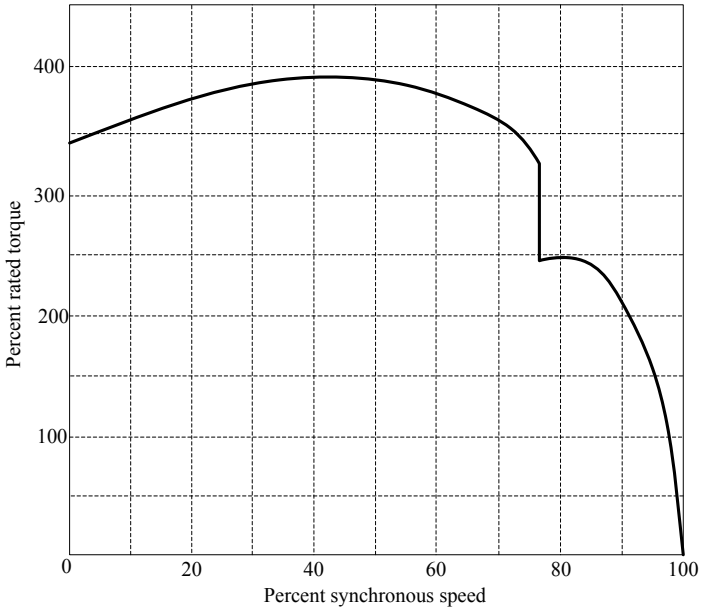

Figure 5.9 Typical torque speed characteristic of a capacitor-start motor [172].

5.3 Reactive Power Management

In this section, a reactive power management algorithm (RPMA) is presented for voltage regulation.

5.3.1 Voltage sensitivity

The voltage sensitivity matrix relates the changes in magnitudes and angles of bus voltages to the changes in the real and reactive power injections at buses. The voltage sensitivity matrix can be calculated by inverting the Jacobian matrix at a specific operating point. The power flow equations are listed in (5.12) [188]:

$$\begin{cases} P_i = \sum_{k=1}^{n} |V_i||V_k|\left(G_{ik}cos(\theta_i - \theta_k) + B_{ik}\sin(\theta_i - \theta_k)\right) \\ Q_i = \sum_{k=1}^{n} |V_i||V_k|\left(G_{ik}sin(\theta_i - \theta_k) - B_{ik}\cos(\theta_i - \theta_k)\right) \end{cases} \tag{5.12}$$

where P_i and $Q_i$are real and reactive power net injection at bus i; $Y_{ik} = -(G_{ik} + jB_{ik})$ is inverse of the impedance of line connecting bus i and k; $V_i\angle\theta_i$ and $V_k\angle\theta_k$ are the voltage phasors at bus i and bus k respectively. The Jacobian matrix is obtained by linearizing the power flow equations:

$$\begin{bmatrix} \Delta P \\ \Delta Q \end{bmatrix} = \begin{bmatrix} \frac{\partial P}{\partial \theta} & \frac{\partial P}{\partial V} \\ \frac{\partial Q}{\partial \theta} & \frac{\partial Q}{\partial V} \end{bmatrix} \begin{bmatrix} \Delta\theta \\ \Delta V \end{bmatrix} \tag{5.13}$$

If the Jacobian matrix is well-conditioned, the voltage sensitivity matrix is derived as below:

$$\begin{bmatrix} \Delta\theta \\ \Delta V \end{bmatrix} = \begin{bmatrix} A & B \\ C & D \end{bmatrix} \begin{bmatrix} \Delta P \\ \Delta Q \end{bmatrix} \tag{5.14}$$

where $A = \frac{\partial P}{\partial \theta}^{-1} + \frac{\partial P}{\partial \theta}^{-1}\frac{\partial P}{\partial V}\left(\frac{\partial Q}{\partial V} - \frac{\partial Q}{\partial \theta}\frac{\partial P}{\partial \theta}^{-1}\frac{\partial P}{\partial V}\right)^{-1}\frac{\partial Q}{\partial \theta}\frac{\partial P}{\partial \theta}^{-1}$, $B = -\frac{\partial P}{\partial \theta}^{-1}\frac{\partial P}{\partial V}\left(\frac{\partial Q}{\partial V} - \frac{\partial Q}{\partial \theta}\frac{\partial P}{\partial \theta}^{-1}\frac{\partial P}{\partial V}\right)^{-1}$, $C = -\left(\frac{\partial Q}{\partial V} - \frac{\partial Q}{\partial \theta}\frac{\partial P}{\partial \theta}^{-1}\frac{\partial P}{\partial V}\right)^{-1}\frac{\partial Q}{\partial \theta}\frac{\partial P}{\partial \theta}^{-1}$, and $D = \left(\frac{\partial Q}{\partial V} - \frac{\partial Q}{\partial \theta}\frac{\partial P}{\partial \theta}^{-1}\frac{\partial P}{\partial V}\right)^{-1}$. Denote the voltage of the target bus to be regulated as V_j and the real and reactive power of the buses with EIDGs as P_l and Q_l. D_{lj} is the sensitivity factor denotes the deviation of voltage at bus j caused by the deviation of

reactive power of the *l*th EIDG. Assuming the real power injections at buses remain constant during the entire islanding process, the voltage deviation at target *j*th bus could be calculated as:

$$\Delta V_j = \sum_l D_{lj} \Delta Q_l \tag{5.15}$$

From (5.15), it is noted that the voltage deviation at bus *j* is determined/impacted not only by EIDGs at the same bus ($j=l$), but also by EIDGs from other buses ($j \neq l$). Therefore, for a weak (heavily loaded) bus with no EIDG, it is possible to regulate its voltage by adjusting reactive power outputs of remote DGs. Hence, the following RPMA is proposed to calculate the amount of reactive power that needs to be generated by DGs to regulate voltage at remote weak buses.

5.3.2 Reactive power management algorithm

Figure 5.10 shows the evolution of voltage at bus 611 during and subsequent to a fault-induced islanding. The voltage evolution can be divided into some stages by t_1, t_2 and t_3 in Figure 5.10. In the beginning, the MG is operating at steady-state and the bus voltage is within the security range. At t_1, a three-phase to ground fault on the utility grid occurs, and the voltage at bus 611 drops to 0.47 p.u.. MG is islanded from the utility grid after t_2, and immediately voltage starts rising afterwards. During the time interval of t_2-t_3, the bus voltage recovers to 0.90 p.u.. After t_3, voltage reaches to a steady-state value but is still out of the security range.

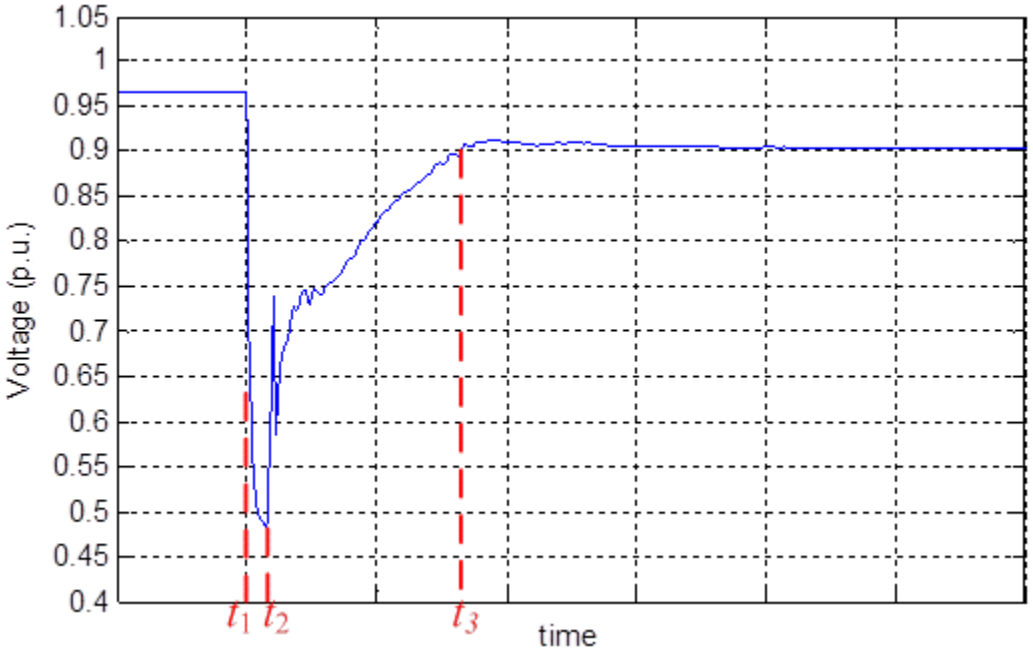

Figure 5.10 Voltage recovery at bus 611 during and subsequent to islanding process.

Based on the evolution of voltage, a two-stage RPMA is proposed. During the interval t_2-t_3, the maximum reactive power (MRP) of EIDGs is generated. It is because V<0.90 p.u. is far from normal steady-state operating condition, and the sensitivity based control may be ineffective. After t_3, a sensitivity-based distributed Q compensation (SBDQC) method could be applied to support the voltage by providing reactive powers from EIDGs.

In SBDQC, based on the bus voltages and the voltage sensitivity factors, a linear programming problem is formulated to solve the reactive power sharing among the EIDGs. The objective function is to minimize the total reactive power from the EIDGs.

$$f = min(Q'_{1,ref} + Q'_{2,ref} + \cdots + Q'_{l,ref}) \tag{5.16}$$

where l is the total number of the EIDGs in the MG, $Q'_{l,ref}$ is the reactive power reference for the controller of the lth EIDG.

The constraints are:

1) The voltage at bus j should stay within its security range:

$$V_j^{lower} \le \left(V_j + \Delta V_j\right) \le V_j^{upper} \tag{5.17}$$

where j is the number of the target bus, which consists of EIDG buses and weak buses (which are prone to have voltage issues); V_j is the voltage of bus j; $V_j^{lower} \le V_j \le V_j^{upper}$ is the voltage security range and is defined as $0.94\ \text{p.u.} \le V_j \le 1.06\ \text{p.u.}$ in this study [189]; ΔV_j is the voltage deviation at bus j and is calculated by (5.15).

2) The reactive power generated by $EIDG_l$ cannot exceed its maximum capability, $Q_{l,max}$.

$$0 < Q'_{l,ref} = \left(Q_{l,ref} + \Delta Q_l\right) \le Q_{l,max} \tag{5.18}$$

A flowchart for the proposed control algorithm is depicted in Figure 5.11. Once the islanding occurs, the algorithm determines whether to use MRP or SBDQC based on the condition whether V_j<0.90 p.u.. Then the calculated results $\left(Q'_{1,ref}, \cdots, Q'_{l,ref}\right)$ are sent to the controllers of $(EIDG_1, \cdots, EIDG_l)$ as the references of the power inverters.

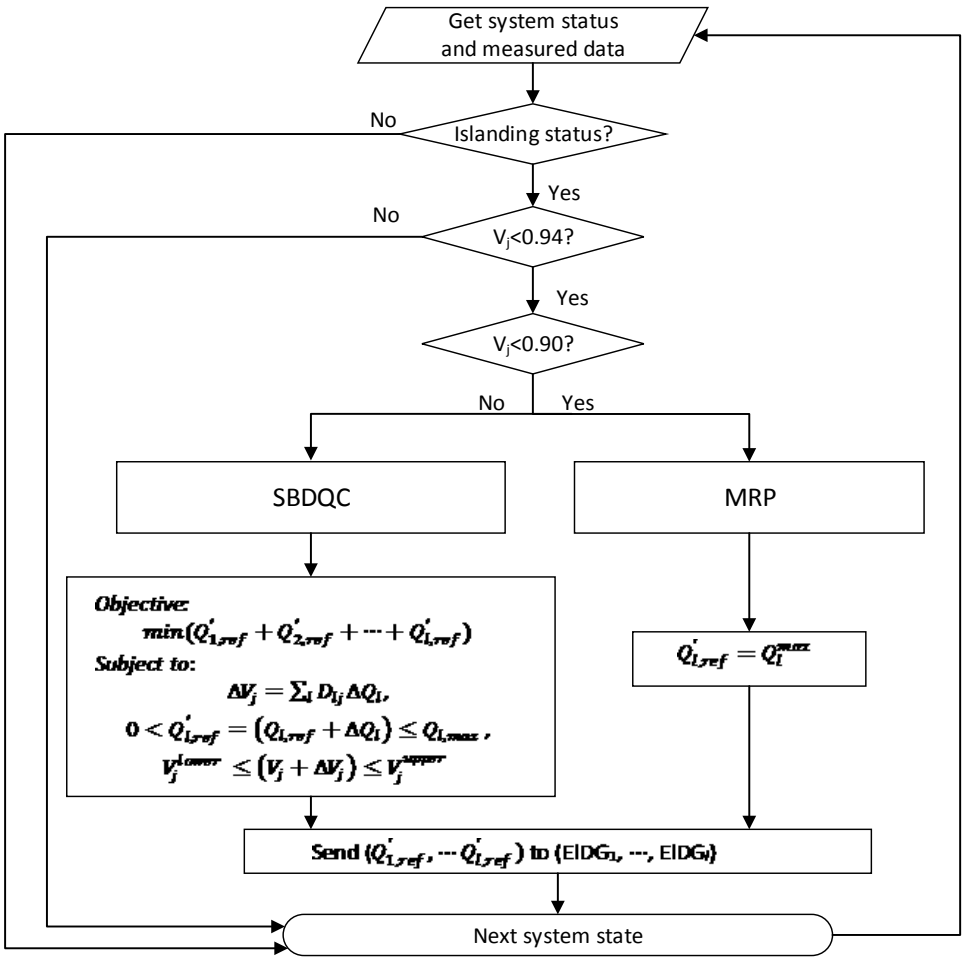

Figure 5.11 Reactive power management algorithm.

5.4 Simulation Results and Discussions

The proposed method has been validated on a MG test-bed described in Section 5.2. Dynamic simulations have been carried out using Simulink/SimPowerSystems [190]. The dynamic simulation system is shown in Figure 5.12.

In the simulation, it is assumed the MG starts at a steady-state operating condition where the voltage at the point of common coupling (PCC) is 1.05 p.u.. Two case studies are presented in this section. In the first case study, in order to find the weakest buses in this MG, both the PV and battery systems are operating at unity power factor with no reactive power output. In the

second case, the proposed RPMA is implemented. There are some assumptions and conditions defined for the simulations:

1) *Weather conditions*: It is assumed to be in a hot summer with 35 ºC ambient temperature and 1000 W/m^2 solar irradiance. The PV could generate at its nominal real power under this weather condition. The battery is also controlled to provide its nominal real power. In this condition, the capabilities of reactive power generation of PV and battery system are both limited to 398kVar.

2) *Buses selection*: From the preliminary simulation results, it has been observed that buses 611 and 652 are the weakest buses in this MG in terms of voltage security, which coincides with the original feeder information [180] and the previous study reported in [173]. Therefore, only the voltage at the weak buses, 611 and 652, and the EIDG buses, 675 and 680, are presented and discussed.

3) *Composition of loads and power sources*: In the MG, the power ratings of the loads and the line parameters are modified by using the method in [16]. The penetration of SPIMs in the studied MG is designed to be 1098.1kVA, which takes 40.53% of the total loads. The rated powers of PV and battery converters are 720kVA, which means they are capable of providing 398kVar reactive power when the nominal real power output is generated. In addition, the conventional loads are kept unbalanced like in the original feeder that loads on Phase B is a little lighter than Phase A and Phase C, but the total loads are designed to be nearly balanced in three phases. The rated power of resources and loads in the MG are listed in TABLE 5.5.

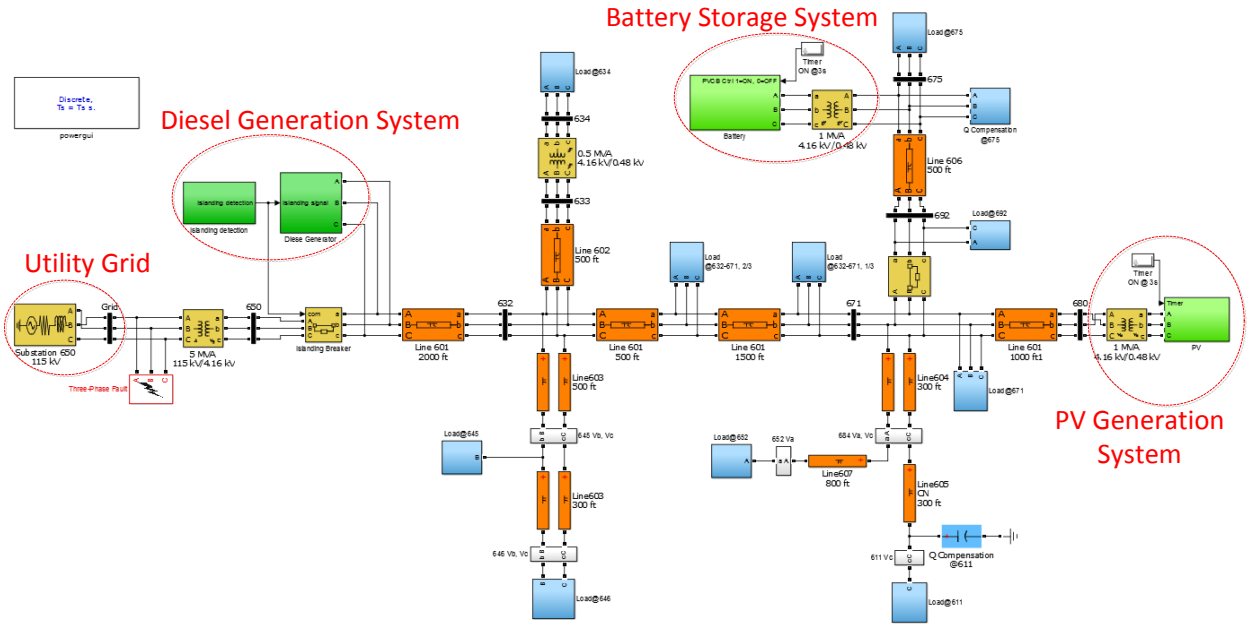

Figure 5.12 Simulation system of the studied microgrid in MATLAB/Simulink.

TABLE 5.5 POWER SOURCES AND LOADS COMPOSITION IN THE STUDIED MICROGRID

	Types	*kW or kVar*	S_{load} *(kVA)*	$(S_{load}/S_{load}^{total})\%$
Loads	Motor loads	*P*=909.6 *Q*=615.2	1098.1	40.53%
	Other loads	*P*=1396.8 *Q*=797.9	1608.6	59.47%
	S_{load}^{total}	*P*=2106.4 *Q*=1413.1	2536.5	*N/A*
	Types	*kW or kVar*	S_{source} *(kVA)*	$(S_{source}/S_{source}^{total})\%$
Power Sources	PV	*P*=600 *Q*=398	720	15.8%
	Battery	*P*=600 *Q*=398	720	15.8%
	Diesel Generator	*N/A*	3125	68.4%
	S_{source}^{total}	*N/A*	4565	*N/A*

5.4.1 Case study 1: without Q compensation

The voltage magnitudes at buses 611, 652, 675, and 680 are shown in Figure 5.13. At *t*=8s, a three phase to ground fault occurs at the utility grid and is not cleared until the MG detects

the fault and islands itself from the utility grid after 7 cycles. The voltage at the PCC drops to as low as 0.5 p.u., triggering a large-scale stalling of the SPIMs. The stalling of SPIMs further slows down the voltage recovery process. The voltage recovery time is found to be around 0.8s in this study. Due to the insufficiency in reactive power, after reaching the steady state, the voltages at buses 611 and 652 only recover to 0.90 p.u.. Even for buses 675 and 680, on which EIDGs are installed, their voltages are well below the lower limit. Ten seconds after the islanding, the SPIMs are cut off from the MG by the equipped thermal protection devices. Since the PV and battery are still generating the nominal real power, the voltage of Phase B on the buses 675 and 680 rises up to the upper limit.

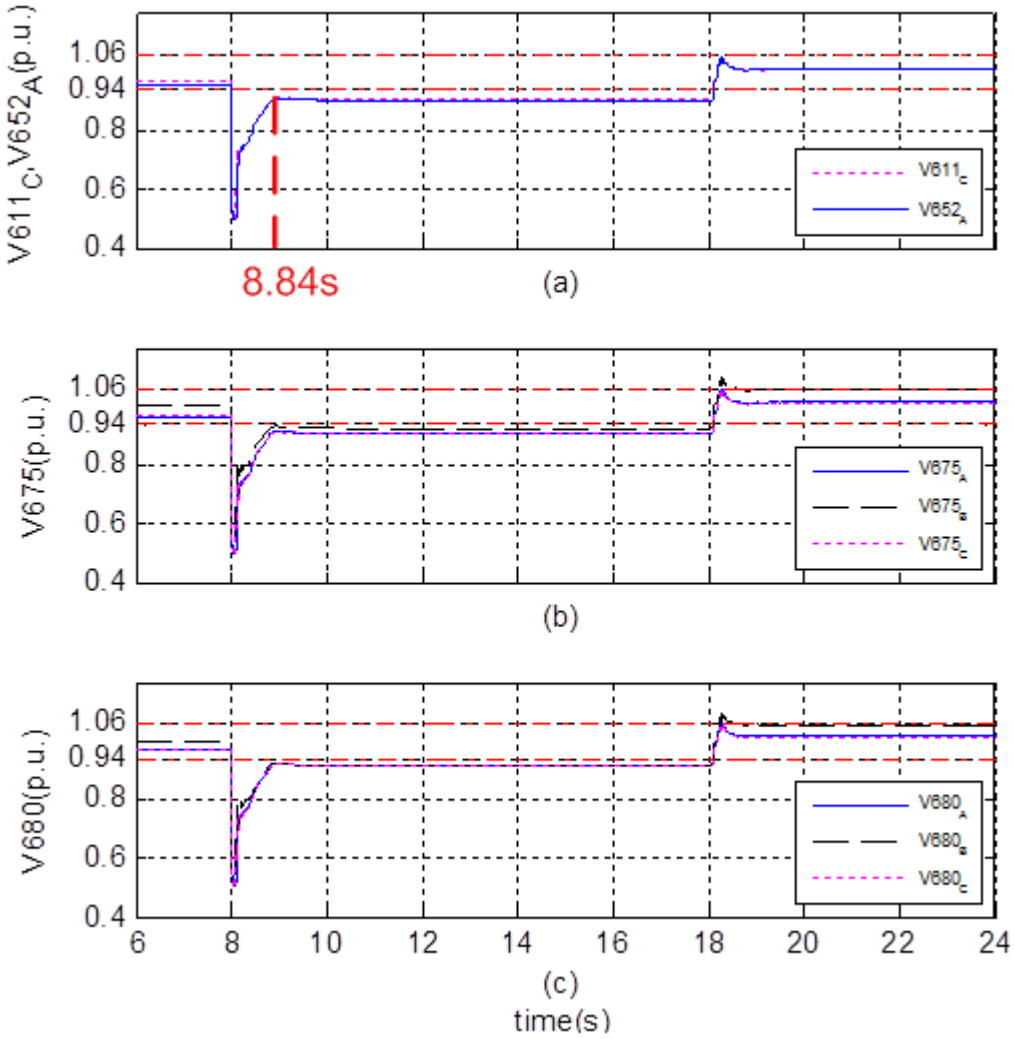

Figure 5.13 Voltage at buses 611, 652, 675, and 680 without Q compensation.

5.4.2 Case study 2: with reactive power management algorithm

Voltage sensitivity factors are basics of the proposed RPMA and are firstly calculated. Based on calculations, the sensitivity factors are close for the three load conditions: without SPIMs, with SPIMs, and with stalled SPIMs. The sensitivity factors used in this study are calculated by averaging the sensitivity coefficients obtained under these three loading conditions. Since the system is three phase unbalanced, these factors are different for each phase. For simplicity, only the sensitivity factors associated with the EIDG buses and the weak buses (675, 680, 611, and 652) are listed in TABLE 5.6.

TABLE 5.6 SENSITIVITY FACTORS BY GENERATING 100 KVAR REACTIVE POWER ON EVERY PHASE FROM EIDGS

	V_{675}			V_{680}			V_{611}	V_{652}
	A	*B*	*C*	*A*	*B*	*C*	*C*	*A*
Q_{675}	0.0268	0.0233	0.0227	0.0238	0.0218	0.0208	0.0208	0.0238
Q_{680}	0.0252	0.0224	0.0205	0.0295	0.0274	0.0248	0.0205	0.0246

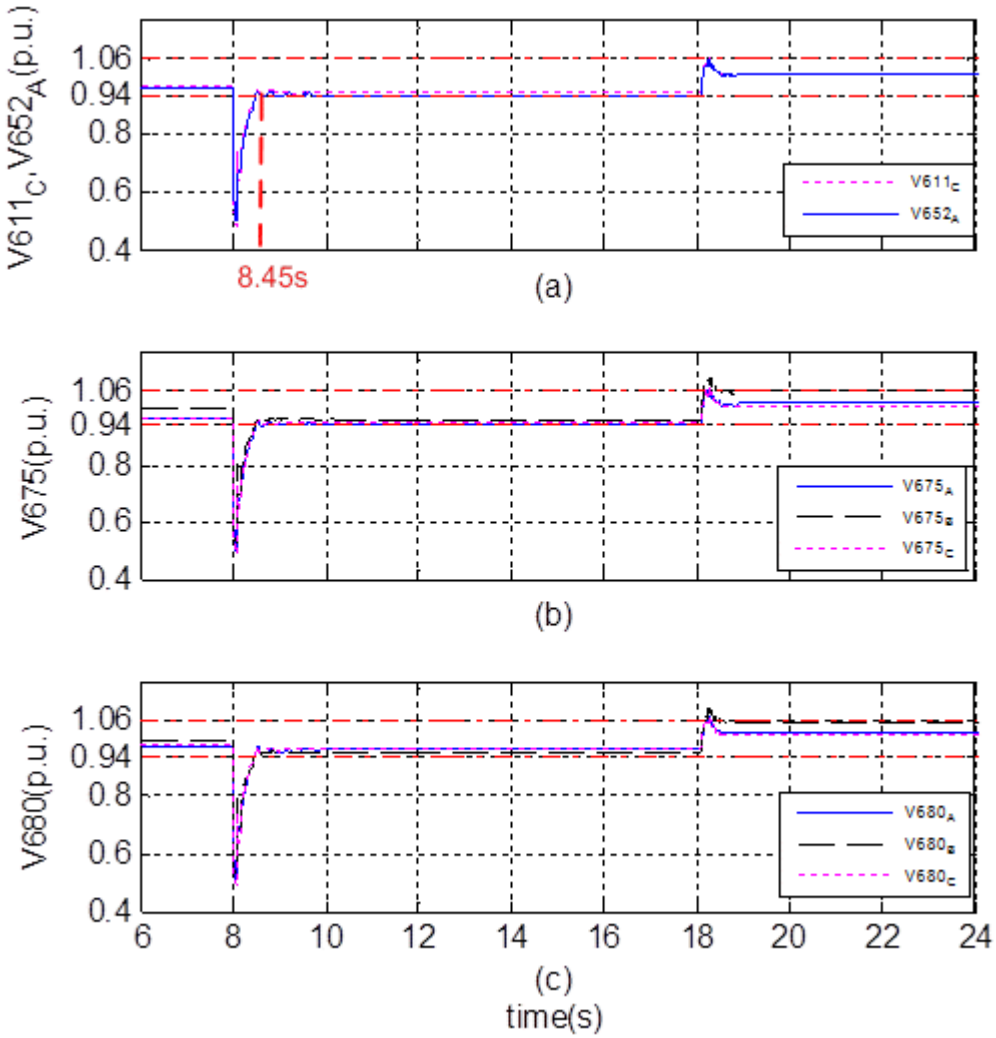

Figure 5.14 Voltage at buses 611, 652, 675, and 680 with distributed Q compensation.

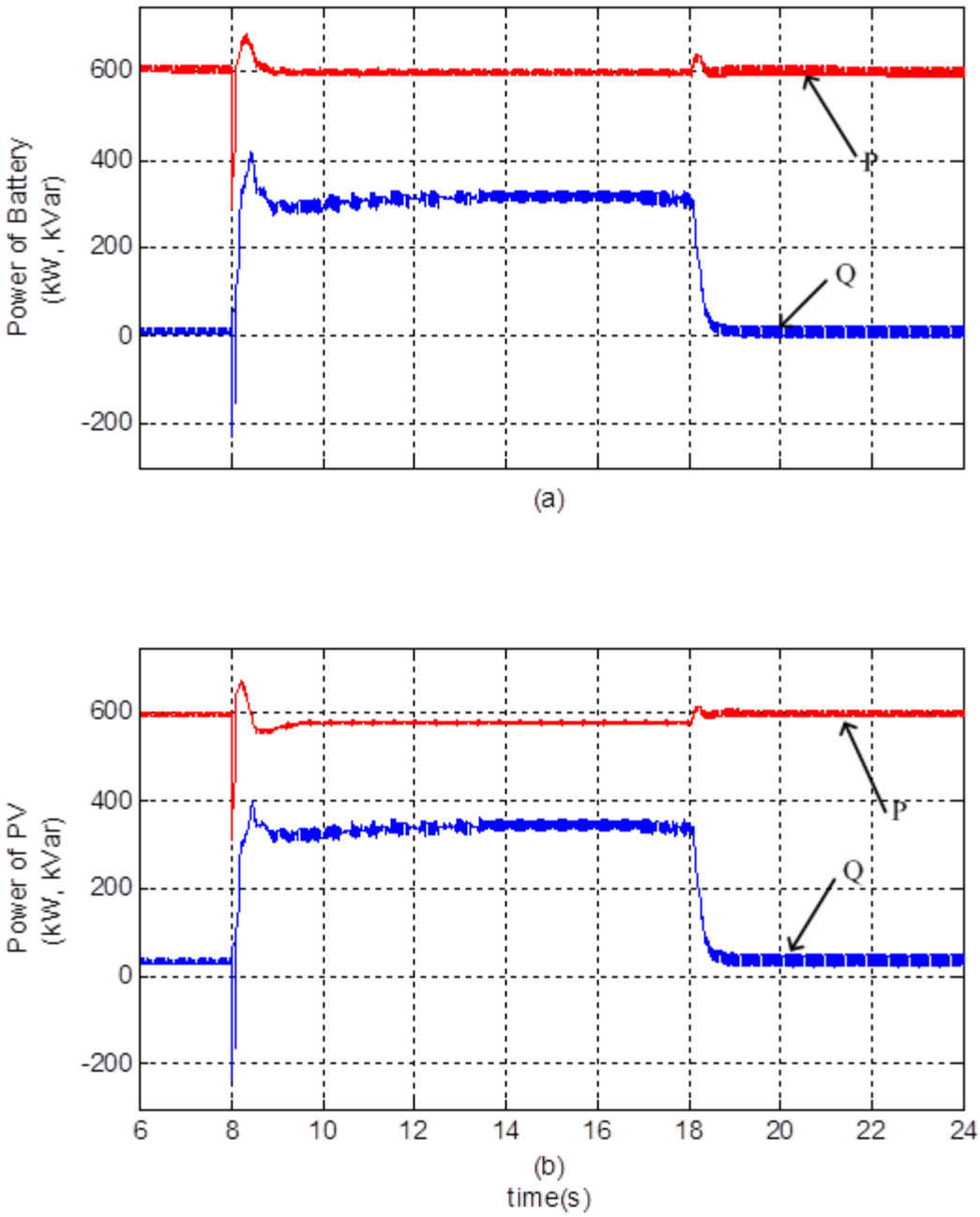

Figure 5.15 Sharing of power between PV and battery.

The RPMA is utilized to maintain the voltage security by sharing the reactive power between the PV and the battery. The voltages shown in Figure 5.14 restore fast during the islanding process and behave well within the security range subsequent to the islanding process. In Figure 5.15, immediately after the islanding, the voltages are compensated by MRP from the

PV and the battery. The time for voltage recovery is shortened to only around 0.4s. In addition, after the voltages recover to 0.90 p.u., the algorithm calculates the best composition of the reactive power from the PV and the battery to maintain the voltages. As shown in Figure 5.15, the SBDQC determines the battery is controlled to generate maximum Q, but the PV does not. In addition, the algorithm automatically reduces the reactive powers from the PV and the battery to avoid the voltages on Phase B of buses 675 and 680 violating the upper limit when the stalling SPIMs are isolated.

In Figure 5.16, the simulation results of the diesel generation system (DGS) are presented. Prior to t=8.0s, the DGS is controlled in P&Q control mode to generate the preset 0.3 p.u. real power, which corresponds around 45% of the total real power. Seven cycles after the fault occurs, the DGS is changed to V&f control mode to provide the references of voltage and frequency. In Figure 5.16(a), after the islanding, it takes around 0.4s for the voltage to restore to the nominal value. In addition, the speed is controlled to be the synchronous speed which guarantees the system frequency is not distorted as shown in Figure 5.16(b). In Figure 5.16(c), the power generated by the DGS rises to 0.45 p.u. to track the extra demands of the stalling SPIMs. After the SPIMs are all isolated from the grid, P_{mec} decreases to 0.1 p.u. to maintain the power balance of the MG.

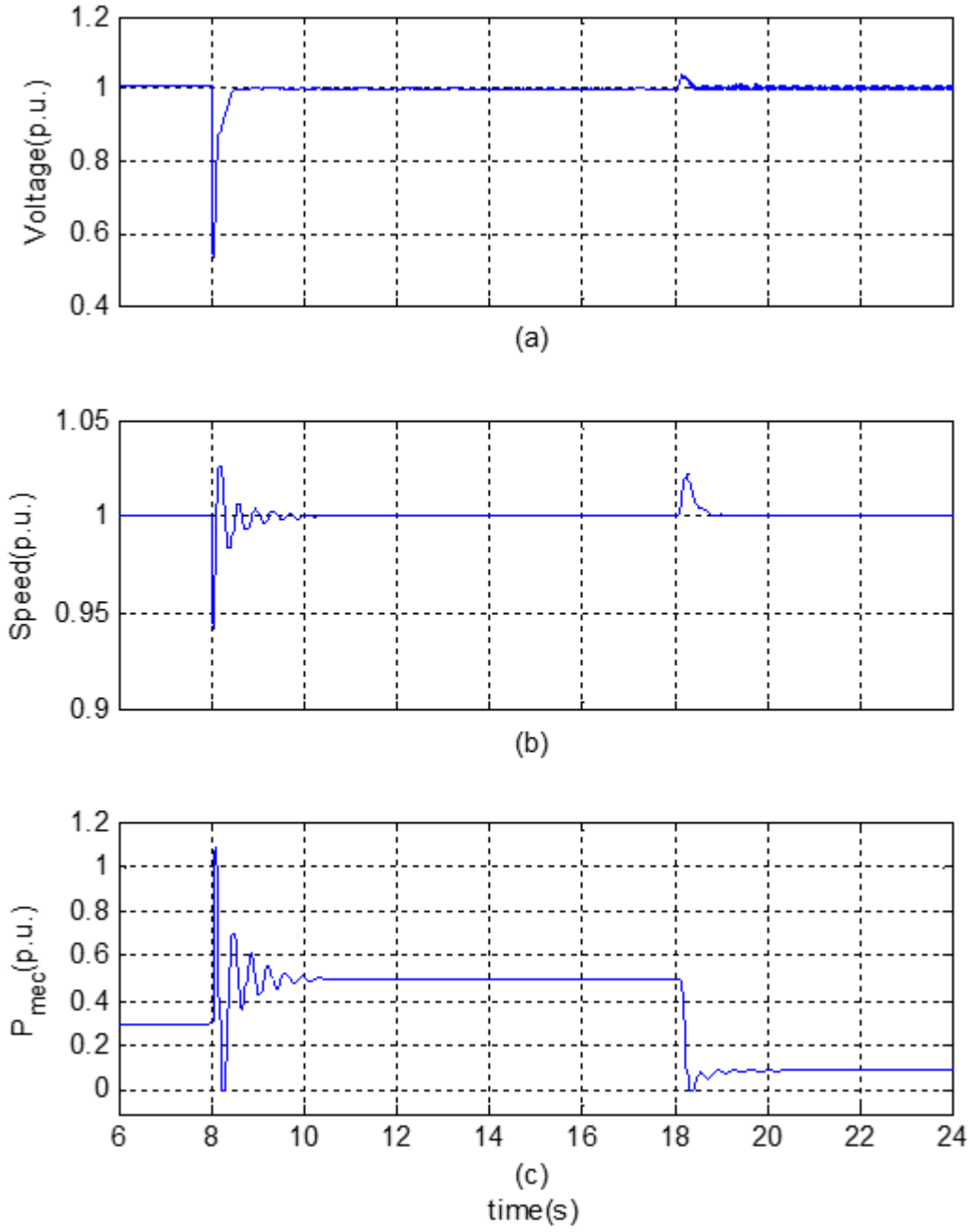

Figure 5.16 Simulation results of the DGS, (a) output voltage, (b) speed, and (c) real power output.

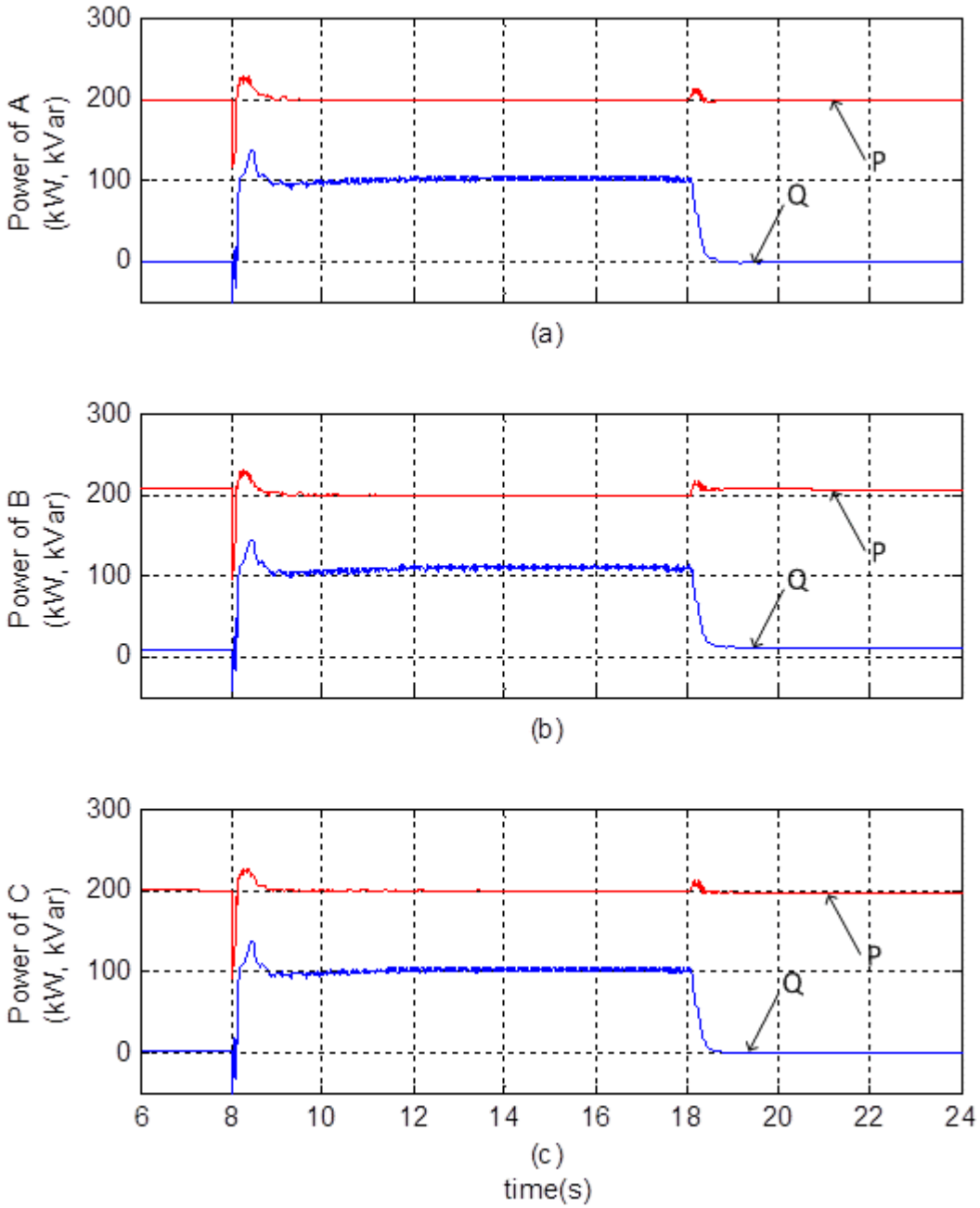

Figure 5.17 P&Q of the battery of (a) Phase A, (b) Phase B, and (c) Phase C.

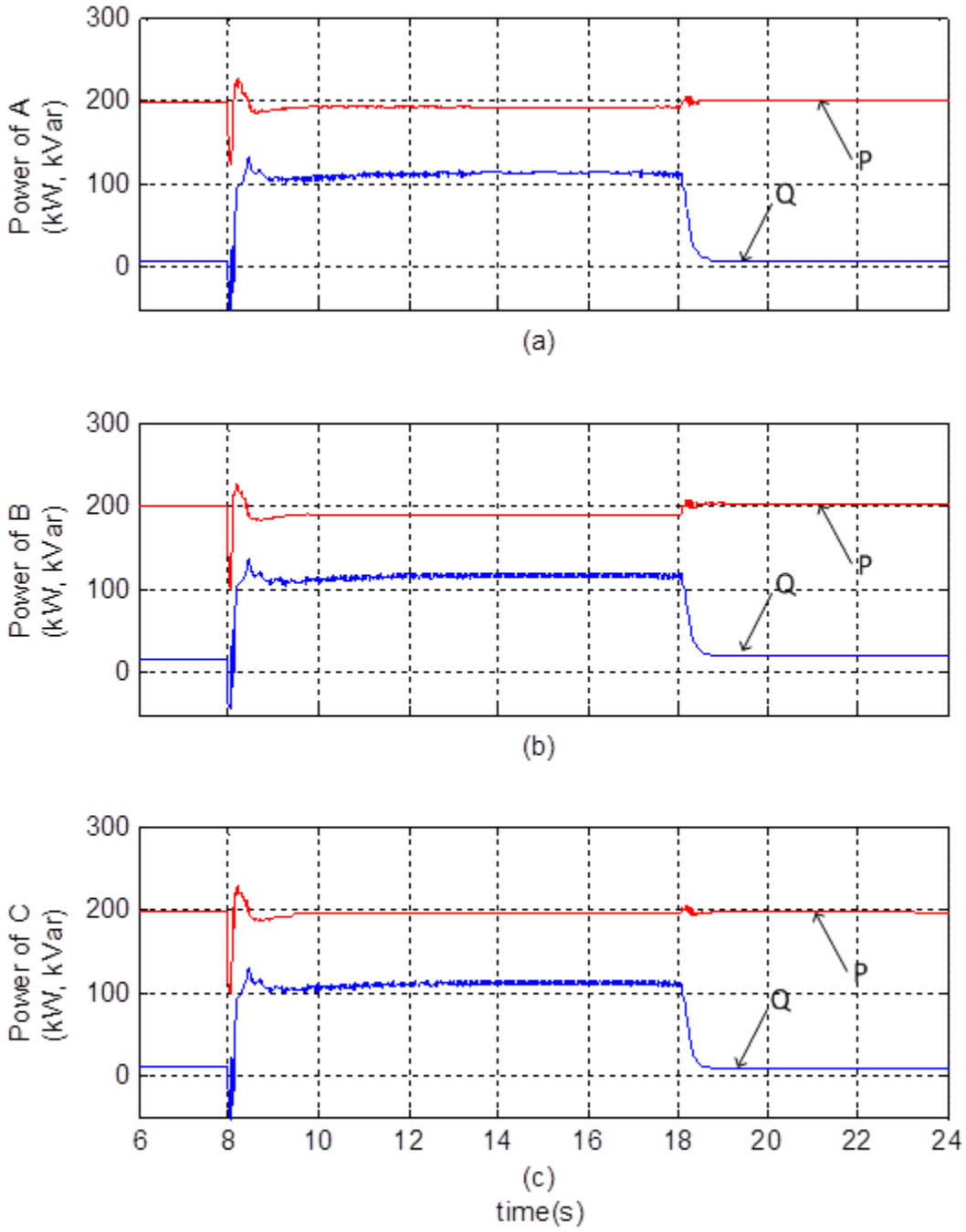

Figure 5.18 P&Q of the PV of (a) Phase A, (b) Phase B, and (c) Phase C.

In addition, to verify the effectiveness of the PQ controller designed to control the three-phase power, P and Q generations of the battery and PV for all three phases are shown in Figure 5.17 and Figure 5.18. It is clearly shown that the real and reactive powers are both averagely

shared by three phases no matter how the three-phase voltages are unbalance at buses 675 and 680.

From the comparison, it can be seen that the RPMA accelerates the voltage recovery process during and subsequent to the islanding process. In addition, by optimally dispatching the reactive power generation from EIDGs, it guarantees all the voltages in the MG behave well within the voltage security limits.

5.5 Conclusion

The voltage security issues in a MG with high penetration of single-phase induction machines under the condition of fault-induced islanding were studied. The stalled SPIMs consume large amount of reactive power and could significantly delay the process of voltage recovery. To accelerate the voltage recovery process while avoiding voltage violations, a voltage-sensitivity-based reactive power management algorithm was proposed in this chapter. The effectiveness of the proposed algorithm has been validated by the simulation results conducted on a modified version of the IEEE standard 13-bus test feeder with three DGs.

CHAPTER 6 SUMMARY AND FUTURE WORK

6.1 Conclusion

In Chapter 2, we presented the safety control of PEVs in distribution networks by using finite state machine with variables (FSMwV). First, basic DES theories based on finite state machine and supervisory control are introduced. Then a novel control synthesis under the modeling framework of FSMwV was proposed. An offline safety control synthesis procedure that takes the advantage of both event disablement and enforcement in order to prevent the controlled system from venturing into illegal states and an online safety control synthesis procedure based on the limited/variable lookahead policies to address the practical concern of real world implementation have been developed. In the end, the theoretical result has been implemented to control PEVs in distribution networks.

In Chapter 3, a voltage stability incorporated optimization method was proposed to maximize the injection of PEVs in DNs without violating power limits and causing voltage stability issues. We first presented an optimization injection method to maximize the injection of PEVs without causing the voltage stability issue in the DN. The simulation results on the IEEE 33-Bus test feeder show that the proposed optimization injection method can better utilize the power resources of DN to maximize the injection of PEVs. This method provides a clear reference to DNO to manage the charging of the PEVs in DNs.

In Chapter 4, we introduced a universal demonstration platform to further explore the active management of PEVs in the DNs. The platform is composed of software for the master station (MS) and the remote terminal units (RTUs) and the hardware demonstration set of charging stations. The management algorithm for the MS and the RTUs are flexible to integrate priority

algorithm of charging to meet the demands from PEV owners. Based on the ADAM-6066 modules, the RTUs are able to communicate with MS and charging stations and carry out the demands to charge PEVs or not. The demonstrated method is suitable for applications in active distribution networks to manage PEVs and can be extendable to the management of renewable energy sources.

In Chapter 5, we studied the voltage security issues in a MG with high penetration of single-phase induction machines under the condition of fault-induced islanding. The stalled SPIMs consume large amount of reactive power and could significantly delay the process of voltage recovery. To accelerate the voltage recovery process while avoiding voltage violations, a voltage-sensitivity-based reactive power management algorithm was proposed in this chapter. The effectiveness of the proposed algorithm has been validated by the simulation results conducted on a modified version of the IEEE standard 13-bus test feeder with three DGs.

6.2 Future Work

First we will not only continue our work in modeling the power systems through discrete event systems, but also extend it to model power systems as a hybrid machine. The continuous variables in power systems, such as voltages, currents and powers and the discrete events, such as the participation of the capacitors and DGs will be jointly modelled and controlled. The hybrid method will be adapted to model standalone devices, *e.g.*, wind generation system and solve the power quality issues in DNs.

In addition, we will improve the demonstration platform. To save the cost, an embedded controller with monitor, such as digital signal processor (DSP) will be used to replace the computers for remote terminal units (RTUs). On the other hand, the platform will be extended to manage and control renewable energy sources and energy storage. Therefore, the flexibility,

extendibility and capabilities of the platform are enhanced and will be more competent to demonstrate the active management of DNs.

From the viewpoint of distribution network, the coordination of energy storage and the DGs will bring more challenges and opportunities. We will continue our previous work on distribution networks to propose active management strategies to improve system reliability and stability. A microgrid-based distribution network (MDN) changes its original function in a large power grid. A MDN is no longer only a PQ node, and could play a more important role. For example, a MDN could enhance the margin of voltage stability, provide reactive power support to the grid, and guarantee the security of critical loads during blackout. We will explore these promising research areas.

APPENDIX A

Based on the single-line equivalent system model for a node *k* in a DN in Figure A.1, the equivalent node voltage collapse index (*ENVCI*) is used to investigate the impact of the injection of PEVs to DN [165].

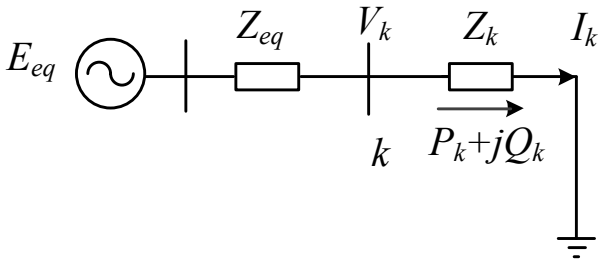

Figure A.1 Single-line model.

The outgoing power at node *k* has to satisfy the following simple power flow equations:

$$P_k + jQ_k = V_k \cdot \left(\frac{E_{eq} - V_k}{Z_{eq}}\right)^* \tag{A.1}$$

If the voltage phasors at the two nodes of the equivalent single line model are expressed in the rectangular coordinates, i.e., $E_{eq} = |E_{eq}|\angle\theta_{eq} = e_{eq,x} + je_{eq,y}$, $V_k = |V_k|\angle\theta_k = v_{k,x} + jv_{k,y}$, and $Z_{eq} = R_{eq} + jX_{eq}$, then (A.1) can be separated into a real part and an imaginary part as follows:

$$\begin{aligned} P_k R_{eq} + Q_k X_{eq} &= v_{k,x}(e_{eq,x} - v_{k,x}) + v_{k,y}(e_{eq,y} - v_{k,y}) \\ P_k X_{eq} - Q_k R_{eq} &= e_{eq,y} v_{k,x} - e_{eq,x} v_{k,y} \end{aligned} \tag{A.2}$$

The solvability of (A.2) can be judged by singularity of its Jacobian matrix, i.e.,

$$J = \begin{bmatrix} e_{eq,x} - 2v_{k,x} & e_{eq,y} - 2v_{k,y} \\ e_{eq,y} & -e_{eq,x} \end{bmatrix} \tag{A.3}$$

$$det(J) = 2(e_{eq,x} v_{k,x} + e_{eq,y} v_{k,y}) - (e_{eq,x}^2 + e_{eq,y}^2) = 0 \tag{A.4}$$

ENVCI can be represented as:

$$ENVCI = 2\left(e_{eq,x}v_{k,x} + e_{eq,y}v_{k,y}\right) - \left(e_{eq,x}^2 + e_{eq,y}^2\right) \quad \text{(A.5)}$$

The expression of *ENVCI* can be also re-written in polar coordinates as

$$ENVCI = 2\left|E_{eq}\right||V_k|\cos(\theta) - \left|E_{eq}\right|^2 \quad \text{(A.6)}$$

where θ is the angle deference of θ_{eq} and θ_k.

Whenever the $ENVCI_n$ of at least one node in the system is very low, it indicates that the system approaches its voltage collapse point. Under a given operating condition, obviously, the node with the lowest value of $ENVCI_n$ is the weakest node that may cause system instable under that condition. This method relieves the required computing burden and is able to real-time follow the variation of loads and generators.

REFERENCES

[1] C. Gellings, "Power to the people," *IEEE Power&Energy Magazine,* pp. 52-63, 2011.

[2] A. Keane and M. O'Malley, "Optimal allocation of embedded generation on distribution networks," *IEEE Trans. Power Systems,* vol. 20, pp. 1640-1646, 2005.

[3] G. Celli and F. Pilo, "Optimal sectionalizing switches allocation in distribution networks," *IEEE Trans. Power Delivery,* vol. 14, pp. 1167-1172, 1999.

[4] H. Khani, M. Moallem, S. Sadri, and M. Dolatshahi, "A new method for online determination of the location of switched capacitor banks in distribution systems," *IEEE Trans. Power Delivery,* vol. 26, pp. 341-351, 2011.

[5] C. S. Chang and Z. M. Yu, "Distributed mitigation of voltage sag by optimal placement of series compensation devices based on stochastic assessment," *IEEE Trans. Power Systems,* vol. 19, pp. 788-795, 2004.

[6] S. Bhattacharya, T. Zhao, G. Wang, S. Dutta, S. Baek, Y. Du, *et al.*, "Design and development of generation-I silicon based solid state transformer," in *Proc. IEEE-APEC*, Palm Springs, CA, 2010.

[7] C. L. Hsu, S. Y. Yang, and W. B. Wu, "3C intelligent home appliance control system - example with refrigerator," *Expert Systems with Applications,* vol. 37, pp. 4337-4349, 2010.

[8] A. A. Gumaste, "Electrigence: electrical distribution networks with added intelligence for home/office automation and control," in *Proc. IEEE International Symposium on Power Line Communications and Its Applications*, Piscataway, NJ, 2007.

[9] T. Bopp, A. Shafiu, I. Cobelo, I. Chilvers, N. Jenkins, G. Strbac, *et al.*, "Commercial and technical integration of distributed generation into distribution networks," in *Proc. of CIRED Inter. Conference Electric Distribution*, Barcelona, Spain, 2003.

[10] T. Senjyu, Y. Miyazato, A. Yona, N. Urasaki, and T. Funabashi, "Optimal distribution voltage control and coordination with distributed generation," *IEEE Trans. Power Delivery,* vol. 23, pp. 1236-1242, 2008.

[11] M. E. Elkhatib, R. El-Shatshat, and M. M. A. Salama, "Novel coordinated voltage control for smart distribution networks with DG," *IEEE Trans. Smart Grid,* vol. 2, pp. 598-605, 2011.

[12] C. Hird, H. Leite, N. Jenkis, and H. Li, "Network voltage controller for distributed generation," *Proc. Indus. Electr. Eng. Gener. Transm. Distr.,* vol. 151, pp. 150-156, 2004.

[13] T. Sansawatt, J. O'Donnell, L. F. Ochoa, and G. P. Harrison, "Decentralised voltage control for active Distribution Networks," in *Proc. Inter. Univer. Power Eng. Conf.*, Glasgow, Scotland, 2009.

[14] P. H. Divshali, S. H. Hosseinian, and M. Abedi, "Enhancing small signal stability and reactive power-sharing accuracy in autonomous microgrids by a new decentralized reactive power controller," *Electric Power Components and Systems,* vol. 40, pp. 1820-1841, 2013.

[15] P. Piagi and R. H. Lasseter, "Autonomous control of microgrids," in *Proc. IEEE PES General Meeting*, Montreal, 2006.

[16] Q. Fu, F. Montoya, A. Solanki, A. Nasiri, V. Bhavaraju, T. Abdallah*, et al.*, "Microgrid generation capacity design with renewables and energy storage addressing power quality and surety," *IEEE Trans. Smart Grid,* vol. 3, pp. 2019-2027, 2012.

[17] J. Kim, J. Jeon, S. Kim, C. Cho, J. Park, H. Kim*, et al.*, "Cooperative control strategy of energy storage system and microsources for stabilizing the microgrid during islanded operation," *IEEE Trans. Power Electronics,* vol. 25, pp. 3037-3048, 2010.

[18] F. A. Viawan, A. Sannino, and J. Daalder, "Voltage control with on-load tap changers in medium voltage feeders in presence of distributed generation," *Electric Power Systems Research,* vol. 77, pp. 1314-1322, 2007.

[19] L. Yu, D. Czarkowski, and F. d. León, "Optimal distributed voltage regulation for secondary networks with DGs," *IEEE Trans. Smart Grid,* vol. 3, pp. 959-967, 2012.

[20] C. Rehtanz, *Autonomous Systems and Intelligent Agents in Power System*. Berlin, Germany: Springer, 2003.

[21] C. M. Colson, M. H. Nehrir, R. K. Sharma, and B. Asghari, "Improving sustainability of hybrid energy systems Part II: managing multiple objectives with a multiagent system," *IEEE Trans. Sustainable Energy,* 2013.

[22] S. McArthur and E. Davidson, "Concepts and approaches in multi-agent systems for power applications," in *Proc. Inter. Conf. Intell. Syst. Appl. Power Syst.*, 2005.

[23] M. E. Baran and I. M. El-Markabi, "A multiagent-based dispatching scheme for distributed generators for voltage support on distribution feeders," *IEEE Trans. Power Systems,* vol. 22, pp. 52-59, 2007.

[24] A. Dimeas and N. Hatziargyriou, "Operation of a multiagent system for microgrid control," *IEEE Trans. Power Systems,* vol. 20, pp. 1447-1455, 2005.

[25] A. Molderink, V. Bakker, M. Bosman, J. Hurink, and G. Smit, "Management and control of domestic smart grid technology," *IEEE Trans. Smart Grid,* vol. 1, pp. 109-119, 2010.

[26] P. Vovos, A. Kiprakis, A. Wallace, and G. Harrison, "Centralized and distributed voltage control: impact on distributed generation penetration," *IEEE Trans. Power Systems,* vol. 22, pp. 476-483, 2007.

[27] B. Zhao, X. Zhang, and J. Chen, "Integrated microgrid laboratory system," *IEEE Trans. Power Systems,* vol. 27, pp. 2175-2185, 2012.

[28] Z. Jiang and R. A. Dougal, "Hierarchical microgrid paradigm for integration of distributed energy resources," in *Proc. IEEE PES General Meeting-Conversion and Delivery of Electricity Energy in 21st Centrury*, Pittsburgh, PA, 2008.

[29] C. X. Dou, D. L. Liu, X. B. Jia, and F. Zhao, "Management and control for smart microgrid based on hybrid control theory," *Electric Power Components and Systems,* vol. 39, pp. 813-832, 2011.

[30] J. M. Guerrero, J. C. Vasquez, J. Matas, L. Vicuña, and M. Castilla, "Hierarchical control of droop-controlled AC and DC microgrids—a general approach toward standardization," *IEEE Trans. Industrial Electronics,* vol. 58, pp. 158-172, 2011.

[31] E. Naderi, I. Kiaei, and M. Haghifam, "NaS technology allocation for improving reliability of DG-enabled distribution networks," in *Proc. IEEE International Confer. Probability Methods Applied to Power Systems*, 2010.

[32] C. Wang and M. Nehrir, "Analytical approaches for optimal placement of distributed generation sources in power systems," *IEEE Trans. Power Systems,* vol. 19, pp. 2068-2076, 2004.

[33] M. Sedghi, M. Aliakbar-Golkar, and M. R. Haghifam, "Distribution network expansion considering distributed generation and storage units using modified PSO algorithm," *International Journal of Electrical Power and Energy Systesms,* vol. 52, pp. 221-230, 2013.

[34] A. Piccolo and P. Siano, "Evaluating the impact of network investment deferral on distributed generation expansion," *IEEE Trans. Power Systems,* vol. 24, pp. 1559-1567, 2009.

[35] W. El-Khattam, K. Bhattacharya, Y. Hegazy, and M. M. A. Salama, "Optimal investment planning for distributed generation in a competitive electricity market," *IEEE Trans. Power Systems,* vol. 19, pp. 1674-1684, 2004.

[36] Y. M. Atwa, E. F. El-Saadany, M. M. A. Salama, and R. Seethapathy, "Optimal renewable resources mix for distribution system energy loss minimization," *IEEE Trans. Power Systems,* vol. 25, pp. 360–370, 2010.

[37] G. Celli, E. Ghiani, S. Mocci, and F. Pilo, "A multiobjective evolutionary algorithm for the sizing and siting of distributed generation," *IEEE Trans. Power Systems,* vol. 20, pp. 750-757, 2005.

[38] I.-S. Bae, J.-O. Kim, J.-C. Kim, and C. Singh, "Optimal operating strategy for distributed generation considering hourly reliability worth," *IEEE Trans. Power Systems,* vol. 19, pp. 287-292, 2004.

[39] M. Shaaban, Y. Atwa, and E. El-Saadany, "DG allocation for benefit maximization in distribution networks," *IEEE Trans. Power Systems,* vol. 28, pp. 639-649, 2013.

[40] N. Pogaku, M. Prodanovic, and T. C. Green, "Modeling, analysis and testing of autonomous operation of an inverter-based microgrid," *IEEE Trans. Power Electronics,* vol. 22, pp. 613-625, 2007.

[41] J. He and Y. W. Li, "An enhanced microgrid load demand sharing strategy," *IEEE Trans. Power Electronics,* vol. 27, pp. 3984 - 3995, 2012.

[42] H. S. Ko, G. G. Yoon, and W. P. Hong, "Active use of DFIG-based variable-speed wind-turbine for voltage regulation at a remote location," *IEEE Trans. Power Systems,* vol. 22, pp. 1916-1925, 2007.

[43] H. Li, F. Li, and Y. Xu, "Adaptive voltage control with distributed energy resources: algorithm, theoretical analysis, simulation, and field test verification," *IEEE Trans. Power Systems,* vol. 25, pp. 1638-1647, 2010.

[44] K. Turitsynn, P. Sulc, S. Backhaus, and M. Chertkov, "Options for control of reactive power by distributed photovoltaic generators," *Proceedings of IEEE,* vol. 99, pp. 1063-1073, 2011.

[45] R. Shivarudraswamy and D. N. Gaonkar, "Coordinated voltage regulation of distribution network with distributed generators and multiple voltage-control devices," *Electric Power Components and Systems,* vol. 40, pp. 1072-1088, 2012.

[46] Y. Kim, S. Ahn, P. Hwang, G. Pyo, and S. Moon, "Coordinated control of a DG and voltage control devices using a dynamic programming algorithm," *IEEE Trans. Power Systems,* vol. 28, pp. 42-51, 2013.

[47] R. Tonkoski, L. Lopes, and T. El-Fouly, "Coordinated active power curtailment of grid connected PV inverters for overvoltage prevention," *IEEE Trans. Sustainable Energy,* vol. 2, pp. 139-147, 2011.

[48] Q. Zhou and J. W. Bialek, "Generation curtailment to manage voltage constraints in distribution networks," *IET Gener., Trans. Distr.,* vol. 1, pp. 492 – 498, 2007.

[49] Y. Wang, P. Zhang, N. Kanan, W. Li, and W. Xiao, "Online overvoltage prevention control of photovoltaic generators in microgrids," *IEEE Trans. Smart Grid,* vol. 3, pp. 2071-2078, 2012.

[50] W. Freitas, J. C. M. Vieira, A. Morelato, and W. Wu, "Influence of excitation system control modes on the allowable penetration level of distributed synchronous generators," *IEEE Trans. Energy Conversion,* vol. 20, pp. 474-480, 2005.

[51] M. Duvall, "Grid Integration of Plug-In Hybrid Electric Vehicles," Electric Power Research Institute2009.

[52] K. Clement, E. Haesen, and J. Driesen, "The impact of charging plug-in hybrid electric vehicles on the distribution grid," *IEEE Trans. Power Systems,* vol. 25, pp. 371-380, 2008.

[53] J. Zhao, Y. Chen, Z. Chen, F. Lin, C. Wang, and H. Zhang, "Modeling and control of discrete event systems using finite state machines with variables and their applications in power grids," *Systems & Control Letters,* vol. 61, pp. 212-222, 2012.

[54] J. Zhao, Z. Chen, F. Lin, C. Wang, and H. Zhang, "Safety control of PHEVs in distribution networks using finite state machines with variables," in *Proc. North American Power Symposium*, 2011.

[55] W. Kempton and J. Tomic, "Vehicle-to-grid power fundamentals: Calculating capacity and net revenue," *Jour. Power Sources,* vol. 144, pp. 268-279, 2005.

[56] New York Independent System Operator, "Alternative route: electrifying the transportation sector," New York ISO, NY 2009.

[57] M. H. Albadi and E. F. El-Saadany, "Demand response in electricity markets: an overview," in *Proc. IEEE PES General Meeting*, 2007.

[58] K. Marchese, S. A. Pourmousavi, and M. H. Nehrir, "The application of demand response for frequency regulation in an islanded microgrid with high penetration of renewable generation," in *Proc. IEEE North America Power Symposium*, 2013.

[59] N. C. Scott, D. J. Atkinson, and J. E. Morrell, "Use of load control to regulate voltage on distribution networks with embedded generation," *IEEE Trans. Power Systems,* vol. 17, pp. 510-515, 2002.

[60] N. Lu and D. P. Chassin, "A state queueing model of thermostatically controlled appliances," *IEEE Trans. Power Systems,* vol. 19, pp. 1666-1673, 2004.

[61] S. Shao, M. Pipattanasomporn, and S. Rahman, "Demand response as a load shaping tool in an intelligent grid with electric vehicles," *IEEE Trans. Smart Grid,* vol. 2, pp. 624-631, 2011.

[62] G. Strbac, "Demand side management: benefits and challenges," *Energy Policy,* vol. 36, pp. 4419-4426, 2008.

[63] Y. Zong, D. Kullmann, A. Thavlov, O. Gehrke, and H. W. Bindner, "Application of model predictive control for active load management in a distributed power system with high wind penetration," *IEEE Trans. Smart Grid,* vol. 3, pp. 1055-1062, 2012.

[64] R. Walling, R. Sain, R. Dugan, J. Burke, and L. Kojovic, "Summary of distributed resources impact on power delivery," *IEEE Trans. Power Delivery,* vol. 23, pp. 1636-1644, 2008.

[65] Y. Baghzouz, "General rules for distributed generation - feeder interaction," in *Proc. IEEE PES General Meeting*, 2006.

[66] G. Carpinelli, G. Celli, F. Pilo, and A. Russo, "Distributed generation siting and sizing under uncertainty," in *Proc. IEEE Porto Power Tech Conference*, 2001.

[67] P. Mahat, Z. Chen, B. Bak-Jensen, and C. L. Bak, "A simple adaptive overcurrent protection of distribution systems with distributed generation," *IEEE Trans. Smart Grid,* vol. 2, pp. 428-437, 2011.

[68] H. H. Zeineldin, A. Saif, M. M. A. Salama, and A. F. Zobaa, "Three-dimensional non-detection zone for assessing anti-islanding detection schemes," *Electric Power Components and Systems,* vol. 38, pp. 621-636, 2010.

[69] P. Mahat, Z. Chen, and B. Bak-Jensen, "Review of islanding detection methods for distributed generation," in *Proc. Inter. Conf. Elec. Utility Dereg. Restruct. Power Tech.*, 2008.

[70] M. Garmrudi, H. Nafisi, A. Fereidouni, and H. Hashemi, "A novel hybrid islanding detection technique using rate of voltage change and capacitor tap switching," *Electric Power Components and Systems,* vol. 40, pp. 1149-1159, 2012.

[71] W. Xu, G. Zhang, C. Li, W. Wang, G. Wang, and J. Kliber, "A power line line signaling based technique for anti-islanding protection of distributed generators—part I: scheme and analysis," *IEEE Trans. Power Delivery,* vol. 22, pp. 1758-1766, 2007.

[72] M. A. Refern, O. Usta, and G. Fielding, "Protection against loss of utility grid supply for a dispersed storage and generation unit," *IEEE Trans. Power Delivery,* vol. 8, pp. 948-954, 1993.

[73] F. Pai and S. Huang, "A detection algorithm for islanding-prevention of dispersed consumer-owned storage and generating units," *IEEE Trans. Energy Conversion,* vol. 16, pp. 346-351, 2001.

[74] G. Hung, C. Chang, and C. Chen, "Automatic phase shift method for islanding detection of grid connected photovoltaic inverter," *IEEE Trans. Energy Conversion,* vol. 18, pp. 169-173, 2003.

[75] V. Menon and M. H. Nehrir, "A hybrid islanding detection technique using voltage unbalance and frequency set point," *IEEE Trans. Power Sytems,* vol. 22, pp. 442-448, 2007.

[76] S. M. Brahma, "Fault location in power distribution system with penetration of distributed generation," *IEEE Trans. Power Delivery,* vol. 26, pp. 1545-1553, 2011.

[77] Q. Zhou, C. Wang, B. Zheng, and J. Zhao, "Fault location for distribution networks with distributed generation sources using a hybrid PSO/DE algorithm," in *Proc. IEEE PES General Meeting*, Vancouver, BC, CA, 2013.

[78] I. S. Baxevanos and D. P. Labridis, "Implementing multiagent systems technology for power distribution network control and protection management," *IEEE Trans. Power Deliv.,* vol. 22, pp. 433-443, 2007.

[79] B. Russell and C. Benner, "Intelligent systems for improved reliabiliy and failure diagnosis in distribution systems," *IEEE Trans. Smart Grid,* vol. 1, pp. 48-56, 2010.

[80] F. Blaabjerg, R. Teodorescu, M. Liserre, and A. Timbus, "Overview of control and grid synchronization for distributed power generation system," *IEEE Trans. Industrial Electronics,* vol. 53, pp. 1398-1409, 2006.

[81] X. She, A. Q. Huang, and R. Burgos, "Review of solid-state transformer technologies and their application in power distribution systems," *IEEE Journal of Emerging and Selected Topics in Power Electronics,* vol. 1, pp. 186-198, 2013.

[82] A. Sundaram and M. Gandhi. (2008, Sept.). Solid-State Fault Current Limiters. Available: http://energy.gov/sites/prod/files/ESPE%202008%20Peer%20Review%20-%20Solid%20State%20Fault%20Current%20Limiters%20-%20Ashok%20Sundaram,%20EPRI%20and%20Mahesh%20Gandhi,%20Silicon%20Power.pdf

[83] C. Meyer, S. Schroder, and R. Doncker, "Solid-state circuit breakers and current limiters for medium-voltage systems having distributed power systems," *IEEE Trans. Power Electronics,* vol. 19, pp. 1333-1340, 2004.

[84] S. Hwang, X. Liu, J. Kim, and H. Li, "Distributed digital control of modular-based solid-state transformer using DSP+FPGA," *IEEE Trans. Industrial Electronics,* vol. 60, pp. 670-680, 2013.

[85] E. Zabala, E. Perea, and J. Rodriguez, "Improvement of the Quality of Supply in Distributed Generation networks through the integrated application of power electronic techniques," in *Proc. Inter. Conf. Integr. Renew. Energy Sour. Distr. Energy Res.*, 2004.

[86] H. Tao, A. Kotsopoulos, J. Duarte, and M. Hendrix, "Family of multiport bidirectional DC-DC converters," *IEE Proceedings: Electric Power Applications,* vol. 153, pp. 451-458, 2006.

[87] F. Deng and Z. Chen, "A Control Method for Voltage Balancing in Modular Multilevel Converters," *IEEE Trans. Power Electronics,* vol. 29, pp. 66 - 76, 2014.

[88] K. Ilves, S. Norrga, L. Harnefors, and H. Nee, "On energy storage requirements in modular multilevel converters," *IEEE Trans. Power Electronics,* vol. 29, pp. 77-88, 2014.

[89] R. Gustavsson, "Dependable ICT support of power grid operations " BTH2006.

[90] F. Pritchard, "Reading deeper: advanced metering and asset management," *IEEE Power and Energy Magazine,* vol. 8, pp. 85-87, 2010.

[91] M. Paolone, A. Borghetti, and C. A. Nucci, "Development of an RTU for synchrophasors estimation in active distribution networks," in *Proc. IEEE Bucharest PowerTech*, Bucharest, Romania, 2009.

[92] A. Borghetti, C. A. Nucci, M. Paolone, G. Ciappi, and A. Solari, "Synchronized phasors monitoring during the islanding maneuver of an active distribution network," *IEEE Transactions on Smart Grid,* vol. 2, pp. 82-91, 2011.

[93] J. Liu, J. Tang, F. Ponci, A. Monti, C. Muscas, and P. Pegoraro, "Trade-offs in PMU deployment for state estimation in active distribution grids," *IEEE Trans. Smart Grid,* vol. 3, pp. 915-924, 2012.

[94] D. Laverty, D. Morrow, R. Best, and P. Crossley, "Differential ROCOF relay for loss-of-mains protection of renewable generation using phasor measurement over internet protocol," in *Proc. CIGRE/IEEE PES Joint Symp. Integr. Wide-Scale Renew. Res. Into the Power Deliver. Syst.*, 2009.

[95] A. Timbus, M. Larsson, and C. Yuen, "Active management of distributed energy resources using standardized communications and modern information technologies," *IEEE Trans. Industrial Electronics,* vol. 56, pp. 4029-4037, 2009.

[96] C. Sastry, V. Srivastava, R. Pratt, and S. Li, "Use of residential smart appliances for peak-load shifting and spinning reserves: cost/benefit analysis," Pacific Northwest National Laboratory, Richland, Washington2010.

[97] J. Fuller and G. Parker, "Modeling of GE appliances: cost benefit study of smart appliances in wholesale energy, frequency regulation, and spinning reserve markets," Oacific Northwest National Laboratory, Richmond, WA2012.

[98] R. Thomas, "Putting an action plan in place," *IEEE Power&Energy Magazine,* vol. 7, pp. 27-31, 2009.

[99] F. Ongaro, S. Saggini, and P. Mattavelli, "Li-Ion battery-supercapacitor hybrid storage system for a long lifetime, photovoltaic-based wireless sensor network," *IEEE Trans. Power Electronics,* vol. 27, pp. 3944-3952, 2012.

[100] S. Lukic, S. Wirasingha, F. Rodriguez, J. Cao, and A. Emadi, "Power management of an ultracapacitor/battery hybrid energy storage system in an HEV," in *Proc. IEEE Vehicle Power and Propulsion Conference*, 2006.

[101] M. Glavin, P. Chan, S. Armstrong, and W. Hurley, "A stand-alone photovoltaic supercapacitor battery hybrid energy storage system," in *Proc. EPE Power Electronics and Motor Control Conference*, 2008.

[102] E. Cutter, "Benefit analysis of energy storage, case study with Sacramento municipal utility district," EPRI, Palo Alto, CA2011.

[103] E. Cready, J. Lippert, J. Pihl, I. Weinstock, and P. Symons, "Technical and economic feasibility of applying used EV batteries in stationary applications: A Study for the DOE energy storage systems program," Sandia National Labs., Albuquerque, NM2003.

[104] U. Wang. (2011, 08 08). Chevy Volt Batteries For Neighborhood Energy Storage. Available: http://www.forbes.com/sites/uciliawang/2011/08/08/chevy-volt-batteries-for-neighborhood-energy-storage/

[105] S. Carter. (2011, 08 13). Nissan Using Old LEAF Batteries In New Solar Charging Stations. Available: http://nissan-leaf.net/2011/08/13/nissan-using-old-leaf-batteries-in-new-solar-charging-stations/

[106] D. Bral, C. Wang, and C. P. Yeh, "Economical and legal considerations of home-based wind power systems in eastern michigan," in *Proc. IEEE PES General Meeting*, Pittsburg, PA, 2008.

[107] "HERO," ed. Detroit, MI, 2013.

[108] M. Roger, C. Miller, S. McElmurry, G. Xu, W. Shi, and C. Wang, "HERO: A smartphone application for real-time emissions feedback," *Environmental Modelling & Software,* submitted.

[109] Federal Energy Regulatory Commission, "A ntional assessment of demand response potential," Federal Energy Regulatory Commission, Washington, D.C.2009.

[110] H. Xin, Z. Qu, J. Seuss, and A. Maknouninejad, "A self-organizing strategy for power flow control of photovoltaic generators in a distribution network," *IEEE Trans. Power Systems,* vol. 26, pp. 1462-1473, 2011.

[111] P. Tenti, H. Paredes, and P. Mattavelli, "Conservative power theory, a framework to approach control and accountability issues in smart microgrids," *IEEE Trans. Power Electronics,,* vol. 26, pp. 664-673, 2011.

[112] L. Y. Wang, C. Wang, G. Yin, and Y. Wang, "Weighted and constrained consensus for distributed power dispatch of scalable microgrids," *Asian Journal of Control,* submitted.

[113] R. Lasseter, "Smart distribution: Coupled microgrids," *Proceedings of the IEEE,* vol. 99, pp. 1074-1082, 2011.

[114] R. H. Lasseter, "CERTS microgrid," in *Proc. IEEE International Confer. System of Systems Engineering*, San Antonio, TX, 2007.

[115] R. H. Lasseter, "Extended CERTS microgrid," in *Proc. IEEE PES General Meeting*, Piscataway, NJ, 2008.

[116] R. Lasseter, A. Akhil, C. Marnay, J. Stephens, and J. Dagle, "Integration of distributed energy resources: The CERTS MicroGrid concept," Department of Energy, Washington, D.C. 2003.

[117] B. Kroposki, T. Basso, and R. DeBlasio, "Microgrid standards and technologies," in *Proc. IEEE PES General Meeting*, Piscataway, NJ, 2008.

[118] N. Hatziargyriou, H. Asano, R. Iravani, and C. Marnay, "Microgrids," *IEEE Power & Energy Magazine,* vol. 5, pp. 78-94, 2007.

[119] F. Lin, M. P. Polis, C. Wang, L. Y. Wang, and H. Zhang, "Hierarchical control and management of virtual microgrids for vehicle electrification," in *Proc. IEEE Transportation Electrification Conference and Expo*, Dearborn, MI, 2012.

[120] P. J. Ramadge and W. M. Wonham, "Supervisory Control of a Class of Discrete Event Processes," *SIAM Journal on Control and Optimization,* vol. 25, pp. 206-230, Jan 1987.

[121] C. G. Cassandras and S. Lafortune, *Introduction to Discrete Event Systems*. New York, NY: Springer, 1999.

[122] F. Lin and W. M. Wonham, "On Observability of Discrete-Event Systems," *Information Sciences,* vol. 44, pp. 173-198, Apr 1988.

[123] J. E. Hopcroft, R. Motwani, and J. D. Ullman, *Introduction to Automata Theory, Languages, and Computation: Pearson New International Edition*: Pearson Education, 2013.

[124] S. L. C. G. Cassandras, *Introduction to Discrete Event Systems*: Kluwer, 1999.

[125] P. J. G. Ramadge and W. M. Wonham, "The Control of Discrete Event Systems," *Proceedings of the IEEE,* vol. 77, pp. 81-98, Jan 1989.

[126] J. L. Peterson, *Petri Net Theory and the Modeling of Systems*. Upper Saddle River, NJ: Prentice-Hall, 1987.

[127] L. E. Holloway, B. H. Krogh, and A. Giua, "A survey of Petri Net methods for controlled discrete event ystems," *Discrete Event Dynamic Systems,* vol. 7, pp. 151-190, 1997.

[128] Y. Li and W. M. Wonham, "Control of Vector Discrete-Event Systems .1. The Base Model," *IEEE Trans. Automatic Control,* vol. 38, pp. 1214-1227, Aug 1993.

[129] Y. Li and W. M. Wonham, "Control of Vector Discrete-Event Systems-II - Controller Synthesis," *IEEE Trans. Automatic Control,* vol. 39, pp. 512-531, Mar 1994.

[130] G. Cohen, S. Gaubert, and J. P. Quadrat, "Timed-event graphs with multipliers and homogeneous min-plus systems," *IEEE Transactions on Automatic Control,* vol. 43, pp. 1296-1302, Sep 1998.

[131] Y. L. Chen and F. Lin, "Modeling of discrete event systems using finite state machines with parameters," in *IEEE International Conference on Control Applications*, 2000.

[132] K. T. Cheng and A. S. Krishnakumar, "Automatic generation of functional vectors using the extended finite state machine model," *ACM Transactions on Design Automation of Electronic Systems,* vol. 1, pp. 57-79, 1996.

[133] Y. Yang, A. Mannani, and P. Gohari, "Implementation of supervisory control using extended finite-state machines," *International Journal of Systems Science,* vol. 39, pp. 1115-1125, 2008.

[134] A. Mannani, Y. Yang, and P. Gohari, "Distributed extended Finite-State Machines: Communication and control," *WODES 2006: Eighth International Workshop on Discrete Event Systems, Proceedings,* pp. 161-167, 2006.

[135] A. Voronoc and K. Akesson, "Verification of supervisory control properties of finite automata extended with variables," Chalmers University of Technology, Göteborg, Sweden2009.

[136] M. Skoldstam, K. Akesson, and M. Fabian, "Modeling of discrete event systems using finite automata with variables," *Proceedings of the 46th IEEE Conference on Decision and Control,* pp. 5438-5443, 2007.

[137] B. Gaudin and P. H. Deussen, "Supervisory control on concurrent discrete event systems with variables," in *2007 American Control Conference*, 2007, pp. 4033-4038.

[138] T. L. Gall, B. Jeannet, and H. Marchand, "Supervisory Control of Infinite Symbolic Systems using Abstract Interpretation."

[139] S. L. Chung, S. Lafortune, and F. Lin, "Limited Lookahead Policies in Supervisory Control of Discrete Event Systems," *IEEE Transactions on Automatic Control,* vol. 37, pp. 1921-1935, Dec 1992.

[140] N. Benhadjalouane, S. Lafortune, and F. Lin, "Variable Lookahead Supervisory Control with State Information," *IEEE Transactions on Automatic Control,* vol. 39, pp. 2398-2410, Dec 1994.

[141] J. Prosser, J. Selinsky, H. Kwatny, and M. Kam, "Supervisory Control of Electric-Power Transmission Networks," *IEEE Transactions on Power Systems,* vol. 10, pp. 1104-1110, May 1995.

[142] L. H. Fink, "Discrete events in power systems," *Discrete Event Dynamic Systems-Theory and Applications,* vol. 9, pp. 319-330, 1999.

[143] I. A. Hiskens, "Power system modeling for inverse problems," *IEEE Transactions on Circuits and Systems I-Regular Papers,* vol. 51, pp. 539-551, Mar. 2004.

[144] H. S. Zhao, Z. Q. Mi, and H. Ren, "Modeling and analysis of power system events," in *2006 Power Engineering Society General Meeting*, 2006, pp. 1468-1473.

[145] H. Heymann, F. Lin, and G. Meyer, "Synthesis of minimally restrictive legal controllers for a class of hybrid systems," *Hybrid Systems IV, Lecture Notes in Computer Science,* vol. 1273, pp. 134-159, 1997.

[146] M. Heymann, F. Lin, and G. Meyer, "Synthesis and viability of minimally interventive legal controllers for hybrid systems," *Discrete Event Dynamic Systems-Theory and Applications,* vol. 8, pp. 105-135, Jun 1998.

[147] Y. Li, F. Lin, and Z. H. Lin, "A generalized framework for supervisory control of discrete event systems," *International Journal of Intelligent Control Systems,* vol. 2, pp. 139-159, 1998.

[148] C. Roe, F. Evangelos, J. Meisel, A. P. Meliopoulos, and T. Overby, "Power system level impacts of PHEVs," in *2009 42nd Hawaii International Conference on System Sciences*, Big Island, HI, 2009.

[149] K. Clement-Nyns, E. Haesen, and J. Driesen, "The Impact of Charging Plug-In Hybrid Electric Vehicles on a Residential Distribution Grid," *IEEE Transactions on Power Systems,* vol. 25, pp. 371-380, Feb 2010.

[150] R. C. Green, L. F. Wang, and M. Alam, "The impact of plug-in hybrid electric vehicles on distribution networks: A review and outlook," *Renewable & Sustainable Energy Reviews,* vol. 15, pp. 544-553, Jan 2011.

[151] K. Clement, E. Haesen, and J. Driesen, "Stochastic analysis of the impact of plug-in hybrid electric vehicles on the distribution grid," in *CIRED International Conference Electricity Distribution*, Prague, Czech Republic, 2009.

[152] V. A. Ajjarapu and C. Christy, "The continuation power flow: A tool for steady – state voltage stability analysis," *IEEE Transactions on Power Systems,* vol. 7, pp. 416-423, 1992.

[153] A. Araposthatis, S. Sastry, and P. Varaiya, "Analysis of power flow equation," *Electric Power & Energy Systems,* vol. 3, pp. 115-126, 1981.

[154] A. Lof, T. Smed, and G. Anderson, "Fast calculation of a voltage stability index," *IEEE Transactions on Power Systems,* vol. 7, pp. 54-64, 1992.

[155] P. Kessel and H. Glavitsch, "Estimating the voltage stability of a power system," *IEEE Transactions on Power Delivery,* vol. 1, pp. 346 - 354, 1986.

[156] M. Moghavvemi and O. Faruque, "Real-time contingency evaluation and ranking technique," *IEEE Proceeding on Generation, Transmission and Distribution,* vol. 145, pp. 517-524, 1998.

[157] A. Mohamed, G. B. Jasmon, and S. Yusoff, "A static voltage collapse indicator using line stability factors," *Journal of Industrial Technology,* vol. 7, pp. 73-85, 1989.

[158] S. A. Arefifar and W. Xu, "Online tracking of power system impedance parameters and field experiences," *IEEE Transactions on Power Delivery,* vol. 24, pp. 1781-1788, Oct 2009.

[159] G. Fusco, A. Losi, and M. Russo, "Constrained least squares methods for parameter tracking of power system steady-state equivalent circuits," *IEEE Transactions on Power Delivery,* vol. 15, pp. 1073-1080, Jul 2000.

[160] F. Gubina and B. Strmcnik, "A simple approach to voltage stability assessment in radial network," *IEEE Transactions on Power Systems,* vol. 12, pp. 1121-1128, 1997.

[161] G. Jasmon and L. Lee, "New contigency ranking technique incorporating a voltage stability criterion," *IEE Porceedings Generation, Transmission and Distribution,* vol. 140, pp. 87-90, 1993.

[162] G. B. Jasmon and L. Lee, "Distribution network reduction for voltage stability analysis and load flow calculations," *Electric Power and Energy System,* vol. 13, 1991.

[163] M. J. H. Sterling, A. M. Chebbo, and M. R. Irving, "Reactive power dispatch incorporating voltage stability," *IEE Proceedings Generation. Transmission, and Distribution, ,* vol. 139, pp. 253-260, May 1992.

[164] B. Venkatesh, R. Ranjan, and H. B. Gooi, "Optimal reconfiguration of radial distribution systems to maximize loadability," *IEEE Transactions of Power Systems,* vol. 19, pp. 260-266, 2004.

[165] Y. Wang, C. Wang, F. Lin, W. Li, L. Y. Wang, and J. Zhao, "A new transfer impedance based system equivalent model for voltage stability analysis," *International Journal of Electrical Power & Energy Systems,* vol. 62, pp. 38-44, 2014.

[166] P. Kundur, *Power System Stability and Control*. New York: McGraw-Hill, 1994.

[167] MathWorks. (2013). *Optimization Toolbox User's Guide*.

[168] R. D. Zimmerman, C. E. Murillo-Sánchez, and R. J. Thomas, "MATPOWER: Steady-state operations, planning and analysis tools for power systems research and education," *IEEE Transactions Power Systems,* vol. 26, pp. 12-19, Feb 2011.

[169] I. E. Commission, "IEC 60870-5-104, Transmission protocols: Network access for IEC 60870-5-101, using standard transport profiles ", ed. Switzerland, Jun. 2006.

[170] C. Gerkensmeyer, M. Kintner-Meyer, and J. DeSteese, "Technical callenges of pug-in hybrid electric vehicles and impacts to the US power system: distribution system analysis," Pacific Northwest National Laboratory, Richland, WashingtonJan. 2010.

[171] F. Katiraei, A. R. Iravani, and P. W. Lehn, "Micro-grid autonomous operation during and subsequent to islanding process," *IEEE Transactions on Power Delivery,* vol. 20, pp. 248-257, Jan 2005.

[172] A. E. Fitzgerald, C. Kingsley, and S. Umans, *Electric Machinery*. Boston, MA: McGraw-Hill, 2003.

[173] R. Yan and T. K. Saha, "Investigation of voltage stability for residential customers due to high photoviltaic penetrations," *IEEE Transactions on Power Systems,* vol. 27, pp. 651-662, 2012.

[174] E. Liu and J. Bebic, "Distribution system voltage performance analysis for high penetration photovoltaics," National Renewable Energy Laboratory, Golden, CO2008.

[175] K. Turitsyn, P. Sulc, S. Backhaus, and M. Chertkov, "Options for Control of Reactive Power by Distributed Photovoltaic Generators," *Proceedings of the IEEE,* vol. 99, pp. 1063-1073, Jun 2011.

[176] J. McDonald, "Microgrids beyond the hype: utilities need to see a benefit," *IEEE Electrification Magazine,* vol. 2, pp. 6 - 11, Mar. 2014.

[177] C. K. Sao and P. W. Lehn, "Control and power management of converter fed microgrids," *IEEE Transactions on Power Systems,* vol. 23, pp. 1088-1098, Aug 2008.

[178] S. Barsali, M. Ceraolo, P. Pelacchi, and D. Poli, "Control techniques of Dispersed Generators to improve the continuity of electricity supply," in *2002 IEEE Power Engineering Society Winter Meeting, Conference Proceedings*, 2002, pp. 789-794.

[179] R. Aghatehrani and R. Kavasseri, "Reactive Power Management of a DFIG Wind System in Microgrids Based on Voltage Sensitivity Analysis," *IEEE Transactions on Sustainable Energy,* vol. 2, pp. 451-458, Oct 2011.

[180] W. H. Kersting, "Radial distribution test feeders," in *IEEE PES Winter Meeting*, Columbus, OH, 2001.

[181] J. A. P. Lopes, C. L. Moreira, and A. G. Madureira, "Defining control strategies for microgrids islanded operation," *IEEE Trans. on Power Systems,* vol. 21, pp. 916-924, May 2006.

[182] F. P. Demello, R. J. Koessler, J. Agee, P. M. Anderson, J. H. Doudna, J. H. Fish*, et al.*, "Hydraulic-turbine and turbine control-models for system dynamic studies," *IEEE Trans. Power Systems,* vol. 7, pp. 167-179, Feb 1992.

[183] R. Gagnon, B. Sauliner, G. Sybille, and P. Giroux, "Modeling of a generic high performance of no storage wind-diesel system using MATLAB/Power systems blocks set," presented at the European Wind Energy Association Global Wind Power Conference, 2002.

[184] IEEE, "IEEE recommended practice for excitation system models for power system stability studies," in *Revision of IEEE 521.5-1992*, ed: IEEE Standard, 2005.

[185] J. Zhao, K. Graves, C. Wang, G. Liao, and C. Yeh, "A Hybrid Electric/Hydro Storage Solution for Standalone Photovoltaic Applications in Remote Areas," in *2012 IEEE Power and Energy Society General Meeting*, 2012.

[186] D. Linden, *Handbook of Batteries*. New York, NY: McGraw Hill, Inc., 1995.

[187] A. H. K. Alaboudy, H. H. Zeineldin, and J. L. Kirtley, "Microgrid Stability Characterization Subsequent to Fault-Triggered Islanding Incidents," *IEEE Trans. Power Delivery,* vol. 27, pp. 658-669, Apr 2012.

[188] A. Bergen and V. Vittal, *Power Systems Analysis*. Upper Saddle River, NJ: Prentice Hall, 1999.

[189] IEEE Standards Coordinating Committee 21, "IEEE Guide for Design, Operation, and Integration of Distributed Resource Island Systems With Electric Power Systems," in *IEEE Standard 1547.4*, ed. New York, NY, 2011.

[190] The MathWorks. (2003). *SimPowerSystems User's Guide*.

ABSTRACT

MANAGEMENT OF PLUG-IN ELECTRIC VEHICLES AND RENEWABLE ENERGY SOURCES IN ACTIVE DISTRIBUTION NETWORKS

by

JUNHUI ZHAO

August 2014

Advisor: Dr. Caisheng Wang

Co-Advisor: Dr. Feng Lin

Major: Electrical Engineering

Degree: Doctor of Philosophy

Near 160 million customers in the U.S.A. are served via distribution networks (DNs). The increasing penetration level of renewable energy sources (RES) and plug-in electric vehicles (PEVs), the implementation of smart distribution technologies such as advanced metering/monitoring infrastructure, and the adoption of smart appliances, have changed distribution networks from passive to active. The next-generation of DNs should be efficient and optimized system-wide, highly reliable and robust, and capable of effectively managing highly-penetrated PEVs, RES and other controllable loads. To meet new challenges, the next-generation DNs need active distribution management (ADM).

In this thesis, we study the management of PEVs and RES in active DNs. First, we propose a novel discrete-event modeling method to model PEVs and other loads in distribution networks. In addition, a new optimization algorithm to integrate as many PEVs as possible in DNs without causing voltage issues, including the violation of voltage security ranges and voltage stability issues, is studied. To further explore the active management of PEVs in the DNs, we develop a universal demonstration platform, consisting of software packages and hardware remote terminal

units. The demonstration platform is designed with the capabilities of measurement, monitoring, control, automation, and communications.

Furthermore, we have studied the reactive power management in microgrids, a special platform to integrate distributed generations and energy storage in DNs. To solve possible voltage security issues in a microgrid with high penetration of single-phase induction machines under the condition of fault-induced islanding, a voltage-sensitivity-based reactive power management algorithm is proposed.

AUTOBIOGRAPHICAL STATEMENT

JUNHUI ZHAO

Education

2014 Doctor of Philosophy, Wayne State University, Detroit, MI, USA
2013 Master Degree in Engineering, Wayne State University, Detroit, MI, USA
2009 Master Degree in Engineering, Chongqing University, Chongqing, China
2006 Bachelor Degree in Engineering, Xi'an University of Technology, Xi'an, Shaanxi, China

Selected Honors and Awards

- Best Poster Winner in IEEE SEM Spring Conference, 2014
- Rumble Fellowship, Wayne State University, 2013
- Grand Prize, Michigan Clean Energy Venture Competition, 2012

Selected Publications

Journal

1. ***J. Zhao***, C. Wang, B. Zhao, F. Lin, Q. Zhou, and Y. Wang, "A review of active management for distribution networks: current status and future development trends," *Electric Power Components and Systems*, vol. 42, no. 3-4, pp. 280-293, 2014.
2. ***J. Zhao,*** Y. L. Chen, Z. Chen, F. Lin, C. Wang and H. Zhang, "Modeling and control of discrete event systems using finite state machines with variables and their applications in power grids," *Systems & Control Letters*, vol. 61, no. 1, pp. 212-222, Jan. 2012.
3. S. Alyami, Y. Wang, C. Wang, ***J. Zhao***, and B. Zhao, "Adaptive real power capping method for fair overvoltage regulation of distribution networks with high penetration of PV systems," *IEEE Trans. Smart Grid*, (in publication).
4. Y. Wang, C. Wang, F. Lin, W. Li, L. Y. Wang, and ***J. Zhao***, "Incorporating generator equivalent model into voltage stability analysis," *IEEE Trans. Power Systems*, vol. 28, no. 4, pp. 4857-4866, Nov. 2013.

Conference

1. ***J. Zhao***, D. Shi, R. Sharma and C. Wang, "Microgrid reactive power management during and subsequent to islanding process," in *Proc. IEEE PES T&D*, Chicago, IL, Mar. 2014.
2. ***J. Zhao***, Y. Wang, C. Wang, F. Lin, and L. Y. Wang, "Maximizing the penetration of plug-in electric vehicles in distribution network," in *Proc. of IEEE Transportation Electrification Conference & Expo*, Dearborn, MI, June 2013.
3. ***J. Zhao***, K. Graves, C. Wang, G. Liao and C. P. Yeh, "A hybrid electric/hydro storage solution for standalone photovoltaic applications in remote areas," in *Proc. IEEE-PES General Meeting*, San Diego, CA, July 2012.
4. ***J. Zhao***, Z. Chen, F. Lin, C. Wang and H. Zhang, "Safety control of PHEVs in distribution networks using finite state machines with variables," in *Proc. North American Power Symposium*, Boston, MA, Aug. 2011.